Circadian patterns in key physiological processes of the marine diatom Phaeodactylum tricornutum

Thesis

UNRESTRICTED.

Circadian patterns in key physiological processes of the marine diatom *Phaeodactylum tricornutum*

MARIA RAGNI

Laurea in Scienze Ambientali

Università degli studi di Napoli "Parthenope"

Italia

DOCTOR OF PHILOSOPHY

Sponsoring Establishment

Stazione Zoologica "Anton Dohrn"

Naples, Italy

Director of studies:

Dr. Maurizio Ribera d'Alcalà
Stazione Zoologica "A. Dohrn"
Naples (Italy)

Supervisors:

Prof. Roberto Di Lauro
Stazione Zoologica "A. Dohrn"
Naples (Italy)

Prof. Marlon R. Lewis
Dalhousie University, Halifax
(Canada)

Submission date: 1 February 2005
Award date: 27 April 2005

Abstract

Circadian rhythms are a widespread feature among all the levels of organismal complexity, from bacteria to humans. Nevertheless their ecological relevance in marine phytoplankton has not been clearly assessed.

In this study the diatom *P. tricornutum* was used as a model for giving an integrated picture of the circadian patterns of phytoplankton photophysiology in relation to the external light field and for assessing the interaction between the cell cycle and the temporal control of processes like pigment synthesis and photosynthesis.

The results suggest that light/dark shifts are crucial for regulating the timing of different cell activities, including the synthesis of photoprotectant pigments (i.e., diadinoxanthin). The photosynthetic processes run at different paces in different stages of the cell cycle and different times of the day. This would imply a synchronization of cell processes due to both internal and external entrainer/s. When the external trigger is removed (e.g., in absence of light/dark shifts), the time distribution of the cell cycle stages quickly flattens, the efficiency of the use of light lowers, as well as the flexibility in facing light variations. Though, this does not always involve the loss of synchronization of processes like pigment synthesis, or the activation/inactivation of the photosynthetic machinery.

The results from an *in situ* experiment support the occurrence of a circadian regulation of photophysiological processes in natural phytoplankton, at least in the upper layer of the water column, where solar radiation can act as a signal for the entrainment of circadian rhythms, whether or not mediated by specific photoreceptors.

The overall picture is that the presence of systems for the circadian control of physiological activity would be a successful feature in marine phytoplankton, which is reasonable also in an evolutionary perspective, since the day/night cycle is a permanent pattern in the Earth system.

Contents

List of used symbols and abbreviations IV

Chapter 1

Circadian variability in organismal physiology 1

1.1 Features and components of circadian clocks 3
1.2 Diel periodicity in marine algae 5
1.3 The adaptive significance of circadian clocks in microalgae 7
1.4 Questions and aims of the work 12

Chapter 2

Light signals underwater 15

2.1 Methodological approach 17
2.1.1 Parameterization of solar radiation at the sea surface 17
2.1.2 Parameterization of underwater attenuation 19
2.2 Results 21
2.2.1 Model validation 21
2.2.2 Diel and depth variability of band ratios 24
2.2.3 The impact of chlorophyll fluorescence 26
2.3 Discussion 28

Chapter 3

Experimental approaches and protocols 31

Scheme of the experimental activity 32
3.1 The species object of investigation: *Phaeodactylum tricornutum* 33
3.2 Experimental strategies 34
3.2.1 Culture conditions 34
3.2.2 Experiments in artificial light regime 35
3.2.2.1 "Long" experiments 35
3.2.2.2 "Short" experiments 36
3.2.3 Experiments in natural light regime 38
3.2.3.1 "Long" experiments 39
3.2.3.2 In situ experiment 40
3.3 Analytical procedures (on samples) 40
3.3.1 Flow cytometry (FCM) 40
3.3.2 Cell cycle studies 41
3.3.3 Pigments determination (HPLC) 41
3.3.4 Absorption measurements 42
3.3.5 Photosynthetic parameters 43
3.3.5.1 $NaH^{14}CO_3$ incubations (PvsE experiments) 43

3.3.5.2 Variable fluorescence 45
3.4 In situ profiles 48
3.4.1 FRRF 48
3.4.2 Irradiance profiles 49

Chapter 4
Diel periodicity in the photosynthetic machinery of marine phytoplankton. The *P. tricornutum* model 50
4.1 Background 50
4.2 Circadian patterns of pigment concentrations and photosynthetic parameters in PT grown in artificial light 55
4.2.1 Pigments 55
4.2.2 Absorption coefficients 60
4.2.3 PvE coefficients 64
4.2.4 Variable fluorescence 66
4.2.5 Summary 68
4.3 Circadian patterns of pigment concentrations and photosynthetic parameters in PT grown in natural light 70
4.3.1 Pigments 70
4.3.2 PvsE coefficients 72
4.3.3 Variable fluorescence 74
4.3.4 Summary 78
4.4 The effect of changes in light regime on the diel variability of pigment content and fluorescence-derived parameters 79
4.4.1 The effect of growth irradiance 79
4.4.1.1 Pigments 79
4.4.1.2 Variable fluorescence 80
4.4.2 The effect of light shifts 82
4.4.2.1 Pigments 82
4.4.2.2 Variable fluorescence 83
4.4.3 The effect of the duration of photoperiod 84
4.4.3.1 16: 8 LD cycles 84
4.4.3.2 24 : 0 LD cycles 85
4.4.4 Summary 87
4.5 Circadian patterns of pigment concentrations and photosynthetic parameters in situ 88
4.5.1 Pigments 90
4.5.2 PvsE parameters 92
4.5.3 Variable fluorescence 94
4.5.4 Summary 97
4.6 Synthesis of the chapter 97

Chapter 5
The time course of the cell cycle of *P. tricornutum* in different light regimes 100
5.1 Background 100

5.2 Results 104
5.2.1 Circadian patterns of growth, geometrical parameters and cell cycle stages of PT cells grown in artificial light 104
5.2.1.1 Size/shape dependent properties of PT cells 104
5.2.1.2 Cell cycle stages and growth rates 105
5.2.1.3 Summary 109
5.2.2 Circadian patterns of growth, geometrical parameters and cell cycle stages of PT cells grown in natural light 110
5.2.2.1 Size/shape dependent properties of PT cells 110
5.2.2.2 Cell cycle stages and growth rates 111
5.2.2.3 Summary 114
5.2.3 Circadian patterns of growth, geometrical parameters and cell cycle stages of rapidly dividing PT cells grown in artificial light 115
5.2.3.1 Summary 118
5.2.4 Size/shape dependent properties and pigment composition of the three different morphotypes of PT 118

Chapter 6
Towards an integrated view of the diel biological activities of a marine phytoplankter 121
6.1 Rationale of the experiments 124
6.2 Cell growth and pigments 124
6.3 Photosynthetic machinery 135
6.4 Time patterns in LL 139
6.5 Cell cycle 147
6.6 Conclusions 154

Acknowledgments 157
References 159

List of used symbols and abbreviations

Symbol/ abbreviation	Definition	Relashionhip	Used unit of measurement
$a(\lambda)$	Spectral absorption coefficient of the water sample	$a_w(\lambda) + a_{CDOM}(\lambda) + a_{sus}(\lambda)$	m^{-1}
$a^*_{chl}(\lambda)$, $a^*_{cell}(\lambda)$	Chl *a*-specific and cell-specific spectral absorption coefficient, (or optical cross section)	a_{pig}/Chl *a* a_{pig}/cellN	$m^2(mgChla)^{-1}$ m^2cell^{-1}
$a_{CDOM}(\lambda)$, $a_{det}(\lambda)$, $a_w(\lambda)$	Spectral absorption coefficient of dissolved organic matter, detritus, pure water		m^{-1}
$a_{pig}(\lambda)$	Spectral absorption coefficient of pigments	$a_{sus}(\lambda) - a_{det}(\lambda)$	m^{-1}
$a_{sus}(\lambda)$	Spectral absorption coefficient of the suspension	$a_{det}(\lambda) + a_{pig}(\lambda)$	m^{-1}
α^B α^{chl}, α^{cell}	Photosynthetic efficiency (light limited slope of the PvsE curve)		$gC(gChl\ a \cdot \mu molquanta \cdot m^{-2}s^{-1}h)^{-1}$ $pgC\ (cell \cdot \mu molquanta \cdot m^{-2}s^{-1}h)^{-1}$
α_{PAM}	light limited slope of the rETR light curve (PhytoPAM technique)		elctrons/quanta
$b_b(\lambda)$, $b_{bw}(\lambda)$, $b_{bp}(\lambda)$	spectral backscattering coefficients: total, of seawater, of particulate		m^{-1}
βcar	βcarotene		$\mu g/l$ pg/cell
Chl *a*	Chlorophyll *a*		$\mu g/l$ pg/cell
Chl c_2	Chlorophyll c_2		$\mu g/l$ pg/cell
Ddx	Diadinoxanthin		$\mu g/l$ pg/cell
Dtx	Diatoxanthin		$\mu g/l$ pg/cell
$E_d(\lambda,z)$, $E_{dd}(\lambda,z)$, $E_{ds}(\lambda,z)$	Global, direct and diffuse spectral downwelling irradiance at the depth z and wavelength λ	$E_d(\lambda,z)=E_{dd}(\lambda,z)+E_{ds}(\lambda, z)$	$Wm^{-2}nm^{-1}$ $\mu molquanta \cdot m^{-2}s^{-1}$
$E_f(\lambda, z)$	Irradiance produced by chlorophyll a fluorescence at depth z and wavelength λ	Eq. 2.5	$Wm^{-2}nm^{-1}$ $\mu molquanta \cdot m^{-2}s^{-1}$
E_g	Growth irradiance		$\mu molquanta \cdot m^{-2}s^{-1}$

E_k, E_{kPAM}	Compensation irradiance, or photoacclimation index	P^B/α^B $rETR_{MAX}/\alpha_{PAM}$	μmolquanta·$m^{-2}s^{-1}$
$E_{0d}(\lambda, z)$	Scalar downwelling irradiance at the depth z and wavelength λ		$Wm^{-2}nm^{-1}$
F_0, F_m	Minimum and maximum fluorescence yield measured in the dark		r.u.
F_0', F_m'	Minimum and maximum fluorescence yield measured under a background irradiance		r.u.
F_v/F_m	Maximum quantum yield of PSII	$(F_0 - F_m)/ F_m$	
F_v'/F_m'	Effective quantum yield of PSII under a background irradiance	$(F_0' - F_m')/ F_m'$	
FALS	Forward angle light scattering		r.u.
FCP	Fucoxanthin-chlorophyll proteins		
FRRF	Fast repetition rate fluoromentry		
FCM	Flow cytometry		
Fucox	Fucoxanthin		μg/l pg/cell
Φ_f	Fluorescence quantum yield		
G_1	Gap 1, phase of the cell cycle		% of cells
G_2	Gap 2, phase of the cell cycle		% of cells
θ	Solar zenith angle		degrees
$K_d(\lambda)$, $K_{dd}(\lambda)$, $K_{ds}(\lambda)$	Diffuse attenuation coefficient for global, direct and diffuse downwelling irradiance	$K_d(\lambda) = K_{dd}(\lambda)+K_{ds}(\lambda)$	m^{-1}
λ	wavelength *in vacuo*		nm
LHCP	Light harvesting chlorophyll-protein complex		
μ	Growth rate		d^{-1}, h^{-1}
$\overline{\mu}_d(\lambda)$	Spectral downwelling average cosine		
M	Mytosis, phase of the cell cycle		% of cells

NPQ	Non-photochemical quenching		
PAM	Pulse amplitude modulation technique		
PAR	Photosynthetically available radiation		μmolquanta $m^{-2}s^{-1}$
P^{B}_{max}, P^{chl}_{max}, P^{cell}_{max}	Maximum photosynthetic rate		gC(gChl *a*·h)$^{-1}$ pgC (cell·h)$^{-1}$
PPC	Photoprotectant caroenoids		μg/l pg/cell
PSC	Photosynthetic carotenoids		μg/l pg/cell
PSP	Photosynthetic pigments		μg/l pg/cell
PT	*P. tricornutum*		
rETR, $rETR_{MAX}$	Relative electron transport rate, maximum relative electron transport rate		μmolelctrons·$m^{-2}s^{-1}$
RC	Reaction center		
RALS	Right angle light scattering		r.u.
RED	Cell red fluorescence		r.u.
S	DNA synthesis, phase of the cell cycle		% of cells
SV_0, SV_M	Stern-Volmer coefficients of NPQ	(F_0/F_0')-1 (F_m/F_m')-1	
σ_{PSII}	Effective cross section of PSII		A^2/q

Chapter 1

Circadian variability in organismal physiology

Among extant photoautotrophs, marine phytoplankters are probably those experiencing the highest variability in their living environment. During its life span, one cell may in fact be exposed to highly different environmental factors, e.g., irradiance (both in intensity and color), different nutrient concentrations, shear rates, density, composition of grazers, etc.

Most of those variations are rarely predictable, therefore tolerance to a wide range of external changes and flexibility in adjusting to them have been key features to be selected for during the evolution of phytoplankton. The proper responses are generally triggered by the variations themselves, or by concurrent signals, with a suite of mechanisms, which may exhibit a high degree of complexity (see, among the others, Falkowski and Raven (1997) and references therein for photoacclimation to changes in light regimes, Platt (1981) and references therein for cell biochemistry, Riebesell *et al.* (1993) and Morel *et al.* (1991) for nutrient assimilation, Villareal and Carpenter (1990) and Moore and Villareal (1996) for the control of bouyancy, Ianora *et al.* (2004) for chemical defense to grazing, etc.). On the other hand, day/night alternation is a persistent feature of the light regime which every cell is exposed to and is, to a certain extent, predictable, whereas other variations of the light environment due, for instance, to changes in atmospheric conditions or of cell position along the water column, can be considered stochastic.

Indeed, the superimposition of periodic changes with random ones is quite frequent in nature and not limited to the time scale of one day. The environment is characterized by several periodical signals at different temporal scales: decadal, seasonal, lunar, diurnal, and tidal, and living organisms display a wide range of biological rhythms in their physiology and behaviour that match the environmental ones.

The most intriguing among these, and probably the most analyzed, are circadian rhythms. In fact, circadian (from 'circa'-about, 'dies'-a day) rhythms very often reflect endogenous biological programs that enable metabolic, physiological or behavioural events to occur at optimal phases of the diel cycle (Suzuki and Johnson, 2001), i.e., with the periodic and predictable component of the environmental variations. These events are regulated by specific molecular systems which allow the proper phasing of the program and are named 'circadian clocks' (Barinaga, 1998).

The fact that the physiological activity of humans, animals and plants follows the course of the day has been known since antiquity. Rhythmical responses in different organisms had already been reported in the 18th century. The French naturalist Jean J. de Mairan observed that movements of higher plants persist even when they are kept in constant darkness (de Mairan, 1729, cited in Somers (1999)). Thirty years later, the German botanist J. G. Zinn (Zinn, 1759) discovered that the leaves of the bean (*Phaseolus coccineus*) raised and lowered even without the light-dark stimulus, and that those movements were almost independent from the temperature, whereas Carl von Linné observed that the time of the day when flowers opened and closed was species-specific ("horologium florae", depicted in 1751 in his *Philosophia Botanica,* cited in http://www.linnean.org/contents/history/linnaeus_biography.html).

The final proof of the existence of endogenous rhythms was the experiment performed by E. Bünning and K. Stern (Bunning and Stern, 1930) where they analyzed the reactions of *Phaseolus multiflorus* and other species at constant temperature and under a given light program (changes of light and darkness) in the laboratory. The experimental setting guaranteed that the movements of the plants were autonomous, i.e. endogenously controlled, and it clearly showed that the movement was rhythmic, and was reset only by the external light signal.

1.1 Features and components of circadian clocks

A common, though not essential, feature of circadian clock controlled rhythms is their self-sustained nature, i.e., they tend to persist even in absence of any external time cues. On the other hand, they are entrained by environmental signals ("zeitgeber", a German term, meaning *time giver*) which reset, and therefore synchronize, the rhythms. Most circadian rhythms in nature are entrained by the day/night light cycle.

The simplest scheme illustrating how these temporal programs work involves a unidirectional pathway, from the input signal to the output phenomena through the following elements:

- the *input signal*, or *environmental oscillator*. This can be a physical, a chemical, or a biological factor that occurs with 24 h periodicity. In photosynthetic organisms, the main factor known to be responsible for rhythmical phenomena is light;
- a *cell receptor* (e.g. photoreceptor).This allows the transduction of the external signals into information for the cell, through an *input pathway*;

- a *circadian oscillator,* or *clock.* This is the core of the system, the endogenous timekeeper. It is phased by the input pathway and generates the *observable rhythm* (output).

Recent and rapid developments in molecular biology and genetics have shed additional light on the existence of internal controls to keep the timing of cellular processes, and have also helped to clarify the molecular mechanisms at the basis of the observed rhythmical phenomena in animals, plants, fungi and bacteria, thus improving the existing models of the

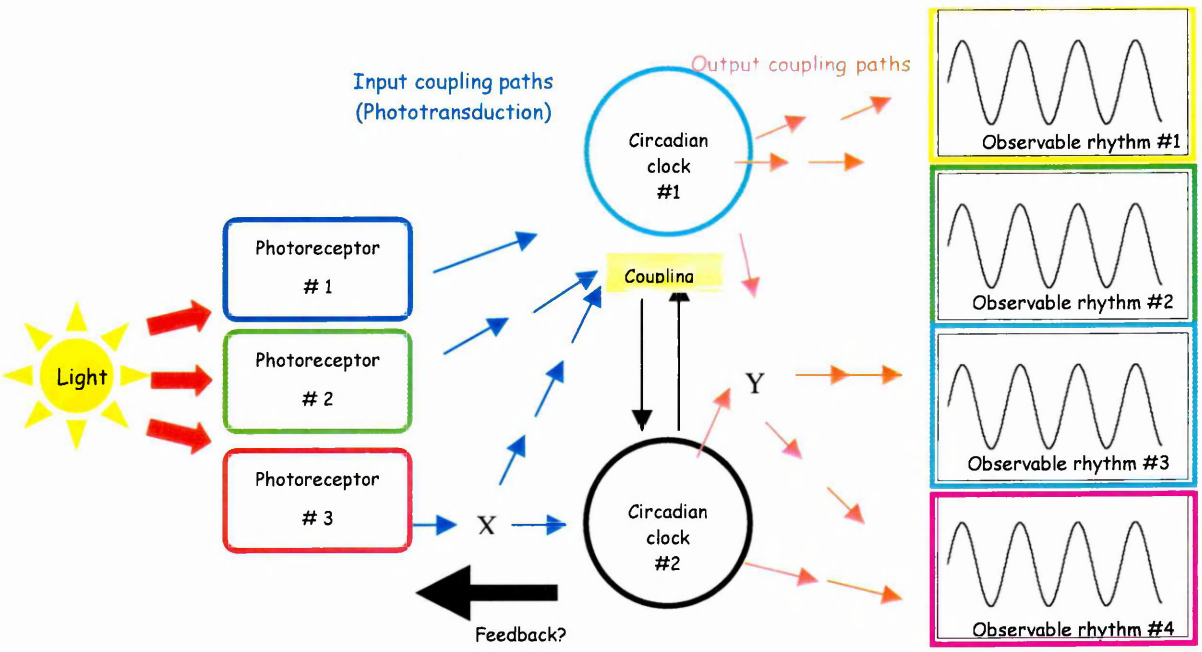

Fig. 1.1. Schematic representation of the different components of the circadian systems, according to Johnson (2001).

circadian oscillators in each system. Those studies indicate that the 24-hour period arises from a system of interconnected feedback loops that control the transcription of a small number of "clock genes". Circadian rhythms are apparently very similar in all species but the genes that make up the clock mechanisms are quite different (comparing animals, plants, fungi and cyanobacteria). The resulting *Circadian oscillator* exerts molecular

control at the transcriptional, transductional and post-transductional levels (*output pathway*). Therefore, circadian rhythms are the result of quite complex systems. A hypothetical representation of the organization of the different components of the circadian clocks is proposed in Johnson (Johnson, 2001) and reproduced in Fig. 1.1, based on more recent studies.

As shown in the scheme, inputs, photoreceptors, clocks and outputs are more than one, and can be coupled in multiple ways, with elements (indicated as X and Y) that can be shared by more than one pathway.

1.2 Diel periodicity in marine algae

Reports of diel periodicity in algae started in the late 50's (Doty and Oguri, 1957; Leedale, 1959). Nevertheless, the observations conducted throughout the following fifteen-twenty years were often misinterpreted, or not well documented until the review by A. Sournia (1974) who put together all the evidence for any kind of circadian variations emerging up to that moment in marine phytoplankton, in order to "sort out evidences, doubts and gaps, referring as often as necessary to laboratory cultures and plant physiology".

First of all he discussed the current terminology on the topic and stated that when dealing with 24 hour cycles, the correct term to use was "circadian" or "diel", whereas "diurnal" was the opposite of "nocturnal", i.e., something occurring between sunrise and sunset; while the term "daily", frequently found in the literature, was not a proper word when referred to circadian rhythms, since it means "once a day" or "every day". The author also pointed out the problem of interference with non-circadian periods, meaning that circadian rhythms can be hidden or confused by periodic variations other than circadian,

either ultradian (periods from 30 minutes to 20 hours) or infradian (from 28 hours to 5 days). Then he went on examining cell division, buoyancy and sinking, vertical migration, chlorophyll *a* content, photosynthesis, respiration, excretion, nutrient uptake, bioluminescence, and indicated some environmental factors as potentially responsible for the entrainment and the modulation of the circadian rhythms: light, temperature, oxygen, CO_2, pH, nutrients, interactions between phytoplankton and zooplankton. Despite this attention, the specific components and mechanisms of phytoplankton circadian systems, and their relation to taxonomic position, remained unexplored, as well as their relation with the external environment. In other words, the questions about the relative weight of internal and external controls and their interactions remained open.

The pioneering work of Sournia was followed, a few years later, by the study of Barbara Prezelin that appeared in two companion papers (Prezelin *et al.*, 1977; Prezelin and Sweeney, 1977). Her work focused on the photosynthetic rhythms in marine dinoflagellates and gave strength to the presence of an endogenous control of several physiological activities in those organisms, confirming previous studies on bioluminescence (Hastings and Sweeney, 1958; Sweeney, 1963) and oxygen evolution (Sweeney, 1960). It took more than a decade to produce a full characterization of the complex circadian system of the dinoflagellate *Gonyaulax polyedra* (Roenneberg and Morse, 1993; Roenneberg, 1996).

In parallel with Prezelin's work, another interesting study was conducted by John Marra on the diatom *Laudaria borealis* (Marra, 1978) under three different artificial light regimes: constant, sinusoidal and irregularly fluctuating light. In the first two cases the maximum photosynthetic rate was observed during the first hours of the light period, whereas under fluctuating light, other peaks occurred following the light variations. Those results were partially confirmed by exposing the culture to natural light regimes, both with

a limpid sky and with variable cloudiness (Marra and Heinemann, 1982), suggesting the action of an endogenous control in conjunction with the capability of responding to rapid fluctuations in light intensity.

Periodical oscillations have also been observed in the pigment content of different phytoplankton groups, such as dinoflagellates (Prezelin *et al.*, 1977; Prezelin and Sweeney, 1977; Latasa *et al.*, 1992), diatoms (Marra, 1978; Owens *et al.*, 1980; Marra and Heinemann, 1982; Post *et al.*, 1984), raphidophytes (Kohata and Watanabe, 1988; Latasa *et al.*, 1992) and prasinophytes (Kohata and Watanabe, 1989). Cellular chlorophyll *a* content generally displayed maxima at the end of photoperiod (Owens *et al.*, 1980; Post *et al.*, 1984), which was often interpreted as reflecting the cell division cycle (CDC), even though the persistence of cyclicity of cellular chlorophyll *a* in the stationary phase (Owens *et al.*, 1980) suggests the existence of an endogenous control of the pigment synthesis. On the other hand, not all pigments are synthesized with the same phase (Kohata and Watanabe, 1988), thus suggesting that there may be the capacity to tune the optimal amount of each pigment pool with the time of the day. This issue will be discussed in depth in the following sections.

1.3 The adaptive significance of circadian clocks in microalgae

The presence of circadian oscillators in cyanobacteria supports the hypothesis that circadian clocks are an ancient invention of evolution, even though it is not clear that the oldest cyanobacteria (traces of their ancestors are from 3.5 bilion years ago) were provided with those systems (Suzuki and Johnson, 2001).

The life tree proposed by Dunlap (Dunlap, 1999), reported in Fig. 1.2, suggests the possibility of more than one independent origin for circadian systems. This is hard to verify

in gene-sequence data because clock genes are among the most quickly evolving genes in the organism, probably because of their close interface with the environment (Dunlap, 1999). In any case, it is a shared opinion that clocks evolved several times to perform very similar functions, thus being an example of convergent evolution (Eriksson and Millar, 2003).

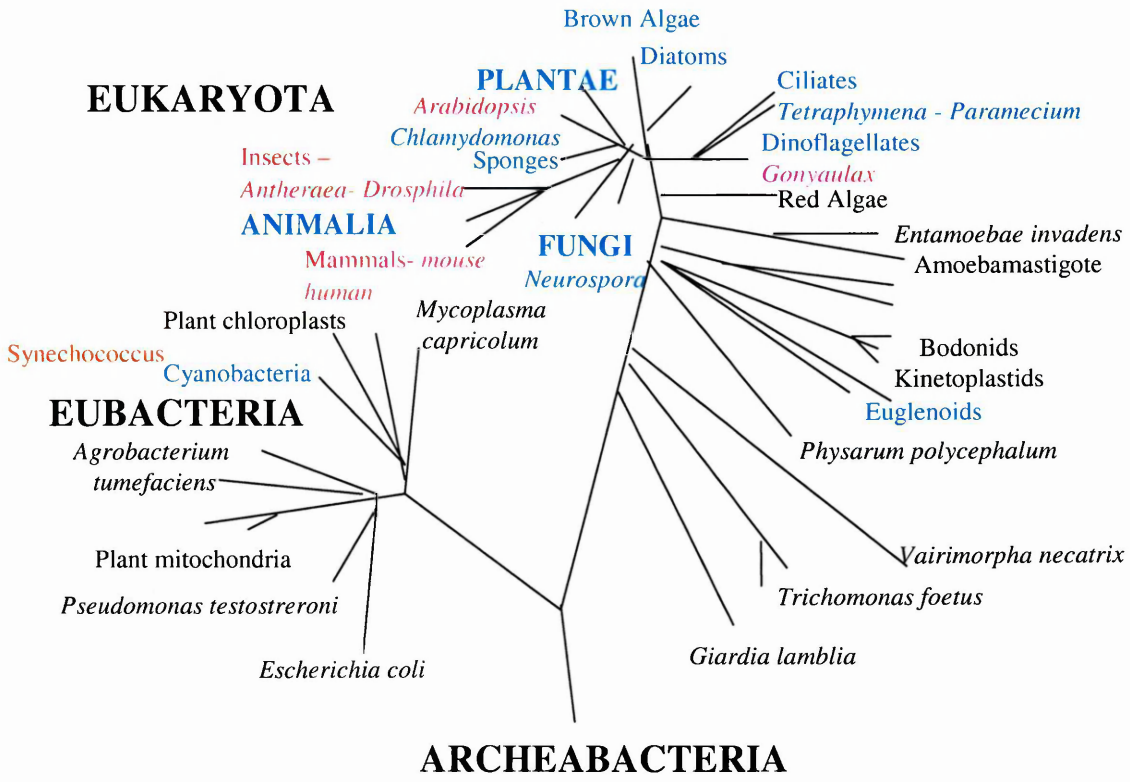

Fig. 1.2. Redrawn from Dunlap (1999), an unrooted universal phylogenetic framework reflecting a maximum-likelihood analysis for the relationships among living organisms. Line segment length corresponds to evolutionary distance. The three major assemblages of organisms, Archaebacteria, Eubacteria, and Eukaryota, diverge from a single ancestor. Shown in blue are phylogenetic groups where circadian rhythms have been described, and in red are those systems where the genetic and molecular analysis of clock mechanism has progressed significantly

The basic hypothesis on the evolutionary persistence of biological clocks is that organisms gain adaptive advantage because of these internal controls. The advantage would reside in the possibility to anticipate periodical variations of environmental variables (physical, chemical and biological) and therefore in being able to efficiently synchronize cellular activities in order to optimally utilize the resources necessary for life and/or predict the imminence of unfavorable conditions (e.g. light or food limitation, the presence of a predator) or to separate physiological activities in different parts of the day. Few studies provide clear evidence for an advantage deriving from the presence of circadian systems, however, or evidence of disadvantage as a consequence of their absence or loss.

Ouyang *et al.* (1998) tested the adaptive significance of circadian control by measuring the relative reproductive fitness of various strains of cyanobacteria (*Synechococcus sp.*) expressing different circadian periods (22h, 25h, 30h). They concluded that the fitness *per se* was improved by the resonance between the endogenous clock and the environmental cycle. In fact strains with circadian periods similar to that of the LD cycle were favored under competition in a way that indicated "the action of a soft selection".

More recently Green *et al.* (2002) analyzed the effects of the loss of circadian regulation on the fitness of *Arabidopsis* plants. They observed that mutants deprived of the circadian rhythmicity flowered later and were less viable than their wild type counterparts, thus demonstrating the adaptative significance of circadian rhythms. Finally (Beaver *et al.*, 2002) genetically tested the links between a circadian system and the reproductive fitness in *Drosophila melanogaster*. They showed that males with loss-of-function mutations in the clock genes *per, tim, cyc* and *ClkJrk* produced ~ 40% fewer progeny than wild type flies.

But why should microalgae have endogenous clocks?

In some groups of microalgae, the organization of temporal programs responds to the need to phase incompatible processes such as nitrogen fixation and oxygen evolution in some cyanobacteria, due to the inactivity of the nitrogen fixing enzyme nitrogenase in the presence of oxygen (Stal and Krumbein, 1985). Another example of temporal separation of processes is the phasing of phototaxis (daytime) and chemotaxis to ammonium (at night) in the green alga *Chlamydomonas reinhardtii* (Byrne *et al.*, 1992). In dinoflagellates, circadian systems seem to solve the need to exploit spatially separated resources, i.e. light (in the euphotic layer) and nutrients (at the base of the mixing layer). This group of algae is in fact typical of stratified column waters where they perform vertical migrations. The timing of such movements is regulated by a complex circadian system triggered by two different zeitgebers (see above for a definition), an exogenous one, light, and a "self selected" one, nitrate, whose cycling depends only on the circadian behavior of the alga, leading to a time-of-day specific exposure (Roenneberg and Merrow, 2002).

Diatoms are one of the most abundant phytoplankton groups. Their success has to be related to their capacity for handling different adaptive solutions (e.g. physiological, biochemical, behavioral) that makes them fitted to many different environments. Some studies highlight the plasticity and complexity of their photosynthetic machinery and strategies: for example, some photosynthetic diatoms are able to grow under heterotrophic conditions using glucose as carbon source (Lewin and Hellebust, 1975), others are capable of C_4 photosynthesis (Reinfelder *et al.*, 2000), and some others live in symbiosis with cyanobacteria (Villareal, 1991). Furthermore, the importance of molecular sensing of environmental signals has recently been supported by studies of calcium-dependent signal

transduction in *Phaeodactylun tricornutum* (Falciatore *et al.*, 2000). The results revealed sensing systems for detecting and responding to fluid motion, osmotic stress and nutrient limitation.

Diatoms are dominant in energetically rich environments, where the effect of turbulence, mixing, or currents may change their position by tens of meters in few hours, resulting in high variations of light conditions (both in intensity and color) that can be more drastic than those due to the diurnal cycle. In this perspective, understanding the adaptive advantages of endogenous programs for such phytoplankters is not trivial. In any case, as it has been already mentioned, day/night alternation is the only persistent feature of the light regime which every organism is exposed to over the course of a typical cell cycle. Hence it may be important and advantageous to optimize growth by means of a temporal organization that allows, for example, to temporally separate light-dependent processes from the ones that do not require light, or to anticipate the occurrence of environmental changes (favorable or unfavorable), or to match the availability of a resource with the maximal capacity to exploit it. In addition, the capability for short term responses may be based on a periodic build-up, i.e. in every moment of the day the cell may be prepared to efficiently face stressing conditions (e.g. damaging light intensities) or to efficiently exploit favorable conditions (e.g. nutrient pulses), that are more likely to occur at that precise time. Several evidences confirm this basic idea, e.g. the occurrence of cell division at night (Vaulot and Chisholm, 1987; Vaulot, 1995), and the concurrent decrease of the photosynthetic capacity (Kaftan *et al.*, 1999), that are widespread features among phytoplankton. In *Chlamydomonas* sensitivity to UV light is enhanced at dusk and dawn and decreases at midday, when the photon arrival of this damaging radiation is maximum (Nikaido and Johnson, 2000).

1.4 Questions and aims of the work

There are many reports of diel periodicity in diatoms (Palmer *et al.*, 1964; Eppley *et al.*, 1967; Chisholm *et al.*, 1980; Owens *et al.*, 1980; Post *et al.*, 1984) but the efforts were often devoted to study or describe the circadian evolution of single parameters, without relating their concurrent variations, nor discussing of their ecological relevance. Therefore, some basic questions remain open. One is about the possible interactions between the cell division cycle and other light-dependent processes, and its relationship with the light regime. As a fact, the understanding of the various daily rhythms is complicated by the phased cell division, which is a recurrent feature in marine phytoplankton (Chisholm *et al.*, 1980). Its periodicity is clearly coupled to the light-dark cycle, although its timing is highly variable within different algal groups and it may be modulated by several environmental factors (light, nutrients, temperature, pH, dissolved oxygen, etc.).

By contrast, as mentioned above, biochemical components (e.g. pigments) as well as photosynthetic parameters are often phased to the light-dark cycle, but it is poorly known whether it occurs because of the "mediation" of the cell cycle or, instead, due to a direct "dependence" on the 24h period of the illumination. In addition, the study of diel patterns of photo-dependent processes is complicated by the overlapping of short term, less regular responses (e.g. photoacclimation and photoprotection) and processes related to the diurnal cycle of illumination. Hence, another question rising is whether photoacclimation and acclimation to the photoperiod cope with each other, and whether they are driven by the same mechanisms. The answer would allow one to assess how important it is for a cell to be ready and efficient in adjusting to fluctuating light conditions, rather than to preserve the cyclicity of cellular processes, in phase with the overall natural day/night alternation.

My study was aimed at analyzing the periodicity of light-dependent processes in diatoms, in order to obtain a more integrated picture of the complex system of relationships among the biological processes mentioned above. The broad underlying question is about the ecological significance of circadian rhythms in marine phytoplankton, but more specific aims are:

- assessing cyclic patterns in the photophysiology of *Phaeodactylum tricornutum* as a model for marine phytoplankton
- assessing to what extent cell cycle and other light-dependent physiological processes are connected (/not connected)
- assessing to what extent photoacclimation and acclimation to the photoperiod are decoupled (/coupled)

Experiments under natural light (both in culture and in situ) were first conducted to understand whether and how the natural light field, with its spectral changes at twilight, is differently perceived by phytoplankton, and how important this difference is. For this reason, as a preliminary investigation, I performed a modelling study devoted to analysis of the variability of underwater irradiance on different time scales, and in its spectral content, and eventually to highlight the potential role of light as carrier of information underwater, like in terrestrial environments. The rationale and results of such a study are reported in the following chapter and more in detail in Ragni and Ribera d'Alcalà, (2004).

Most of the work was dedicated to in culture experiments on the pennate diatom *P. tricornutum*. It is the first diatom in which a persistent diel rhythm in photosynthetic capacity was reported (Palmer *et al.*, 1964). It is a species extensively studied due to the ease of growing, so that much is known about its biology (Geider *et al.*, 1985; Marsot *et al.*, 1991; Quigg and Berdall, 2003), photophysiology (Ting and Owens, 1993;Lohr and

Wilhelm, 1999, 2001; Lavaud *et al.*, 2002a, 2002b) as well as its genome properties (Falciatore and Bowler, 2002; Scala *et al.*, 2002). Moreover the recent sequencing of the genome of the diatom *T. pseudonana* (Armbrust *et al.*, 2004) will provide a new powerful tool for the characterization of the biology of diatoms.

I conducted two classes of culture experiments, under artificial and natural light regimes, aimed at either describing periodical patterns of biophysical (e.g. absorption coefficients) and biochemical (pigments) components of *P. tricotnutum cells* and their effect on the photosynthetic performance or assessing the relevance of light changes and cell cycle in driving the observed circadian variability. The experimental strategy is described in detail in the Methods section and throughout the text. An in situ experiment was carried out in order to test some of the conclusions emerging from the culture experiments on natural populations of phytoplankton.

The results of the different experiments are described in specific sections, each one followed by a short synthesis on the main outcomes. An integrated view of my results is carried out in a separate chapter that precedes the main conclusions of the work.

Chapter 2

Light signals underwater

As described in the previous chapter, circadian rhythms are generally phased by transduction mechanisms elicited by light signals, and detected by specific photoreceptors. Plants make use of both the phytochrome (*phy*) and cryptochrome (*cry*) families of photoreceptors in gathering information from the light environment for setting the clock (Delvin and Kay, 2000). Less is known about algae, even though there is evidence for the involvement and coaction of two photoreceptors, a red and a blue one, in the light transduction pathway of the circadian oscillators of red algae (Granbon and Pedersen, 2001; Luning, 2001) and dinoflagellates (Roenneberg, 1996).

Phytochromes of higher plants allow the detection of variations in the R:FR ratio, which represents a signal either for the starting and ending of the photoperiod or for the shading under canopies (Smith, 2000). However, the presence of this family of photoreceptors in the earliest marine organisms, such as cyanobacteria (Lamparter *et al.*, 1997) and purple bacteria, supports the hypothesis of a marine origin of phytochrome. Plant chryptochromes specifically mediate responses to blue light, and green and blue photoreceptors are known to be implied in processes such as phototaxis in flagellate algae (Hader and Lebert, 1998; Sineshchekov and Govorunova, 2001) and chloroplast migration in diatoms and green algae (Kraml and Herrmann, 1991; Furukawa *et al.*, 1998).

From these observations it is possible to expect that band ratios (e.g. red: far red (R:FR), blue: red (B:R), green: red (G:R)) may act in algae, as in higher plants, as complex

switches controlling relevant processes, such as synthesis or destruction of pigments (Lopez-Figueroa, 1992), migration (Lopez-Figueroa, 1998), and photoadaptation and phototaxis, whether or not mediated by the action of a clock.

By contrast, some other authors (Hughes *et al.*, 1984; Dring, 1988) have stated that in aquatic environments, light intensity is far more important than light quality in regulating photoacclimation and other physiological responses, because of the high degree of variability of spectral ratios with depth. In addition, given the high rate of vertical attenuation of red wavelengths in water, one could might exclude the possibility that red light would play a role below the first few meters of the water column, although inelastic scattering, namely fluorescence and *Raman* scattering, can inject light in red wavelengths at depth. Nevertheless, an overall reassessment of the informational content of the light spectrum and of the role of photoreceptors in the marine environment is still lacking.

During the last two decades a large effort has been devoted to the characterization of the bio-optical properties of the water column, both with measurements and models (Morel, 1988; Sathyendranath and Platt, 1988; Morel, 1991). The wide range of existing bio-optical models has been largely applied so far either to the quantification of photosynthesis or to the reconstruction of the spectral signatures of the ocean as a diagnostic tool for biogeochemical processes in the sea. There has been little effort, however, to estimate the variability of the underwater light field in order to predict photobiological responses and activities of marine organisms. To address this problem, I developed a semi-analytical radiative transfer model to reconstruct spectral irradiance at the sea surface and in the pelagic realm. I focused on the absorption bands of known and putative photoreceptors of algae and studied their diel and vertical variability, trying to generalize with a different approach the results and the hypotheses emerging from the

above mentioned studies. The results were used to identify specific bands and band ratios suited for photoregulative responses in marine algae, focusing on the scales of variability (temporal and spatial), as partially reported in the following and more in detail in Ragni and Ribera d'Alcalà, (2004).

2.1 Methodological approach

The main output of the model is the spectral downwelling irradiance at the ocean surface and in the ocean interior. The inputs include the geographical location, date, time, and a range of environmental parameters. Its structure is based principally on pre-existing models, as described below, but has been modified to address the potential for photoregulation responses by marine phytoplankton.

2.1.1 Parameterization of solar radiation at the sea surface

The intensity of the incident radiation at the sea-surface is a function of the solar inclination angle and of the scattering and absorption properties of the atmosphere; it is estimated from the cosine of the solar zenith angle θ, which depends on the day of the year, time of the day, and latitude of the site of interest. The spectral distribution of the solar flux at the top of the atmosphere is based on Neckel and Labs (1984) data and a spectral resolution of 1 nm is retained throughout the propagation to the sea surface and into the ocean interior.

Under clear skies, the direct (E_{dd}) and diffuse (E_{ds}) components of the global downwelling irradiance (E_d) at the sea surface are computed assuming a vertically homogeneous atmosphere. Molecular scattering (*Rayleigh* scattering) determination is based on measured atmospheric pressure; ozone, oxygen and water vapor absorption coefficients are taken from Bird and Riordan (1986); aerosol scattering computation is

based on an empirical model (Gathman, 1983). Finally Reed's formula (1977) has been included to perform simulations with different levels of cloudiness.

This parameterization however does not adequately capture the narrow time interval before sunrise and after sunset ($\theta > 90°$, the twilight), during which the upper atmosphere continues to diffuse and to reflect sunlight to the earth's surface. This twilight period has been shown to play a key role in higher plant photoregulation responses (Casal *et al.*, 1990) and in circadian rhythms among plants and animals (Roenneberg and Foster, 1997). The duration of twilight varies with latitude of the observer and declination of the sun. To reproduce the surface solar irradiance at zenith angles > 90°, I developed an empirical parameterization of the spectral irradiance at zenith angles from 80 to 96°, based on measured values of spectral downwelling irradiance $E_d(\lambda)$ at the sea-surface, taken over the twilight period. The rate of E_d decrease at dusk varies with wavelength, and a second-degree polynomial equation in time captures 99% of the observed variability. The coefficients of the polynomial are computed at each wavelength, subject to the constraint of the value and the first derivative at 80°, as computed based on a $\cos(\theta)$ dependence, and a value of $2.5 \cdot 10^{-5}$ $Wm^{-2}nm^{-1}$ at 96° for all the wavelengths which is the limit of sensitivity of the radiometer used (Noise Equivalent Irradiance). It is worth mentioning that the error in the cosine response of the radiometer for $60° < \theta < 85°$ is below 10% and that for $\theta > 90°$ only the diffuse component of downwelling radiation is present. The numerical procedure is applicable to all sites, once the atmospheric properties have been parameterized.

2.1.2 Parameterization of underwater attenuation

The fraction of irradiance transmitted through the sea surface, $E_d(0^-)$ is calculated taking into account reflection, refraction and sea surface roughness (Gregg and Carder,

1990). The global (direct, E_{dd}, plus diffuse, E_{ds}) downwelling irradiance, E_d, at a given depth z is derived through the following relationship (Sathyendranath *et al.*, 1988):

$$E_d(\lambda, z) = E_{dd}(\lambda, z') \cdot e^{-K_{dd}(\lambda,z)(z-z')} + E_{ds}(\lambda, z') \cdot e^{-K_{ds}(\lambda,z)(z-z')} \qquad \textit{Eq. 2.1}$$

where z' is a depth where E_{dd}, and E_{ds} are known, and $K_{dd}(\lambda, z)$ and $K_{ds}(\lambda, z)$ are the spectral diffuse (or vertical) downward attenuation coefficients for the direct and the diffuse components of the global downwelling irradiance, respectively. When it is needed scalar downwelling irradiance, E_{0d}, is derived as follows:

$$E_{0d}(z, \lambda) = \frac{E_d(z, \lambda)}{\overline{\mu}_d(z, \lambda)} \qquad \textit{Eq. 2.2}$$

where μ_d is the downwelling average cosine, estimated according to the approximation of Gordon, (1989).

The values for the K coefficients derive from an estimate, at one meter resolution, of the main processes responsible for the attenuation of light in the marine environment: absorption by seawater, phytoplankton, detritus and yellow substance (the colored dissolved matter, CDOM), backscattering by seawater and particulate matter.

In the version used for the simulations reported in the following sections, the spectral absorption and backscattering coefficients are computed according to bio-optical models used for *case I waters*, where the variability in optical properties is largely due to variability of phytoplankton. Therefore the optical properties of the dissolved and particulate matter are parameterized as a function of the concentration of chlorophyll *a*. In particular, the total spectral absorption coefficient, $a(\lambda)$, is derived as proposed by Morel (1991).

$$a(\lambda) = \left[a_w(\lambda) + 0.06 \cdot a_c'(\lambda) \cdot C^{0.65}\right] \cdot \left[1 + 0.2 \cdot e^{-0.014 \cdot (\lambda - \lambda_0)}\right] \qquad \textit{Eq. 2.3}$$

where $a_w(\lambda)$ is the absorption coefficient of pure water, $a_c'(\lambda)$ is a non dimensional statistically derived chlorophyll *a* specific absorption coefficient (normalized by the maximum), 0.06 the value given to the maximal optical cross section of chlorophyll *a* ($a^*_{chl}{}^{max}$), C the chlorophyll *a* concentration. Note that the product of $a^*_{chl}{}^{max}$ by $a_c'(\lambda)$ is the optical cross section of chlorophyll *a*, $a^*_{chl}(\lambda)$, in $m^2(mg\ Chl a)^{-1}$. The last term in brackets accounts for the contribution of the colored dissolved organic matter (CDOM). For the total backscattering coefficient, $b_b(\lambda)$, the bio-optical model utilized follows (Morel, 1988):

$$b_b(\lambda) = \frac{1}{2} b_w(\lambda) + \left[0.002 + 0.02 \cdot \left(\frac{1}{2} - \frac{1}{4}\log C\right) \cdot \left(\frac{550}{\lambda}\right)\right] \cdot \left[0.30 \cdot C^{0.62} - b_w(550)\right] \qquad \textit{Eq. 2.4}$$

with b_w being the total scattering coefficient of pure water.

The optical properties of sea-water are based on tabulated values (Smith and Baker, 1981; Haltrin and Kattawar, 1991; Pope and Fry, 1997). Finally, inelastic or transpectral processes taken into account are *Raman* scattering and chlorophyll *a* fluorescence; they are of particular interest in the orange-red-far red (λ>600 nm), less energetic, part of the spectrum, where solar direct light is rapidly absorbed by water ($K_d \approx 0.2\text{-}2\ m^{-1}$). The relationships used to compute the downward *Raman* irradiance (Marshall and Smith, 1990; Haltrin and Kattawar, 1993) assume an isotropic distribution function for *Raman* scattering. The irradiance produced by chlorophyll *a* fluorescence has the shape of a Gaussian curve and peaks around 685 nm. This radiant flux is quantified as a function of chlorophyll *a* concentration, its specific absorption coefficient, $a^*_{chl}(\lambda)$, and the value of the quantum

yield of fluorescence Φ_f. This diffuse light field is isotropic and its contribution to the plane downwelling irradiance, E_{fd}, is quantified according to the following expression, which is a slight modification (E_{0d} in place of E_0) of Eq. 8 in Maritorena *et al.* (2000):

$$E_{fd}(z) = \frac{\Phi_f}{4} \cdot \frac{C \int_{400}^{700} E_{0d}(z,\lambda) a^*_{chl}(z,\lambda) d\lambda}{(k - K_d)} \qquad \textit{Eq. 2.5}$$

where k represents an attenuation coefficient for the irradiance generated by fluorescence and propagating upward. The assumption is that the error in replacing the scalar irradiance E_0 with only its downwelling component E_{0d}, is less than 20% (Mobley, 1994, section. 1.5).

2.2 Results

2.2.1 Model validation

The validation of the in-water model was performed using data measured in open waters (*case I*) of the Eastern Mediterranean Sea. Pigment profiles and measured surface E_d were used as input for simulations, and measured downwelling irradiance profiles as validation points. Discrete samples and fluorometric downcasts were coupled to compute the vertical distribution of chlorophyll concentration with the resolution of one meter. Irradiance profiles were acquired using a 13 channel (400, 412, 443, 470, 490, 510, 531, 555, 590, 619, 665, 685, 700 nm) spectral radiometer (Satlantic Inc., SeaWiFS Profiling Multispectral Radiometer) following standard SeaWiFS protocols (Mueller and Austin, 1995). As reported in Fig. 2.1, modeled profiles show good agreement with in-situ data in most of the bands. The highest errors are displayed in the near-uv blue region (412, 443 nm), where the mean percent error is about 10% in the first 20 meters and ranges between 50 and 70% in the 20-100 m layer. This discrepancy may derive from an inadequate

parameterization either of the absorption due to dissolved matter (i.e. CDOM) or of the backscattering of particulates in Mediterranean waters. Therefore I reduced the observed difference by modifying the parameterization of the absorption of CDOM (a_{CDOM}).

It is generally accepted that a_{CDOM} follows with the wavelength a roughly exponential law, according to the following expression:

$$a_{CDOM}(\lambda) = a_{CDOM}(\lambda_0) \cdot e^{-S(\lambda-\lambda_0)} \qquad \textit{Eq. 2.6}$$

where S is the slope of the semi-logarithmic expression, and depends on the light reactivity of the chromophores of the different types of DOM. As shown in the *Eq.2.3*, in the general version of our model S has the constant value of 0.014 nm^{-1}, following (Bricaud *et al.*, 1981).

Recent studies (Ferrari, 2000) reported higher values (up to 0.028 nm^{-1}) in the Mediterranean Sea. I found that ~ 0.05 nm^{-1} reproduces our *in situ* data (see Fig. 2.1) which is rather high, but close to the upper limit of the range reported for other open ocean sites (Højerslev and Aas, 2001). Moreover, absorption spectra acquired in several sites of the Mediterranean Sea (WetLab attenuation-absorption meter AC9), seem to confirm what I numerically found, since they in fact exhibit sharp peaks at 412 nm (data not shown), in spite of what is commonly assumed in *case I* waters, where phytoplankton are responsible for the highest peak of absorption at 430-440 nm.

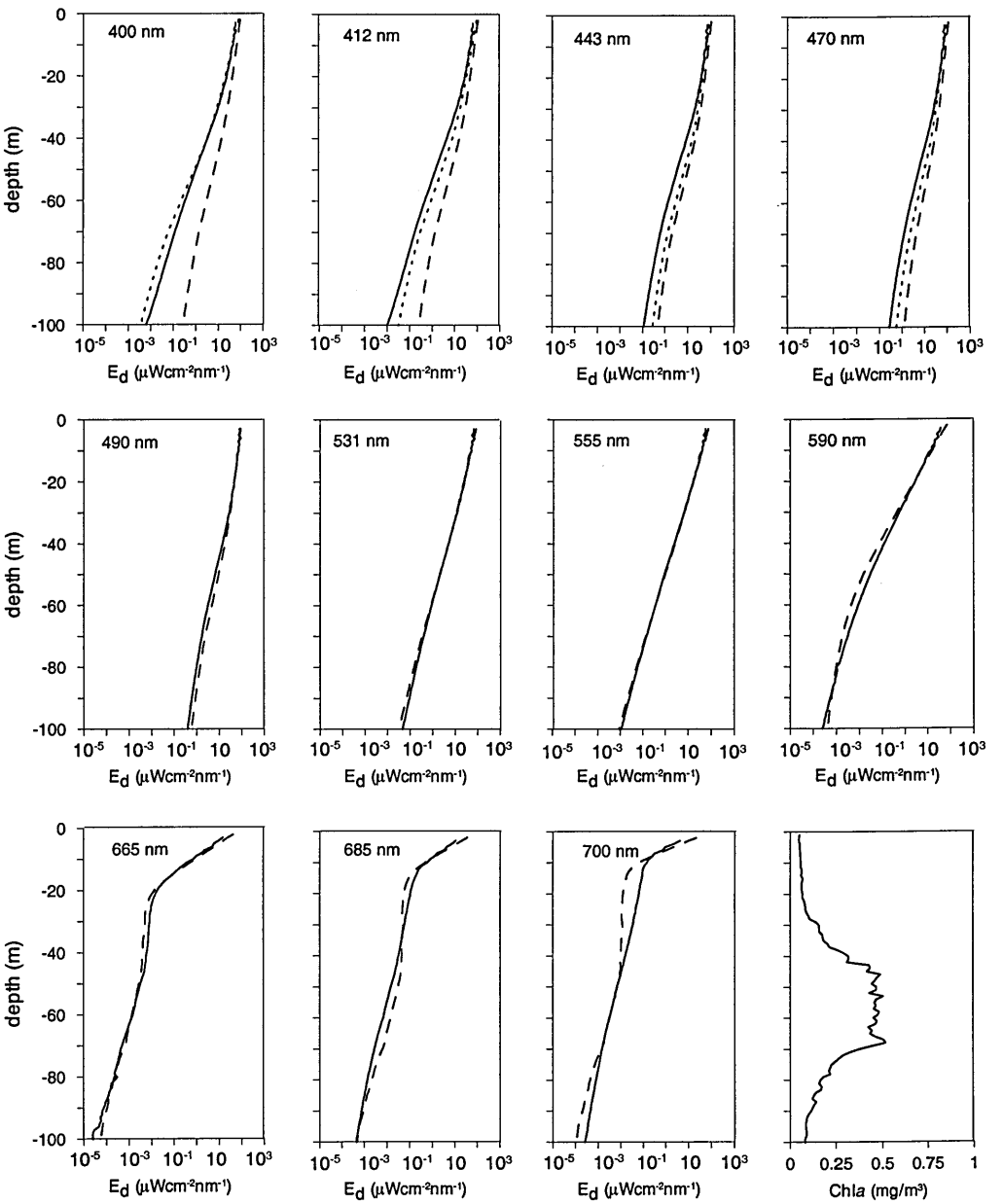

Fig. 2.1. Vertical profiles of measured (solid line) and modelled (dashed and dotted lines) downwelling irradiance at 11 selected wavelengths in a site of the Eastern Mediterranean Sea. Dashed line refers to the general version of the model, dotted line to the version modified for the Mediterranean Sea. The chlorophyll profile (last panel) has been acquired in the same site and used as input for the simulations.

2.2.2 Diel and depth variability of band ratios

I quantified the irradiance integrated over selected wave-bands of the visible spectrum, in particular: blue (B, 400-450 nm), green (G, 500-550), red (R, 630-680), and far-red (FR, 700-750) and analyzed the diurnal and vertical variability of the band ratios R:FR, B:R, G:R. In Fig. 2.2 I report the results of simulations performed at the surface level and at selected depths of the water column. At the sea-surface all the analyzed band ratios display the highest variability at twilight. In particular, R:FR (Fig. 2.2a) shows a steep increase before dawn followed by a slighter decrease, a rather constant value during the central part of the day, and a symmetric behaviour around dusk. The vertical distribution of the band ratios depends on the optical properties of water and its constituents (suspended and dissolved matter). In water R:FR shows a high degree of diel variability. Its value increases with depth, due to the stronger diffuse attenuation coefficient (K_d) of FR vs R. Nevertheless this variability is observed only in the upper 10-15 meters. Below this level, solar incoming irradiance in the 650-750 band is completely lost by water attenuation, and the only red and far red photons present are produced by transpectral processes, i.e. *Raman* scattering and chlorophyll *a* fluorescence. In addition R:FR ratio is rather insensitive to the chlorophyll concentration, as shown in Fig. 2.3a.

Because of the high difference in the attenuation coefficient of B and G vs R light, B:R and G:R ratios reach values up to several thousands as depth increases to 40-50 meters (Fig. 2.2 b, 2.2 c). They also display drastic changes on the diel scale, especially at dawn and dusk, observable even at depth.

Finally, both ratios are affected by the vertical shape of the chlorophyll profile, exhibiting an evident minimum in correspondence of the chlorophyll maximum (Fig. 2.3b-2.3c); moreover B:R significantly varies along with changes in the concentration of chlorophyll *a*.

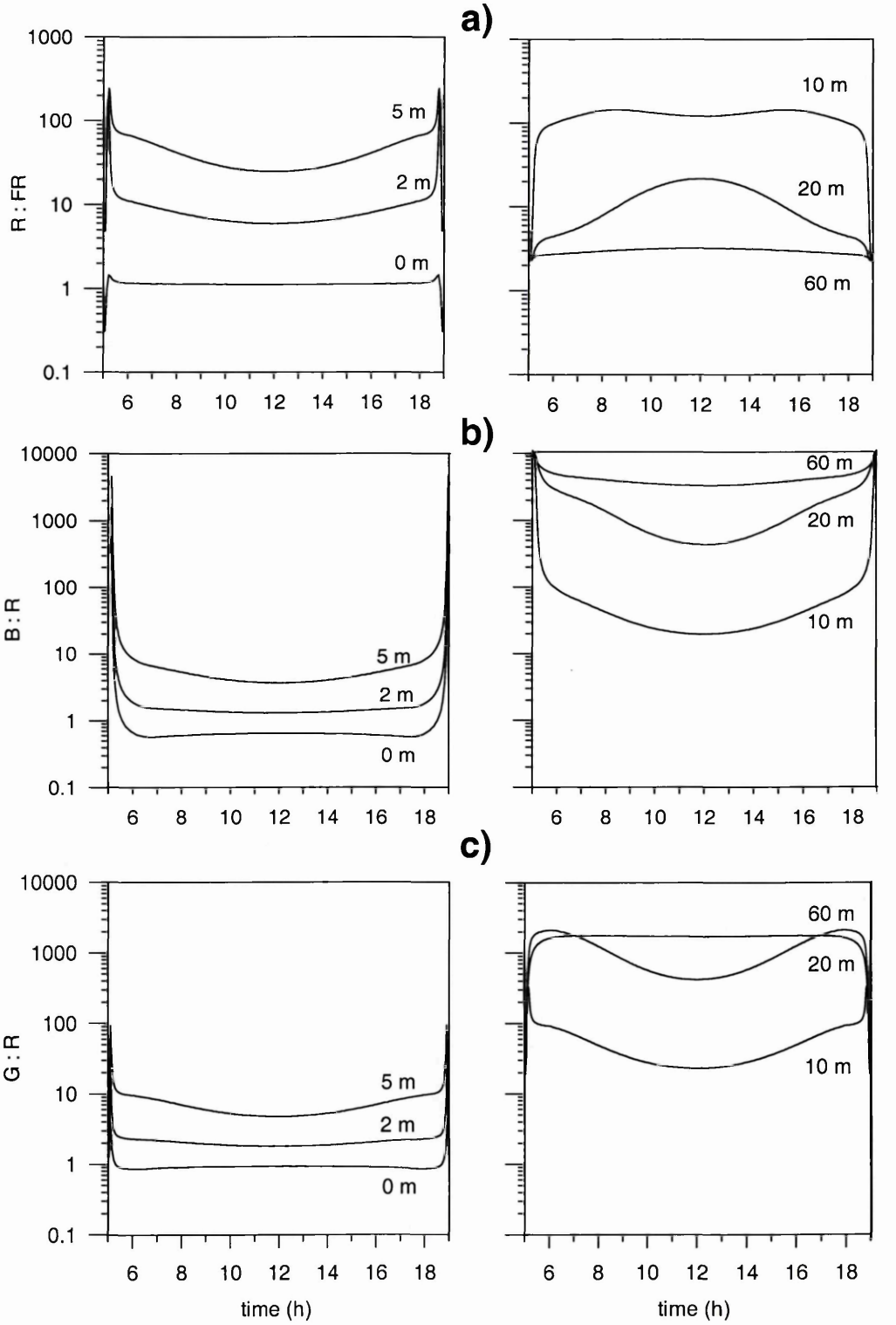

Fig. 2.2 Band ratio variation with time of the day at selected depths of the water column (note the different scales on y axis). Chlorophyll concentration as in Fig.1. Irradiance has been integrated over 50 nm per each indicated band. a) R : FR (630-680: 700-750. b) B : R (400-450: 630-680). c) G : R (500-550: 630-680).

2.2.3 The impact of chlorophyll fluorescence

In Fig. 2.3d, R and FR irradiance are reported in relation to chlorophyll *a* concentration. Simulations were performed using modeled pigment profiles with a Gaussian shape, a deep chlorophyll maximum (DCM) located at 50 meters with concentrations ranging from 0.3 to 12 mg/m^3, constant values for optical cross section of chlorophyll *a* ($a^*_{chl}{}^{max}$ = 0.06 m^2/mgChl*a*), fluorescence quantum yield (Φ_f = 0.02) and solar zenith angle (15°). The resulting R + FR photon irradiance (integrated over the interval 650-750 nm) incident at the depth of the DCM varies from $1.98 \cdot 10^{-2}$ to $2.73 \cdot 10^{-3}$ μmolquanta·m^{-2}s^{-1} and from $2.39 \cdot 10^{-3}$ to $1.31 \cdot 10^{-6}$ μmolquanta·m^{-2}s^{-1} at 100 m, depending on the total amount of chlorophyll. Indeed R-FR irradiance decreases as pigment content increases, since the absorption of B-G light due to more abundant phytoplankton in fact reduces the available excitation energy.

Other simulations were devoted to test the influence of the variability of physiological parameters such as a^*_{chl} and Φ_f on the fluorescence emission (results reported and commented in Ragni and Ribera d'Alcalà, (2004), their Fig. 4). Finally, red fluorescence generated by a single phytoplankton cell was estimated and compared with the background irradiance in the same band (Fig. 2.4). The light emitted by a cell having a chlorophyll *a* content of 1 pg ranges from $3.6 \cdot 10^9$ and $5.7 \cdot 10^{10}$ photons·m^{-2}·s^{-1} when locally incident PAR varies from $4.1 \cdot 10^{18}$ to $4.9 \cdot 10^{19}$. The rate of arrival of red photons on a neighbour cell is a function of the distance between the "source" and the "target" and its size. It ranges from 20% to 0.25% of the emitted flux, as the distance between the two cells varies from 10 to 100 μm. Therefore, in proximity of the DCM, the flux perceivable by one cell due to the emission of another one 100 μm distant is 1-3 orders of magnitude greater

than the background red light field, depending on the chlorophyll *a* concentration in the water column (Fig. 2.4).

Obviously higher or lower cellular pigment content makes the signal from the cell increase or decrease accordingly.

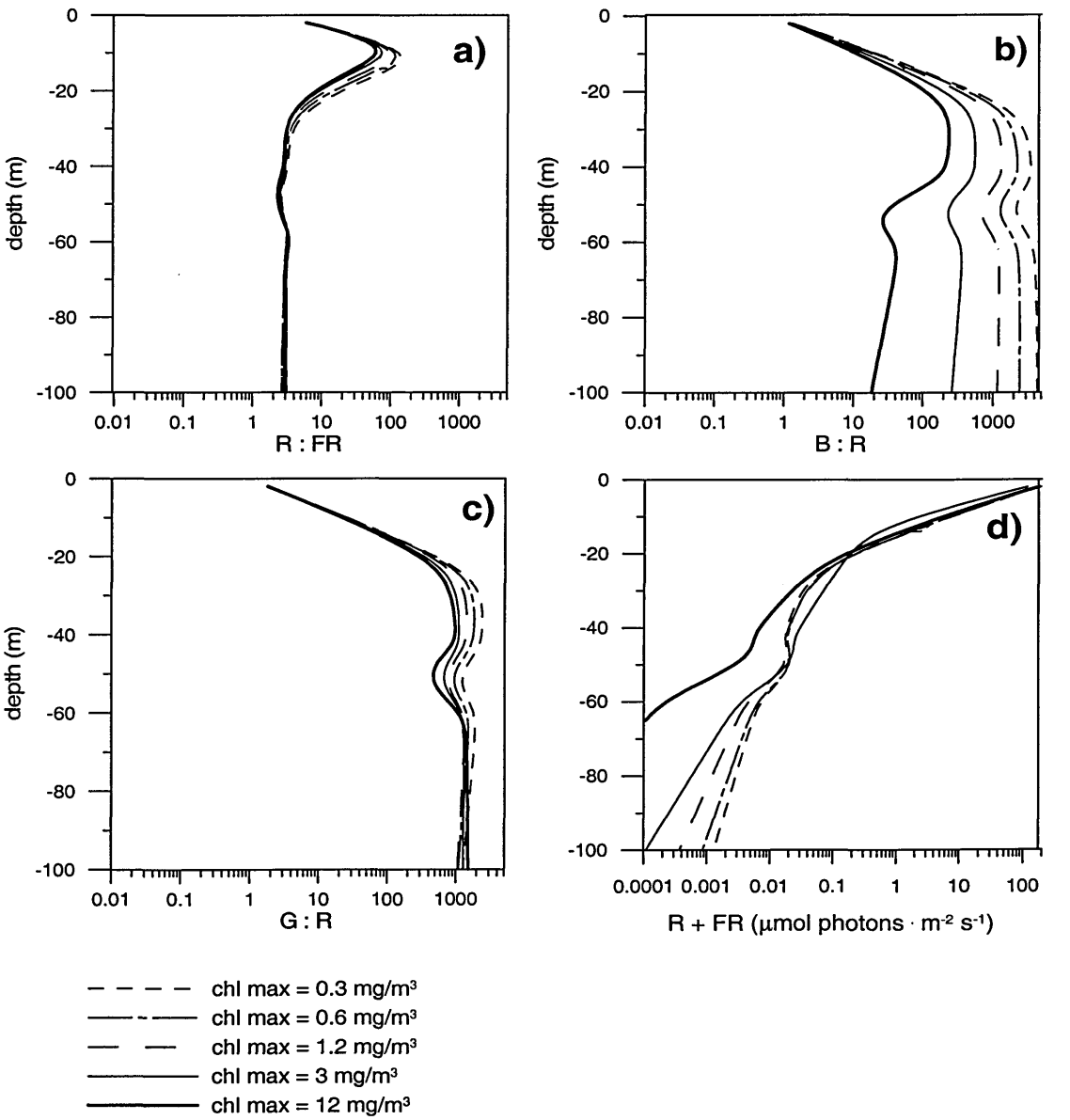

Fig. 2.3 Vertical profiles of spectral bands at different levels of chlorophyll *a* concentration (chlorophyll maximum at 50 m). a) R : FR ratio (630-680: 700-750). b) B : R ratio (400-450: 630-680). c) G : R ratio (500-550: 630-680). c) R + FR (630-680 + 700-750).

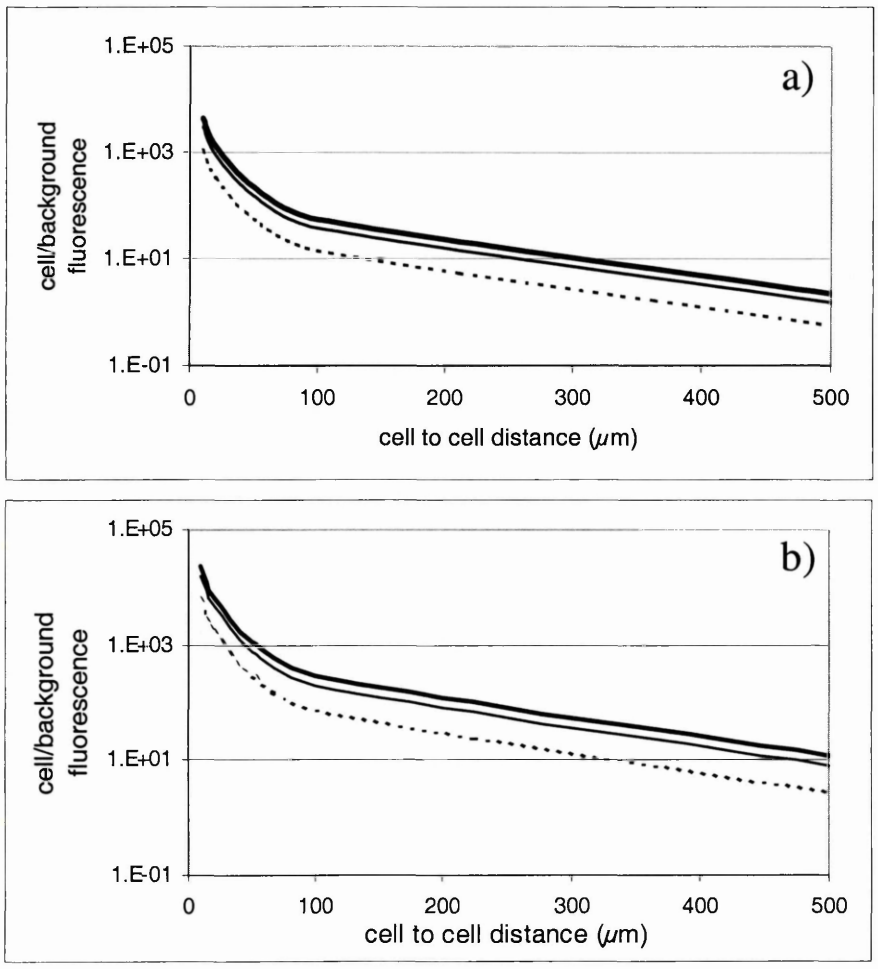

Fig. 2.4. Ratio of cell to background fluorescence (660-710 nm) as a function of the distance between two cells and of the cellular chlorophyll *a* content. Cellular chlorophyll *a* content: (thick line) 9 pg/cell; (thin line) 5 pg/cell; (dotted line) 1 pg/cell. Simulations were performed with $a^*_{chl}{}^{max} = 0.06$ m^2/mg(Chl*a*) and $\Phi_f = 0.02$. Estimates and below reported parameters refer to the depth of the DCM (50 m). a) background chlorophyll *a* concentration = 0.4 mg/m^3; PAR irradiance = $4.9 \cdot 10^{19}$ photons/m^{2}s. b) background chlorophyll *a* concentration = 4 mg/m^3, PAR irradiance = $4.1 \cdot 10^{18}$ photons/m^2·s

2.3 Discussion

The purpose of the study presented in this chapter and entirely reported in Ragni and Ribera d'Alcalà, (2004) was to single out spectral bands and ratios that may contain information on the characteristics of the local environment of marine autotrophs and to

formulate testable hypotheses on their ecological significance. Its link with the present study was to inquire whether and which bands and/or band ratios could act as *zeitgeibers* for circadian regulations in marine phytoplankton.

The diel pattern of R:FR resulting from the simulations matched quite well what already has been reported in the literature (Chambers and Spence, 1984; Lopez-Figueroa, 1992) on the basis of *in situ* measurements and confirmed that R:FR shifts underwater are greater than those displayed above the surface, and theoretically large enough to provide photoperiodic information. Nevertheless, this variability holds only in the upper 10-15 meters. Moreover, fluctuations in meteorological conditions such as sun glitter, clouds, sea roughness, etc. will change the dependence of band ratios on solar angle.

The modeled downwelling irradiance profiles reproduced the measured radiometric data obtained at depth in Mediterranean Sea and by Maritorena *et al.* (2000) and showed that the R and FR light intensities covary below 15-20 m and tend to be very low. The classical phytochrome-mediated responses have been denoted VLFR (Very Low Fluence Response), LFR, (Low Fluence Response) and HIR (High Irradiance Response) depending on the fluence requirements, in terms of the number of photons received and not of the rate of reception; considering that VLFRs require photon fluence between 100 pmol/m^2 and 100 nmol/m^2 (Mancinelli, 1994) one can say that in oligotrophic waters such responses are still possible within the whole euphotic zone, if integrated fluxes over 10 minutes are considered.

It is clear that there are two different regimes in the R:FR band underwater, the first which resembles the terrestrial one with a ratio which varies at dawn and dusk, the second with a constant ratio and weak intensities.

A detailed analysis of the possible hypotheses on the ecological and adaptive role of weak R:FR signals for marine phytoplankton is reported in Ragni and Ribera (2004). As for the scope of the present study a few comments are worth to be made. The R:FR reversal which occurs only at shallow depths cannot be the ubiquitous signal for the start and the end of the photoperiod. On the other hand, the persistence of the R-FR band even at depth, due to the ubiquitous transpectral processes, does not preclude the role of a red photoreceptor as a putative sensor for the start of the light phase of the day. Conveying more complex information, e.g. depth, requires that other bands are involved and used for comparison, i.e., additional photoreceptors. It is intriguing that the R:FR shift is active only when the spectrum is rich in red and far red, i.e., in the very upper layer of the ocean. This layer is the one where the diel variation of irradiance generates significant peak intensities, in the range where photoprotection is necessary for preventing or mitigating light damage. On the other hand, the R:FR trigger, if any, would become inactive below a certain depth, where even at midday the light is below the threshold at which it becomes harmful. Therefore, in parallel with the two R:FR regimes highlighted above in the surface vs the subsurface layer there are two different needs for phytoplankton, with only one (the shallow water) requiring very active photoprotection. I will return to this issue in the next chapters.

Chapter 3

Experimental approaches and protocols

I performed several experiments on cultured suspensions of the diatom *Phaeodactylum tricornutum* (hereafter PT), either in artificial light regime or in natural sun light. During "long" experiments, an extensive set of parameters was measured both over light/dark (LD) cycles and free-running conditions (continuous light (LL) or continuous dark (DD)). On the other hand, "short" experiments where conducted over 12-40 hours to address more specific questions, often rising from the results of the "long" experiments. The suite of investigated parameters was in general reduced, and the sampling frequency varied in consideration of the studied processes (e.g., responses to light shifts). The experimental activity was organized according to the scheme reported below, where arrows and colors evidence sequential-logical interrelations among experiments. The first two experiments (INTRO and PHYSIO) were devoted to give a general picture of the circadian variability of an extensive set of parameters related to the physiology of PT in artificial light. Measurements were conducted both over LD and sequential LL cycles for 4-5 days. The results obtained in artificial light were successively tested under natural light (experiments SPRING and URA) in order to detect analogies and differences between circadian patterns entrained by so different light regimes, i.e. square wave versus quasi-sinusoidal time distribution of irradiance with a significant difference in spectral composition. Given the unfeasibility of realizing continuous light conditions under natural

SCHEME OF THE EXPERIMENTAL ACTIVITY

light at our latitudes, the free running regime was set as continuous dark in natural light experiments (NLE).

Subsequently, specific questions arising from these extensive experiments were tested in short experiments aimed at better clarifying particular aspects, such as the role of the cell cycle, the importance of the duration of photoperiod, the difference between responses to day-night transitions and to unexpected light shifts.

Finally a short *in situ* study (experiment TRICICLO) was conducted with the aim of verifying in the field the results emerging from culture studies and extending to natural phytoplankton populations some of the conclusions of the studies on *P. tricornutum.*

A more detailed description of the rationale of the experiments will be carried out in the following chapters.

3.1 The species object of investigation: Phaeodactylum tricornutum

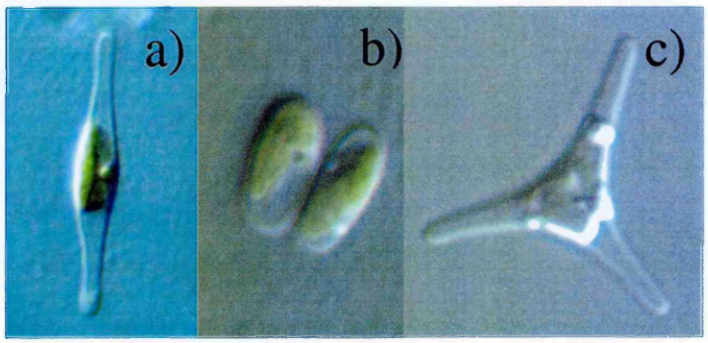

Fig. 3.1. The three morphotypes of *Phaeodactylum tricornutum*: fusiform (a), oval (b), triradiate (c)

P. tricornutum is a rather atypical diatom in that it is polymorphic. It exists as three different morphotypes: oval, fusiform, and triradiate (Borowitzka and Volcani, 1978), shown in Fig. 3.1). Only the oval form has a single silica valve typical of most diatoms, which also confers the capability of slow locomotion (Iwasa and Shimizu, 1972), whereas the valves of the other two consist entirely of organic material. The fusiform morphotype has been reported to have siliceous bands in

the girdle region of the wall, even though the amount of silicon for oval and fusiform cells is similar. All three morphotypes occur in nature but in the conditions used for the experiments reported in this work the fusiform morphotype represented about the 98% of the total, the remaining 2% being the triradiate morphotype. The oval form is usually observed in senescent cultures. It is thought to be dominant in stressing conditions, such as nutrient depletion (De Martino, A., Departement de Biologie, Ecole Normale Superiore, Paris, personal communication). Despite such morphological differences, the organization and structure of the cytoplasmic organelles is similar in all three morphotypes, except for the presence of vacuoles occupying the "arms" of the fusiform and triradiate cells (Borowitzka and Volcani, 1978).

3.2 Experimental strategies

3.2.1 Culture conditions

The CCMP 632 Bohlin clone of the pennate diatom *Phaeodactylum tricornutum* was provided by the Provasoli-Guillard National Center for Culture of Marine Phytoplankton. Cultures were grown axenically in 0.22 μm-filtered seawater, enriched with f/2 Guillard nutrients. The sterility was checked by means of bacterial contamination tests performed some days before the experiments. Cells were generally pre-adapted to experimental conditions for two weeks (i.e. light, nutrient and temperature). The experimental settings changed according to the needs of each experiment. Therefore in the next sections I summarize the aims, the investigated parameters and the experimental settings of each experiment presented in the scheme of pag 32 and discussed in this work. The technical procedures common to all the experiments will be described in detail in section 3.3.

3.2.2 Experiments in artificial light regime

Artificial light experiments (hereafter ALE) were carried out on PT cells grown in controlled culture chambers. Irradiance was provided by fluorescing lamps in "square wave" mode. Temperature was set at 19°C. Cultures were aerated by air-enriched bubbling.

3.2.2.1 "Long" experiments

Exp. "INTRO"

Aim: First characterization of the circadian patterns of a large set of parameters under light-dark alternation and free running conditions. Assessment of the interplay among the different components of the photosynthetic machinery and the coupling with cell cycle

Light regime and experiment duration: two 12:12 LD cycles followed by three 24 LL cycles. Growth irradiance: 150 μmolquanta $m^{-2}s^{-1}$

Sampling frequency: 3 hours

Culture modality: turbidostat-like (after each sampling point fresh medium was added by means of a peristaltic pump. The dilution rate was set according to estimations of average hourly growth rates from growth curves performed prior to the experiment)

Measured parameters: cell concentrations, flow-cytometric parameters, cell cycle stages, pigment concentrations (triplicate samples), absorption spectra on suspensions, PvsE coefficients, FRRF coefficients

Technical notes: Because of the need of large-volume cultures (ca 12 l) a system allowing continuous mixing of the cells was assembled. It consists of a motor which makes the culture tank slowly oscillate, avoiding the sinking and the accumulation of the diatoms at the bottom

Exp. "PHYSIO"

Aim: To confirm the results of the "INTRO" experiment and to investigate more deeply the diel variability of fluorescence-derived parameters by coupling FRRF and Phyto-Pam measurements

Light regime and experiment duration: one 12:12 LD cycle followed by three 24 LL cycles. Growth irradiance: 200 μmolquanta $m^{-2}s^{-1}$

Sampling frequency: 3 hours

Culture modality: turbidostat-like

Measured parameters: cell concentrations, flow-cytometric parameters, pigment concentrations, absorption spectra on filters, FRRF coefficients, Phyto-Pam coefficients

3.2.2.2 "Short" Experiments

Exp. "CICLAC"

Aim: Characterization of the effect of light intensity (either as growth irradiance or as light stress) on the diel patterns of pigment pools and photosynthetic parameters. Changes observed in the D→L transition were compared to those occurring due to light shift from growth irradiance to higher irradiance

Experiment duration: 12 hours

Growth light regime: 12:12 LD cycle - 40 and 200 μmolquanta m^{-2} s^{-1}

Light stress intensity and duration: 400 μmolquanta $m^{-2}s^{-1}$ – 5 hours

Sampling strategy: samples were taken 1 hour before and 1 hour after the DL transition; 1 hour before and 1 hour after the light shift and 5 hours after the light shift (still in high light). Part of the culture was left under the original growth irradiance; concurrent samples from them were taken as controls.

Culture modality during the experiment: batch mode

Measured parameters: cell concentrations, flow-cytometric parameters, pigment concentrations, Phyto-PAM coefficients

EXP: "C24"

Aim: Assessing the relative importance of the photoperiod and cell division cycle in determining the diel patterns of pigments. The experiment was done on PT cells dividing more than once a day, in order to decouple the cell division cycle from the LD cycle

Light regime: 12L:12D, at 200 µmolquanta $m^{-2}s^{-1}$

Experiment duration: 25 h

Sampling frequency: 2 hours

Culture modality during the experiment: batch mode

Measured parameters: cell concentrations (triplicate samples), flow-cytometric data (triplicate samples), pigments concentration, cell cycle stages

Exp. "C36"

Aim: Assessing the relative importance of the photoperiod and cell cycle in determining the diel patterns of pigments, by varying the duration of photoperiod and decoupling the cell division cycle from the LD cycle (as in the previous case).

Strategy: One culture of cells was grown in 12:12LD and brought to16L:8D; another one was grown and studied in 16:8. Then it will be distinguished the case of cells grown under a certain photoperiod (16L:8D or 24L) from that in which a different photoperiod is imposed as "unexpected", i.e. after a different entraining LD regime.

Light regime: 16L:8D, at 200 μmolquanta $m^{-2}s^{-1}$

Experiment duration: 40 h

Sampling frequency: 3 hours

Culture modality during the experiment: batch mode

Measured parameters: cell concentrations (triplicate samples), flow-cytometric data (triplicate samples), pigments concentration, cell cycle stages

Exp. "LL24"

Aim: Verifying the persistence of any circadian periodicity in PT cells grown in 24h LL. Comparison with the patterns observed in free running LL (after adaptation to LD). Part of the culture was darkened for two hours and then exposed again to light in order to verify the importance of dark periods in phasing the photophysiological processes

Growth light regime: 24LL, at 200 μmolquanta $m^{-2}s^{-1}$

Experiment duration: 25 h

Sampling frequency: 2 hours

Culture modality during the experiment: batch mode

Measured parameters: cell concentrations, flow-cytometric data, pigments concentration, Phyto-PAM coefficients

Exp "MORPHO"

Aim: Characterization of the diel patterns of cell geometrical properties and related pigment content of the three different morphotypes of PT, in order to outline possible differences to take into account when dealing with cultures exhibiting different morphotype composition

Growth light regime: 12L:12D, at 50 μmolquanta $m^{-2}s^{-1}$ (oval cells) and 200 μmolquanta $m^{-2}s^{-1}$ (fusiform and triradiate cells)

Experiment duration: 25 h

Sampling frequency: 3 hours

Technical notes: Monoclonal cultures of each morphotype were isolated and provided by Alessandra De Martino (Departement de Biologie, Ecole Normale Superiore, Paris) and maintained for few days in our lab. The fusiform and triradiate shapes were easily maintained by using the usual dilution rates and light conditions; on the contrary the oval cells are known to be rapidly transformed in the other shapes (especially fusiform) when provided with abundant light and nutrients, therefore both the irradiance and the dilution rate used were lower than usual

3.2.3 Experiments in natural light regime

NLE (natural light experiments) on cultures (either PT or a mixed one) were performed during spring Mediterranean cruises on board the R/V Urania, where I was involved with my Lab. The natural day-night cycle was ~12:12. Solar radiation was attenuated by means of neutral screens to protect cells from photodamage. PAR was continuously recorded by means of a Biospherical PAR meter (QSL101) located inside the culture system.

The *in situ* experiment was carried out on April 2004 on board the R/V Copernaut Franca, in the Gulf of Salerno (South Tyrrenian Sea), using both *in situ* profilers and deck measurements on discrete samples of natural phytoplankton population.

3.2.3.1 "Long" experiments

Exp. "SPRING"

Aim: First characterization of the circadian patterns of a large set of parameters in PT under natural day-night alternation and free running (DD) conditions. Assessment of the interplay among the different levels of the photosynthetic machinery and understanding the role of the cell cycle. Comparison with the results of similar experiments in artificial light (EXP. INTRO and PHYSIO)

Light regime and duration: three ~12L:12 LD cycles. Midday irradiance ~350 μmolquanta $m^{-2}s^{-1}$. After one LD cycle, part of the culture was put in DD conditions for three cycles followed by one LD cycle.

Sampling frequency: 3 hours

Culture modality: turbidostat-like

Measured parameters: pigments concentration, absorption spectra on filters, Phyto-PAM coefficients

Exp "URA"

Aim: Characterization of the circadian patterns of a large set of parameters in a mixed phytoplankton culture dominated by PT and *Pyramimonas* sp. (Prasinophyceae) under natural day-night alternation. Assessment of the interplay among the different levels of the photosynthetic machinery. Comparison with the results of similar experiments in artificial light (EXP INTRO and PHYSIO)

Light regime and duration: four cycles ~12:12LD. Midday irradiance ~ 600 μmolquanta m^{-2} s^{-1}

Sampling frequency: 2 hours

Culture modality: turbidostat-like

Measured parameters: pigment concentrations, absorption spectra on filters, FRRF coefficients

3.2.3.2 In situ experiment

EXP "TRICICLO"

Aim: Characterization of circadian patterns of pigment concentrations and photosynthetic parameters in the natural environment. Outlining analogies and differences with the patterns observed in culture, with respect to both diel periodicity and light intensity dependence (vertical distribution).

Duration of the experiment: 25 hours

Sampling strategy: water samples were taken from two depths: 5 and 45 meters, corresponding to 35% and 1% of the incident PAR.

Sampling frequency: 2 hours from 9AM of April 22th to 9AM of the 23th.

Light regime: ~13:11 LD - 0-600 μmolquantam^{-2}s^{-1} at 5m; 0-15 μmolquantam^{-2}s^{-1} at 45m

Measured parameters on discrete samples: pigment concentrations, absorption spectra on filters, Phyto-PAM coefficients, PvsE coefficients (on 4 points), absorption spectra and pigment concentrations on size fractions (on 4 points)

Vertical profiles: CTD, AC9, FRRF, spectral irradiance (on 4 sampling points), surface irradiance

3.3 Analytical procedures (on samples)

3.3.1 Flow cytometry (FCM)

Flow cytometric determinations of cell concentrations, red fluorescence (RED), Forward Angular Light Scattering (FALS) and Right Angular Light Scattering (RALS) were performed using a FACScalibur flow-cytometer (Becton-Dickinson, USA). 1 ml of each sample was fixed in gluteraldehyde (1% final concentration) for 10 minutes, frozen in liquid nitrogen and analysed within few days from the experiment. Fluorescent beads (Coulter, USA) were added to each samples and used as internal standard. Thus, the values of RED, FALS and RALS of a sample are quantified in respect to the properties of the beads and are given in relative units.

3.3.2 Cell cycle studies

The percentage of cells in the different phases of the cell cycle were determined using the flow cytometer FACScalibur, after staining of the DNA. 10 ml of sample (0.5-1 · 10^6 cells) were centrifuged at 3800 rpm for 15 minutes. The supernatant was removed, the pellet suspended in 5 ml of methanol and the sample stored at 4°C until the analysis. This treatment served to remove chlorophyll, whose fluorescence would interfere with that of the stain. Before the flow-cytometric analysis, samples were centrifuged at 3800 rpm for 15 minutes, the pellet washed with 1 ml of 1% phosphate buffered saline (PBS), and the pellet resuspended again in 1 ml of 1% PBS. One µl of RNase and 4 µl of SYTOX Green (final concentration 20 μM) were added to each sample, and the samples incubated at room temperature for 2 hours. The percentage of cells in each of the cell cycle stages was calculated using the software ModFit v2 (Verity, USA).

3.3.3 Pigments determination (HPLC)

Pigment concentrations were determined with the High Performance Liquid Chromatography (HPLC) technique. 10-30 ml aliquots of algal suspensions were filtered on 25 mm glass-fibre filters. In the case of natural phytoplankton samples (Exp. TRICICLO), 1.5-3 liters samples were filtered on 47 mm GF/F. Filters were immediately stored in liquid nitrogen and extracted in methanol just prior to the analysis. HPLC analyses were performed on a Hewlett Packard HPLC 1100 Series instrument, with spectrophotometric and fluorometric detectors, and a reverse phase C8 column. The procedure for identification and quantification of pigments is described in Vidussi *et al.* (1996).

3.3.4 Absorption measurements

The spectral absorption coefficients, a(λ), were measured either on cell suspensions in 1 cm path-length quartz cuvettes or on filtered material (in GF/F filters), with a double beam HP 8453 spectrophotometer equipped with a Labsphere integrating sphere. Medium from the culture (0.22 μm-filtered) was used as reference. A scattering correction independent from wavelength was applied to all the spectra to reflect the assumption that phytoplankton do not absorb at 750 nm. Discrimination of the absorption due to phytoplankton pigments from the total (pigments + cells and detritus) was determined using the oxidant action of sodium hypochlorite on pigments (Ferrari and Tassan, 1999). The optimal amount of NaClO to add for complete removal of pigment absorption was set after performing several tests on differently concentrated cultures. Light absorption due to

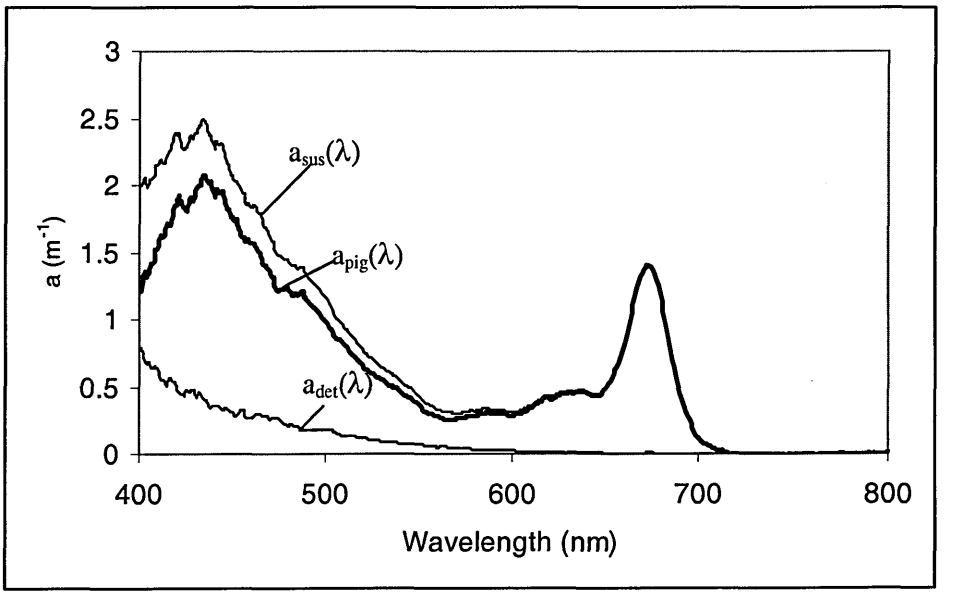

Fig 3.2. An absorption spectrum measured on a suspension of PT. $a_{sus}(\lambda)$ represents the spectral absorption coefficient of the suspension, $a_{pig}(\lambda)$ and $a_{det}(\lambda)$ are its components, as discriminated by the method of Ferrari and Tassan (1999) (see text for details)

hypochlorite steeply increases below 400 nm, thus the addition of NaClO to the suspensions does not introduce artefacts in absorption measurements performed in the range 400-750 nm; nevertheless its effect was assessed on filtered medium (treated with the same amount of NaClO as the samples) and subtracted from all the spectra. The spectral absorption of pigments $a_{pig}(\lambda)$ was calculated by difference between the total absorption coefficient $a(\lambda)$ of the suspension and the one of the "depigmented" (bleached) sample $a_{det}(\lambda)$, as illustrated in Fig. 3.2. Specific absorption coefficients were retrieved by normalizing the a's coefficients either by the chlorophyll concentration ($a^*_{chl}(\lambda)$, in $m^2 mgChl\ a^{-1}$), or by the cell number ($a^*_{cell}(\lambda)$, in $m^2 cell^{-1}$).

3.3.5 Photosynthetic parameters

Photosynthetic performance was studied by means of two different approaches. PvsE experiments measure the assimilation rate of radiocarbon under different irradiance intensities, whereas variable fluorescence techniques give information on PSII functioning and physiology. The latter techniques are instantaneous, thus overcoming many of the problems intrinsically related to the other method, arising from the isolation of phytoplankton in bottles, the choice of the duration of the incubation, etc.

3.3.5.1 $NaH^{14}CO_3$ incubations (PvsE experiments)

Photosynthesis vs Irradiance (PvsE) curves were performed by means of a radial photosynthetron with 9-12 positions (Babin *et al.*, 1994). The irradiance source was a Xenon lamp. In experiments on PT cultures, the incubation duration was 30 minutes and $NaH^{14}CO_3$ was added to 10 ml of sample to a final activity of ca 1 μCi/ml. For incubations of natural samples, the volume of the aliquots was 50 ml, the activity of radiocarbon was

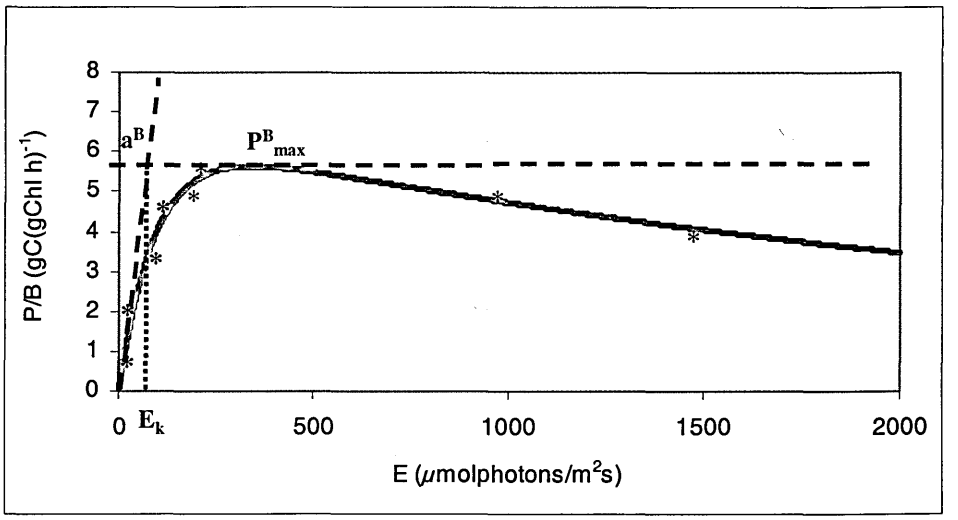

Fig. 3.3. An example of PvsE curve. In blue the parameters retrieved by fitting experimental data (black asterisks) with *Eq. 3.1*

about ca 10 μCi/ml, and the incubation duration was 1h. At the end of the incubation, samples were filtered on 25 mm GF/F. Measurements of ^{14}C were obtained by means of a liquid scintillation counter after the removal of inorganic carbon with 250 μl of HCl.

The photosynthetic coefficients, P^B_{max} (light saturated uptake rate), α^B (photosynthetic efficiency at low irradiance), E_k (light saturation parameter, or photoacclimation index), and β (photoinhibition coefficient), were derived by fitting the data with the equation of optimal curve adaptation as proposed by (Platt *et al.*, 1980) and reported below:

$$P^B = P_S^B\left(1-\exp\left[-\alpha^B\frac{E}{P_S^B}\right]\right)\cdot\exp\left[-\beta\frac{E}{P_S^B}\right] \qquad \textit{Eq. 3. 1}$$

where P^B is the photosynthetic rate at the irradiance E, α^B represents the initial (light-limited) slope of the PvsE curve, β describes the decrease in photosynthetic rate at high irradiance, and $P_S{}^B$ is the parameter equivalent to the light-saturated rate of photosynthesis, i.e. $P_{max}{}^B$, when $\beta = 0$. Finally E_k is given by: $P_{max}{}^B/\alpha^B$, as also evident from the graphic representation reported in Fig. 3.3.

3.3.5.2 Variable fluorescence

FRRF

Fast Repetition Rate Fluorescence measurements were performed using a Fast Tracka FRR fluorometer (Chelsea Instruments Ltd). This technique measures the fluorescence transients induced by a series of brief subsaturating excitation pulses, or flashlets, where intensity, duration and interval between flashlets are independently controlled. It was used both in bench (on cultures) and profiler mode (see section 3.5.1). For bench measurements we used only the dark chamber, while *in situ* measurements were done both in the dark and under solar irradiance. The protocol utilized promotes the saturation of the fluorescence signal and its "relaxation" (decay) by means of differently delivered excitation energy. The settings utilized in the excitation and decay protocols are reported in table 3.1. They were decided after preliminary tests on *P. tricornutum*, following Kolber *et al.*, (1998). As illustrated in Fig. 3.4, the suite of retrieved parameters includes: F_0, F_{max}, σ_{PSII}, and τ_Q, which are respectively the minimal and maximal fluorescence yields, the functional absorption cross-section of the PSII and a kinetic constant of the Q_A^- reoxidation.

Gain		**Saturation flashes N°**	**Flash length (μs)**	**Saturation flashes delay (μs)**
In culture (dilution 1:10)	*In situ*	100	1.10	2.8
1-4	automatic			
Sequences per acquisition N°		**Decay flashes N°**	**Decay flash length (μs)**	**Decay flashes delay (μs)**
In culture	*In situ*	20	1.10	51.6
3	10			

Table 3. 1. FRRF protocols for in culture (banch mode) and *in situ* (profiler) measurements

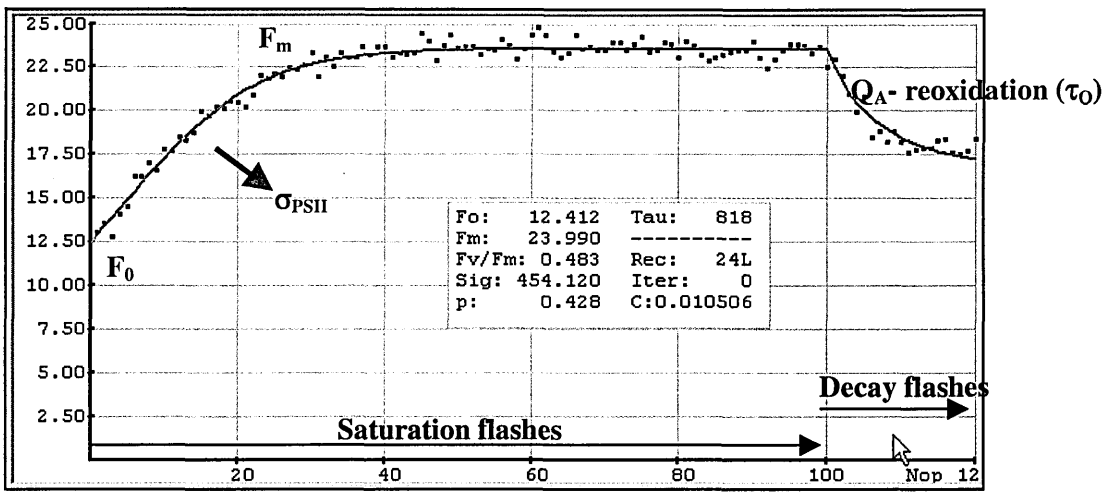

Fig. 3.4. An example of FRRF curve measured on a suspension of PT. On x-axis the number of flashes, on y-axis fluorescence, in r.u. In blue the retrieved parameters (see text for details)

The latter two are derived by using the Frs software (v1.3) provided by Chelsea for fitting the data, according to Kolber *et al.* (1993) and Kolber *et al.*, (1998).

Phyto-PAM

Pulse Amplitude Modulated (PAM) fluorescence measurements were carried out using a Walz Phyto-PAM on 3 ml suspensions in a quartz 10 mm cuvette. The selective amplification of the fluorescence signal is measured with the help of intense, long (45 μsec) -relative to those used in the FRRF technique- pulses of measuring light. Light pulses are generated by an array of light-emitting diodes (LED) in 4 different colors: blue (470 nm), green (520 nm), light red (645 nm) and dark red (665 nm).

The main measurement provides the assessment of the quantum yield of photochemical energy conversion in PSII. The maximal PSII quantum yield, F_v/F_m, is

measured on dark adapted samples by application of the saturation pulse. The dark-adaptation period used was generally 10 minutes. When the saturation pulse is applied during actinic illumination, the observed yield values are lower than after dark-adaptation,

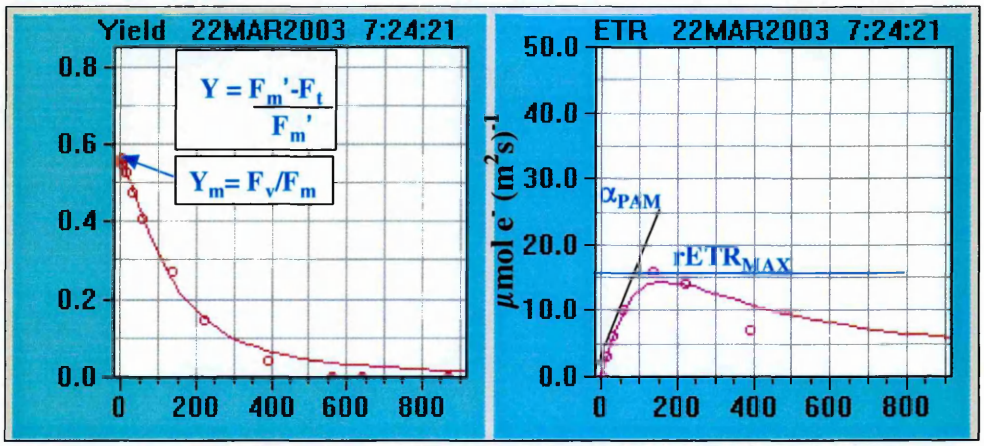

Fig. 3.5. An example of Phyto-PAM "light curves" performed on PT cultures. In blue the retrieved parameters (see text for details)

due to a decrease in the efficiency of energy transformation at PSII reaction centers. This effect may reflect the partial closure of the reaction centers (reduction of primary acceptor Q_A) and/or the increase of non-radiative energy dissipation (as discussed in depth in the next chapter). The product of quantum yield and quantum flux density of absorbed photosynthetically active radiation (PAR) provides a relative measure of the electron transport rate (rETR) in the electron transport chain. The software provided with Phyto-PAM (i.e. PhytoWin) uses a routine for automatically recording light response curves.

After the determination of F_v/F_m (in dark conditions), light intensity is progressively increased to predefined levels (up to10). The sample is illuminated by each "background" irradiance for a defined time period (usually 2 minutes), at the end of which the yield (F_v'/F_m') is determined. Such measurement sequences result in the so-called *light response*

curves of yield and of the derived rETR, shown in Fig. 3.5. Both parameters give information on the photosynthetic performance and light saturation characteristics of a sample. In particular the shape of rETR-curves resemble that of PvsE curves. However, it should be underlined that the short illumination periods applied during Phyto-PAM measurements do not allow full equilibration of the photosynthetic apparatus at the individual PAR-values, contrary to the extended time periods normally applied for PvsE curve recordings. In analogy with the terminology of the PvsE curves, the slope of the rETR vs E curve, is called α, (hereafter α_{PAM}). The value of rETR at saturating light is called $rETR_{MAX}$, and from the ratio between $rETR_{MAX}$ and α_{PAM}, the compensation irradiance, E_{kPAM}, is derived. All these coefficients are retrieved directly by using PhytoWin that fits the data with a theoretical light response function according to a modified version of the photosynthesis model of Eilers and Peeters (1993):

$$ETR = \frac{PAR}{a \cdot PAR^2 + b \cdot PAR + c} \qquad Eq.\ 3.2$$

with the coefficients a, b and c being fitted by minimization of squared deviations.

3.4 In situ profiles

3.4.1 FRRF

FRRF was programmed to carry out two acquisitions delayed by 5 minutes one from the other; this was repeated at each sampling depth. The number of sequences per acquisition was set to 10 (1 second delay among each). Measurements were acquired both in the dark and light chamber in order to compare curves performed under the ambient light with those acquired after 5 minutes in the dark chamber.

3.4.2 Irradiance profiles

In-water profiles of upwelling radiance (L_u) and downwelling plane irradiance (E_d) were acquired using a 13 channel (400, 412, 443, 470, 490, 510, 531, 555, 590, 619, 665, 685, 700 nm) spectral radiometer (Satlantic Inc., SeaWiFS Profiling Multi-channel Radiometer, SPMR). Surface down-welling plane irradiance (E_s, few cm above water) at the same 13 wavelengths and up-welling radiance (L_s, subsurface water at 0.75 m depth) at 7 wavelengths (412, 443, 490, 510, 555, 665 and 684 nm) were measured with a SMSR (Satlantic Inc., SeaWiFS Multi-channel Surface Radiometer). Profiles were acquired following the standard SeaWiFS protocols (Mueller *et al.*, 1995).

Chapter 4

Diel periodicity in the photosynthetic machinery of marine phytoplankton. The *P. tricornutum* model

4.1 Background

The first step of the photosynthetic process is the absorption of light. In the aquatic environment this can be a critical step, due to both the strong and selective attenuation of solar radiation underwater, as widely discussed in Chapter 2, and the "suspended" living of most of the marine photoautotrophs, which may expose them to highly variable light conditions. As a matter of fact, photosynthesis at sea is often limited by light availability. For this reason, several mechanisms for acclimating to varying and/or dim light fields have been developed and selected for in algae (Falkowski and Raven, 1997). These mechanisms are clearly reflected in the high variability of pigment composition, ultrastructural organization of thylakoid membranes, and life strategies found among marine photoautotrophs without a parallel counterpart in terrestrial plants. It is also important to note that variations in the light field require plastic cellular mechanisms to not only capture light, but to also to efficiently dissipate it, when too intense.

Pigment composition, cell size and shape, and spatial organization of thylakoids are the main factors regulating the light absorption of the cells. In particular, changes in these factors lead to variations in the chlorophyll *a*-specific absorption coefficient (or optical cross section), $a^*_{chl}(\lambda)$, the coefficient commonly used to assess the spectrally weighted contribution of phytoplankton on the absorption coefficient of seawater, as explained in

section 2.1.2. For example, acclimation to high light is generally achieved by synthesis of high concentrations of the so-called non-photosynthetic carotenoids, i.e. carotenoids that do not transfer energy to the reaction centres, and a low content of light harvesting pigments. The opposite generally occurs in low light acclimated cells, where chlorophyll *a* (as well as other light-harvesting pigments) accumulates, thus increasing the light capturing capability of the cells, but also decreasing their specific optical cross section because of the pigment *packaging,* i.e. self shading of chromophores within thylakoid membranes. On the other hand, the abundance of non-photosynthetic carotenoids reduces, in fact, the *effective absorption cross section*, σ_{PSII}, a parameter that accounts for the probability that a photon absorbed at a specific wavelength is used for a photochemical reaction. Since pigment complement is so important for coping with the underwater light field dynamics, its size and turnover rate can be considered crucial indexes for understanding algal status and responses.

Each photon captured by the harvesting system has (at least) three possible fates: being diverted to photochemistry (i.e. to the light reactions of photosynthesis), being dissipated as heat, or being re-emitted as fluorescence. The probability of each of the three processes depends on the photophysiological state of the organism in relation to the light environment which it is exposed to. If an algal suspension is illuminated with blue light, the emission of red light by chlorophyll *a* fluorescence is lower than for the same pigment extracted in an organic solvent, which means that the quantum yield of fluorescence (i.e. photons emitted over photons absorbed) is lower in vivo than in vitro. This occurs because fluorescence is *quenched* through alternative pathways, e.g. photochemistry (photochemical quenching) and heat (non photochemical quenching), competing for the de-excitation of the

excited singlet state in vivo. In this perspective, fluorescence-based measurements represent an important tool for studying the status and the functioning of structures and mechanisms for light utilization/dissipation. They are based on the stimulation of chlorophyll *a* fluorescence by means of an artificial light source that causes the closure of the reaction centers (hereafter RC). When RC are "open" they can efficiently trap the excited state energy and deliver it to the photochemical conversion, thus the fluorescence yield is minimum and is indicated with F_0. Conversely, when the RC are closed by the saturating flash (or sequence of flashes) the photochemical yield is very low, and the fluorescence yield becomes maximum (F_m). The maximal change in the fluorescence yield is then achieved in dark adapted state and is expressed as the ratio F_v/F_m, where $F_v = F_m - F_0$. It represents the potential photochemical efficiency of the open centers of PSII. When the measurement of this ratio is performed under actinic light, the actual photochemical efficiency, F_v'/F_m', is lower, due to the partial closure of the reaction centers, which allows the estimation of dissipating processes indicated as non-photochemical quenching (NPQ). A way to quantify NPQ is represented by the Stern-Volmer coefficients reported below:

$$SV_0 = \frac{F_0}{F_0'} - 1 \qquad \textit{Eq. 4 1}$$

$$SV_m = \frac{F_m}{F_m'} - 1 \qquad \textit{Eq. 4 2}$$

where F_0' and F_m' represent the minimum and maximum fluorescence yield as measured under a "background" irradiance. The product between the ambient irradiance and the corresponding F_v'/F_m' gives a relative measure of the electron transport rate (rETR) in the transport chain, thus providing an estimate of the rate of utilization of light in photochemistry.

On the other hand, the classical photosynthetic measurements based on the incorporation of radiocarbon allow the quantification of one of the products of the photosynthetic process, i.e. the amount of carbon compound synthesized, which, in turn depends either on the efficiency of the dark reactions (Calvin cycle) or on processes occurring upstream, like the above described light absorption and utilization in the photochemistry. The light dependence of carbon assimilation is studied in PvsE experiments which consist of the measurement of the rate of C fixation under different irradiances (see section 3.3.5.1).

Many diatoms are quite flexible in responding to rapid changes in the light field and, particularly, in activating photoprotection mechanisms in response to light excess (Lavaud *et al.*, 2002a; Lavaud *et al.*, 2002b). The best-known mechanism of light dissipation in diatoms is related to the formation of the pigment diatoxanthin by enzymatic de-epoxidation of diadinoxanthin (Olaizola *et al.*, 1994; Ting and Owens, 1993). The formation of diatoxanthin in the antenna facilitates the loss of excitation energy from chlorophyll *a* by thermal dissipation of exceeding light, thus preventing the photodamage of the photosynthetic apparatus. The reaction is reversible and the whole process is an example of a xanthophyll cycle similar to the one occurring in higher plants and chlorophytes, which involves violaxanthin, antheraxanthin and zeaxanthin (Demmig, 1987).

Other mechanisms of light dissipation have been reported, one being an electron cycle around PSII, recently demonstrated for *P. tricornutum* (Lavaud *et al.*, 2002b) but already proposed as a mechanism preventing photo-oxidative damage in *Chlorella* (Prasil *et al.*, 1996). However, in spite of the high flexibility of the photosynthetic machinery existing in diatoms, most of the light-dependent processes display regular patterns over the

diel cycle, both in terms of pigment content and functional parameters, as already anticipated in the first chapter. This has been frequently reported in the literature over the last decades (e.g., Palmer *et al.*, 1964; Eppley *et al.*, 1967; Owens *et al.*, 1980; Post *et al.*, 1984; Putt *et al.*, 1988), therefore a key issue of my study has been not only reproducing known patterns but also observing the time course of additional photophysiological parameters which could better elucidate the cellular response to the periodic and random variation in the natural environment.

In the following sections I will report results both from extensive (3-5 days) and short (12-40 hours) experiments on the time variability of photophysiological properties and processes of PT over the diel cycle. The potential for an endogenous control of such mechanisms was tested by doing measurements in free running conditions (continuous light, or continuous dark), in order to verify the persistence of the observed circadian patterns even in absence of external light cues.

The results presented in this chapter are organized in four sections. The first will deal with circadian patterns observed in PT under artificial "square wave" light regime; in the second I will present parallel experiments conducted under natural light; the third will include results from experiments aimed at discriminating the variability of the investigated parameters due to day-night cycles from that driven by responses to the applied light regime (in terms of growth irradiance, length of photoperiod, light shifts); finally, in the last section data from an *in situ* diel cycle will be shown for comparison.

I used the notations of Allali *et al.* (1997) and Trees *et al.* (2000) to distinguish between photosynthetic and non-photosynthetic pigments. The former (PSP) include chlorophylls (i.e. chlorophyll *a, b, c*) and photosynthetic carotenoids (PSC), i.e. carotenoids that are known to transfer excitation energy to chlorophyll *a*; they include:

19'hexanoyloxifucoxanthin, 19'butanoyloxifucoxanthin, fucoxanthin, prasinoxanthin and peridinin. Non photosynthetic pigments are basically carotenoids that, to the best of current knowledge, do not transfer excitation to the reaction centres. They are also indicated as PPC (photoprotective carotenoids) since they are thought to be involved (more or less directly) in photoprotection mechanisms. Among them: βcarotene, diadinoxanthin, diatoxanthin, alloxanthin, antheraxanthin, violaxanthin, zeaxanthin.

In diatoms the major light harvesting chlorophyll-protein complex (LHCP) binds fucoxanthin, chlorophyll *a* and *c* (fucoxanthin-chlorophyll proteins, FCP) (Boczar and Prezelin, 1989). In *P. tricornutum* the commonly detected pigments are: chlorophyll *a*, chlorophyll c_2, fucoxanthin, diadinoxanthin, diatoxanthin, and βcarotene. As already mentioned, diatoxanthin production is generally associated to a photoprotection mechanism, hence its occurrence depends on light conditions (Casper-Lindley and Bjorkman, 1998). Recently Lohr and Wilhelm (1999) reported in PT the presence of small amounts of pigments of the photoprotection cycle typical of higher plants and green algae, i.e. violaxanthin, antheraxanthin, and zeaxanthin, the latter two found only under supersaturating light. See table I for the abbreviations used to indicate pigments hereafter.

4.2 Circadian patterns of pigment concentrations and photosynthetic parameters in PT grown in artificial light

4.2.1 Pigments

Under "square wave" LD regime, in turbidostat-like modality, pigment content displayed a periodical variation over light-dark cycles, with period of about 24 hours and varying phase for different pigments. In Fig 4.1 I report the time course of all detected pigment concentrations in the suspension over LD and LL cycles, as they would have been in

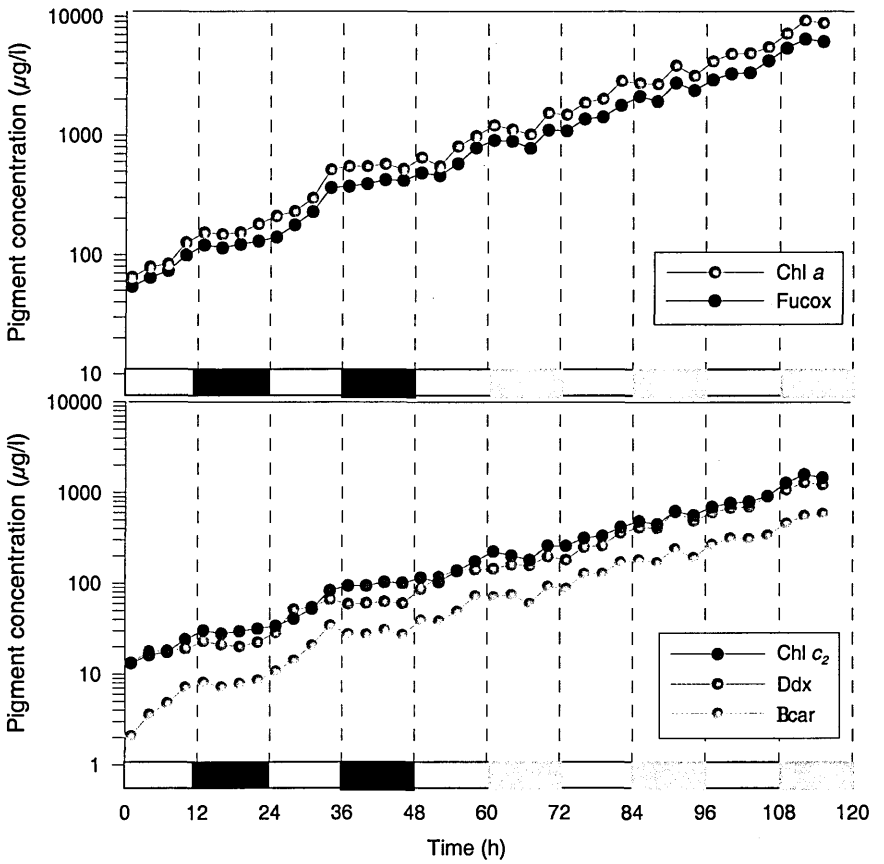

Fig 4.1. Time distribution of pigment concentrations over artificial LD and LL cycles (exp. INTRO). Concentrations have been corrected by the dilution factor applied after each sampling point. Grey boxes indicate "subjective" night periods during continuous light regime

absence of dilution during the experiment INTRO. No significant amounts of Dtx were detected due to both the long adaptation period (at least 2 weeks) and non-saturating growth irradiance.

At a first analysis, all pigments showed similar time patterns in LD, i.e. accumulation during the day and rather constant values at night, while in continuous light pigment content increased quite exponentially over the time. In order to better visualize the data, I rescaled them every 24 hours by the value measured in the first light point (in Fig. 4.2). This representation improves the definitions of the circadian patterns. Pigment content

continuously increased over L periods, displaying maxima just before or after the onset of the dark.

Interestingly, LL cycles were characterized by daily accumulation levels similar to those observed over LD periods. As for the timing, major differences were observed during "subjective" nights, when concentrations still tended to stabilize, like during dark phases, but continued to increase slightly. When normalized by the cell number (Fig. 4.3), pigment concentrations displayed strong circadian variability evidencing some differences from the above described patterns. Cell content of Chl *a*, Chl c_2, Fucox and βcar exhibited similar

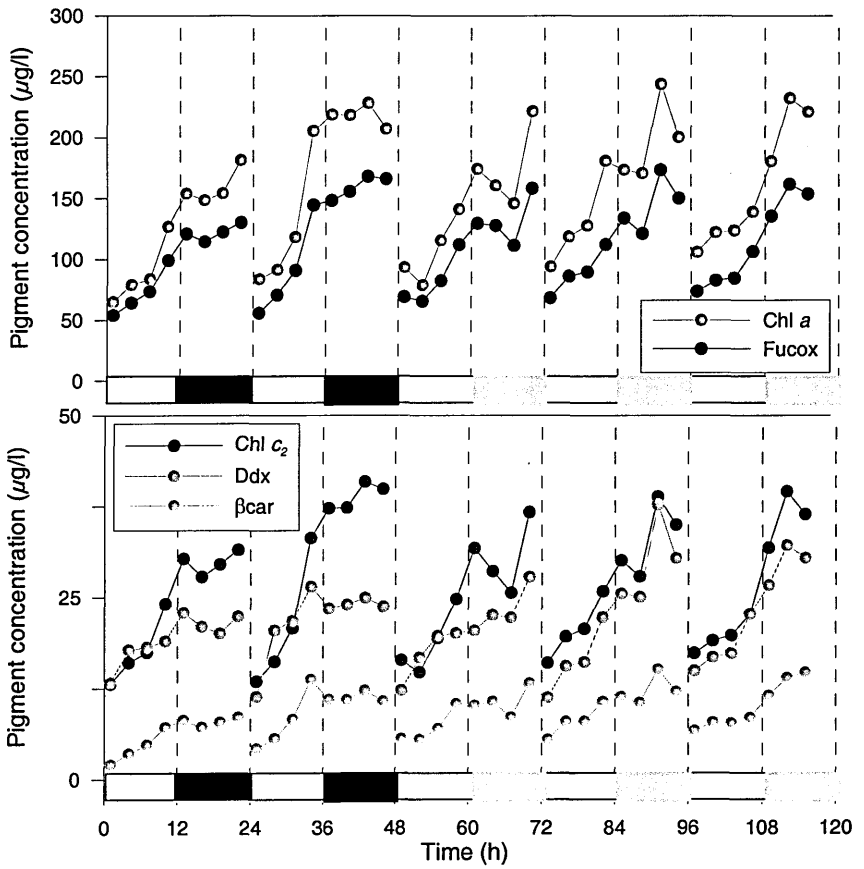

Fig. 4.2. Time distribution of pigment concentrations over LD and LL cycles in the exp. INTRO. Concentrations have been corrected by the dilution factor and rescaled every day by the initial value (i.e. the first of the L period). Grey boxes indicate "subjective" night periods

timing, i.e increase through L periods and rather symmetric decrease over night.

Moreover flow cytometric red fluorescence (RED) displayed the same time distribution as Chl *a*/cell (Fig. 4.4), making me confident of the use of RED as proxy for cellular concentration of chlorophyll *a*. On the other hand, Ddx concentration exhibited different phasing, maximizing its accumulation (in the cell as well as in the suspension) at least 3 hours before the other pigments.

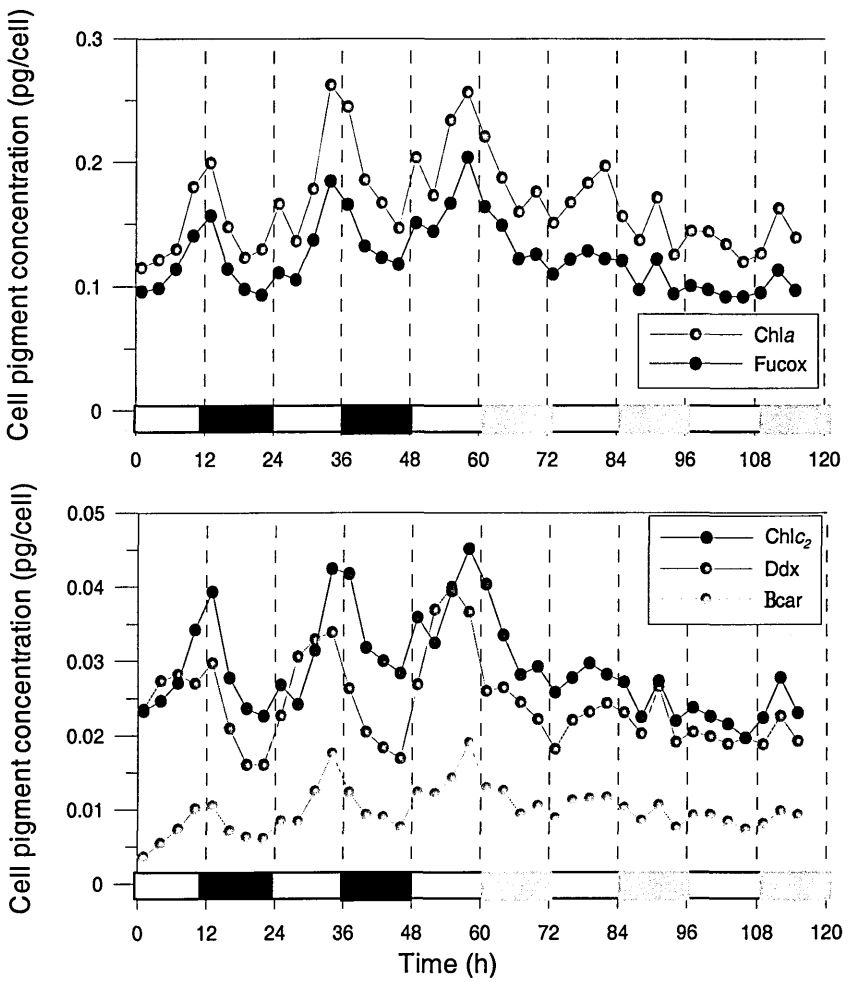

Fig 4.3 Circadian variability of cellular pigment concentrations over artificial LD (white and and black boxes) and LL 24 h (white and grey boxes) cycles (exp INTRO)

This appears particularly clear in the plot of Ddx/Chl *a* ratio (Fig. 4.5), which shows sharp maxima in the first part of the day (i.e at the fourth circadian hour). A clear circadian pattern was shown by βcar/Chl *a* (shown in Fig. 4.5), which was out of phase with the previous; it peaked in the second part of the day, i.e. 3 or 6 hrs after Ddx/Chl *a*. Finally no circadian features were observed in Fucox and Chl c_2 to Chl *a* ratios, which were rather flat over time (data not shown).

In synthesis, the contribution of photoprotectant over photosynthetic pigments, assessed as PPC/PSP and reported in Fig. 4.5, basically matched the distribution of Ddx/Chl *a*. In the continuous light regime, the amplitude of oscillations was reduced and pigment content was lowered to nocturnal values after the first LL cycle (Fig. 4.3). Also in this regime the time pattern of Ddx displayed some differences with respect to the other pigments: while chlorophylls, fucoxanthin and βcarotene decreased during the first "subjective" night as they did over dark periods, cell Ddx exhibited a relative accumulation, as also visible in Ddx/Chl *a* (Fig. 4.5).

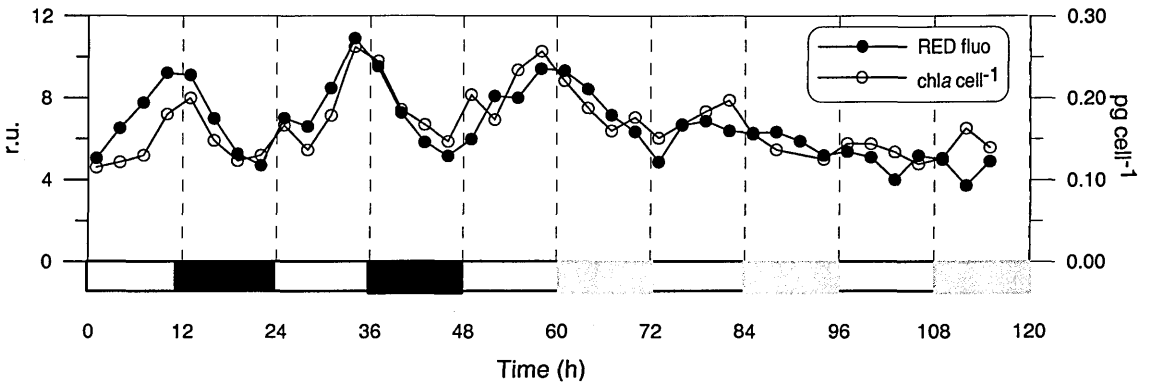

Fig. 4.4 Circadian variability of cellular Chl *a* concentration and red fluorescence (by flow cytometry) over LD and LL cycles (exp INTRO). Grey boxes indicate "subjective" night periods during LL cycles.

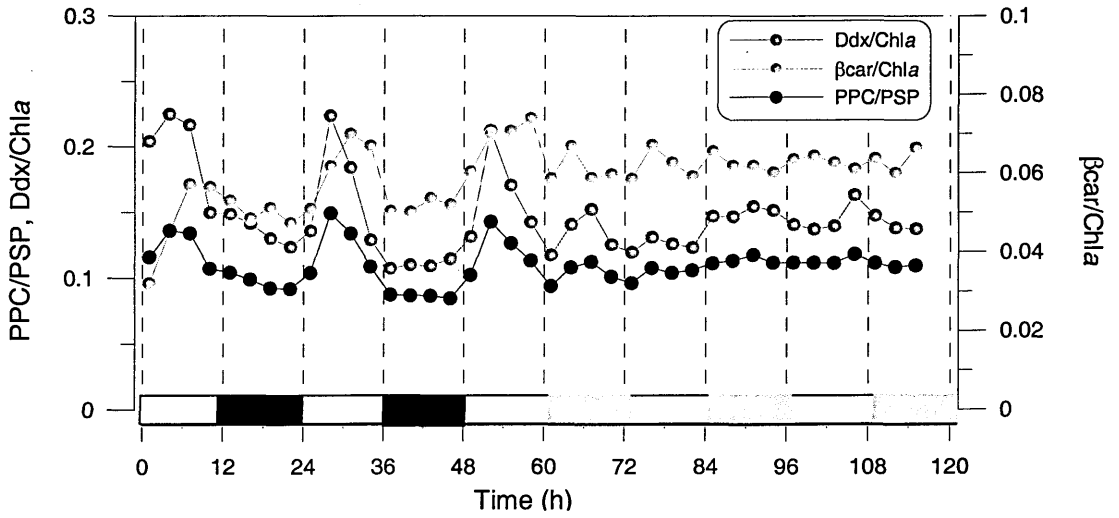

Fig. 4.5 Circadian variability of the indicated pigment ratios over artificial LD and LL cycles (exp. INTRO). Grey boxes indicate "subjective" night periods during LL cycles

4.2.2 Absorption coefficients

The absorption properties of PT varied over light-dark cycles, reflecting the periodical oscillations observed in pigment concentrations. In particular, as shown in Fig. 4.6a, the mean Chl *a*-specific absorption coefficient, a^*_{chl} (averaged over the visible spectrum), was characterized by maxima in the first part of light periods, decreasing values under daylight, minima at the end of the day or the beginning of the night and increasing

values in the dark. Surprisingly, in the LL regime, some periodicity persisted, even if the phase was lost since the first subjective night, when the typically nocturnal increase was much smaller and more prolonged than usual, resulting in a time shift of some hours in the following days.

On the other hand, cell normalized values, a^*_{cell}, exhibited diel oscillations over LD, but a phase delay of 9-12 hours with respect to a^*_{chl} (Fig. 4.6b) and with a maxima which occurred at the end of the day or in the early night. In the continuous light regime, a^*_{cell} kept its diel periodicity over the first unexpected light period, and in the following 9 hours. Afterwards, the time pattern became confused.

The relative contribution of the different pigments to the absorption capability of PT was assessed from their concentration and specific absorption coefficients, according to the following equation:

$$a_{pig(i)}(\lambda) = a^*_{pig(i)}(\lambda) \cdot C_{pig(i)} \qquad \textit{Eq. 4. 3}$$

which assumes that the absorption due to the *ith* pigment ($a_{pig}(i)$, in m^{-1}) is given by the product of its HPLC-derived concentration ($C_{pig(i)}$, in $mg \cdot m^{-3}$) and its specific absorption coefficients ($a^*_{pig(i)}(\lambda)$, in $m^2 \cdot mg^{-1}$, taken from Bidigare *et al.* (1990). Then the contribution on the Chl *a*-specific and cell-specific absorption coefficients was retrieved dividing a_{pig} by Chl *a* concentration and cell number, respectively, and averaging them over the visible wavelength range (400-700 nm). The estimated $a_{pig(i)}$ represents the theoretical absorption coefficient of the *ith* pigment, i.e. that which would be hypothetically measured if the pigments was free in solution and not packed into cells. The results of this analysis are reported in Fig 4.7. The time course of the derived absorption coefficients basically reflected that exhibited by pigment to Chl *a* ratios and by cell pigment content. Among

chlorophyll specific coefficients (panel a), a^*_{chl}(Fucox) and a^*_{chl}(Chl c_2) were flat over time, whereas a^*_{chl}(Ddx) and a^*_{chl}(βcar) displayed the expected circadian oscillations. On a cell basis, all absorption coefficients (a^*_{cell}) oscillated as the concentrations of the corresponding pigments did within cells. Fucox was responsible for most of the absorption capability of PT, (followed by Chl *a*) while βcarotene was the least efficient in light harvesting; intermediate values were estimated for Ddx and Chl c_2. In synthesis, PPC contributed 12-19.5% of the absorption capability of PT (not shown). The implications of the reported pattern will be discussed in detail in Chapter 6.

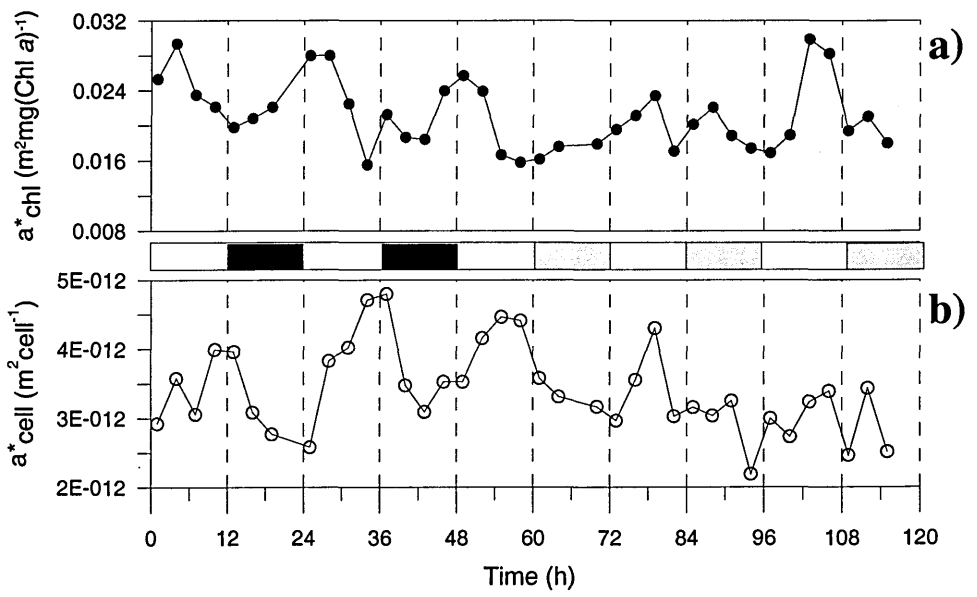

Fig. 4.6 Circadian variability of specific mean absorption coefficients (averaged on the interval 400-700 nm) over artificial LD and LL cycles (exp INTRO). a) Chl *a*-specific absorption coefficients (b) cell-specific absorption coefficients

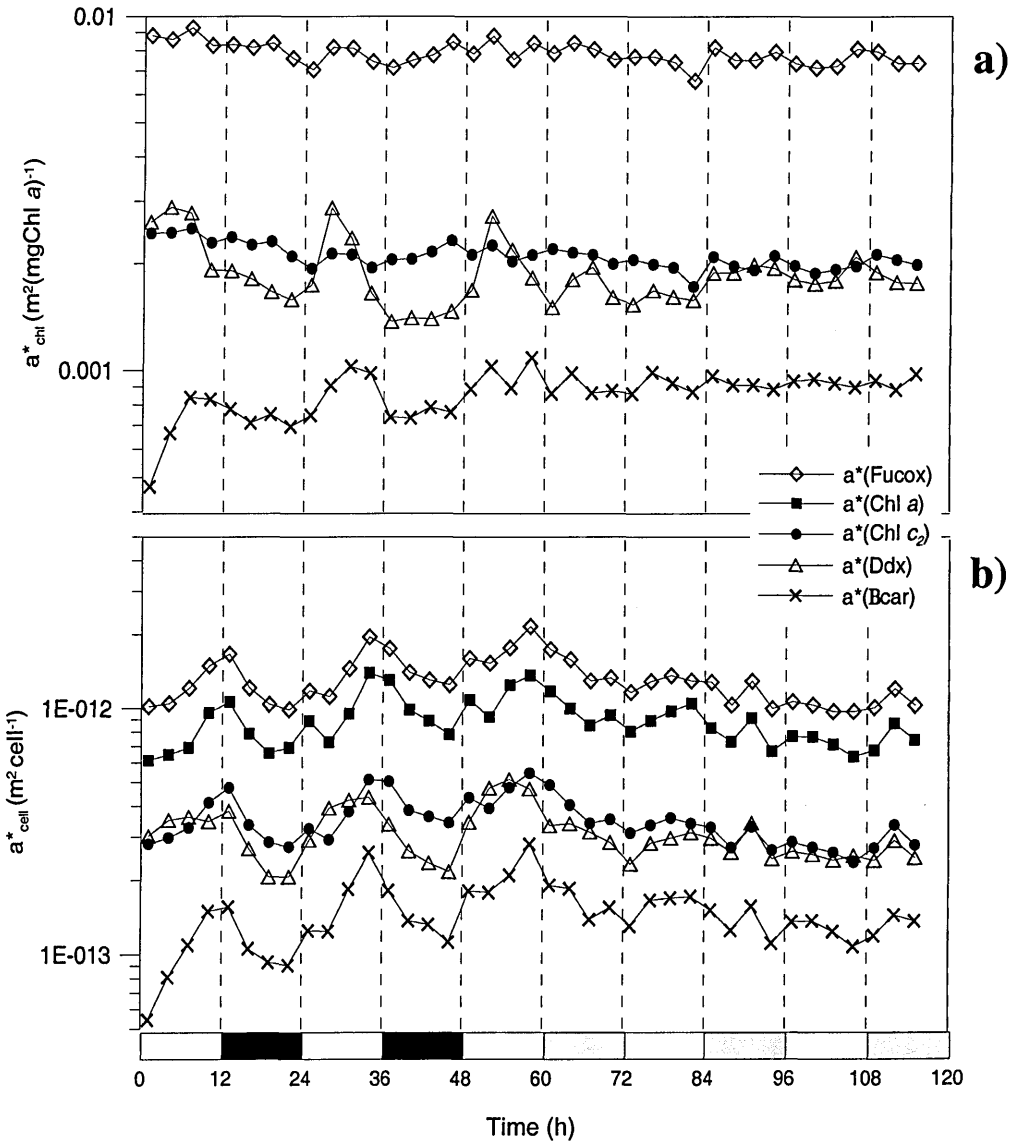

Fig. 4.7. Time pattern of absorption coefficients (averaged over the visible spectrum) of the indicated pigments in artificial LD and LL cycles (exp. INTRO). Coefficients were retrieved using *Eq 4.3* and normalizing them by Chl *a* concentration (a) and by cell number (b)

4.2.3 PvE coefficients

Carbon-based estimates of primary production revealed a strong dependence of photosynthetic coefficients on the day-night cycle. As reported in Fig 4.8 and 4.9 the highest rates of C-fixation were performed during the central part of L periods while low

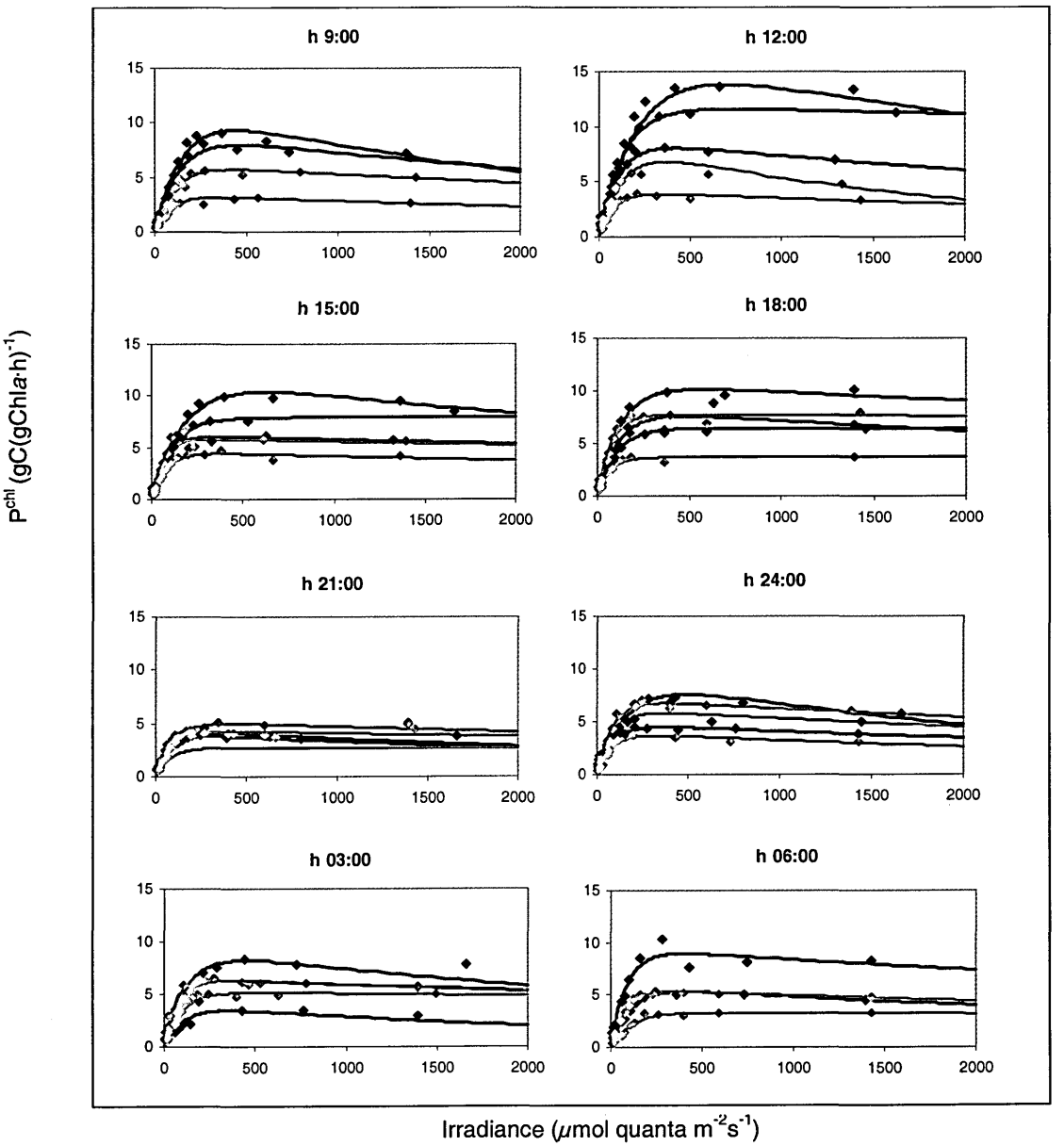

Fig. 4.8. PvsE curves measured in artificial LD (black) and LL (red) cycles. Dots represent P^{chl}, i.e., the amount of carbon fixed per Chl *a* unit in the time unit, measured under 12 irradiance levels. Curves were derived by fitting the data with *Eq. 3.1*. Labels indicate local time of the samples, while data from the curves are plotted vs "circadian time" in the following figure

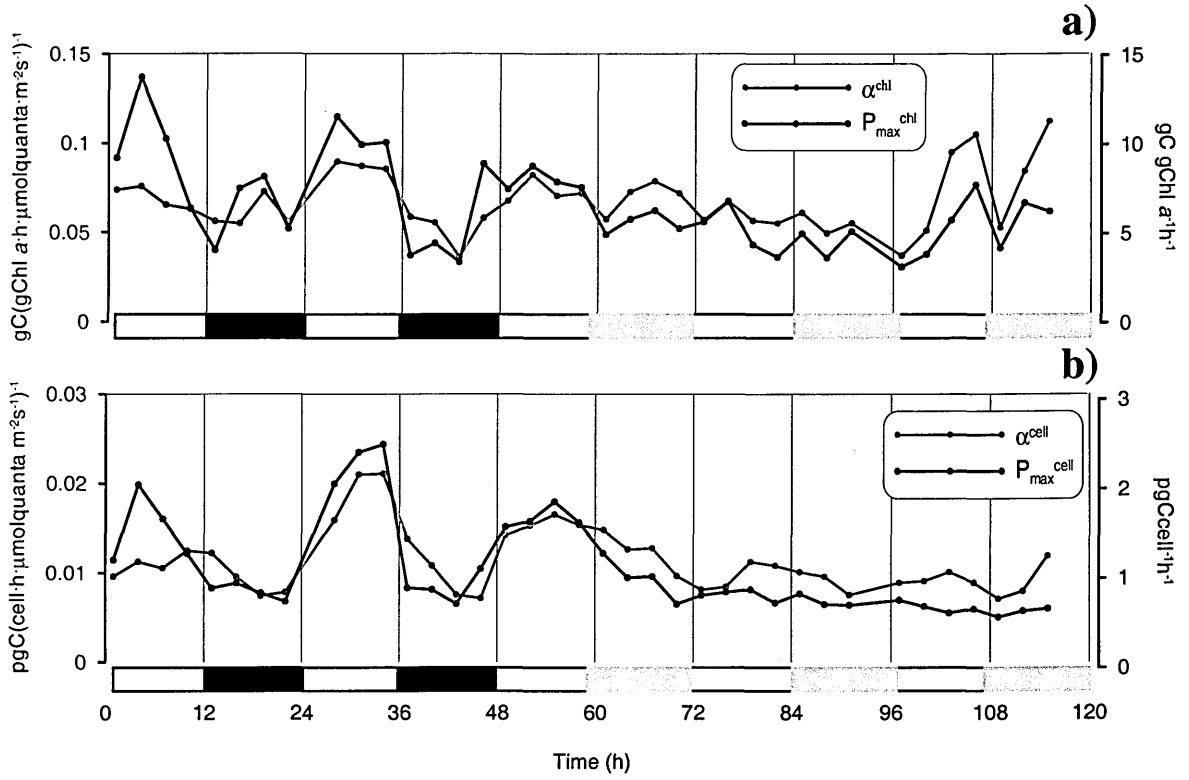

Fig. 4.9 Circadian distribution of PvsE parameters over artificial LD and LL cycles (exp. INTRO). a) chlorophyll normalized PvsE coefficients (P^{chl}_{max} and α^{chl}), as derived from curves of Fig. 4.8. b) cell normalized coefficients (P^{cell}_{max} and α^{cell})

and rather constant values were measured in the dark. In particular chlorophyll-normalized photosynthetic coefficients P^{chl}_{max} and α^{chl} displayed parallel diel oscillations over LD cycles, while in continuous light conditions both parameters lost any periodicity and varied in an irregular way, displaying lower values, often similar to the "nocturnal" ones (red curves and dots in Fig. 4.8).

When calculated on a cellular basis (data reported in Fig. 4.9b), the same photosynthetic parameters exhibited more regular but similar time distribution under LD cycles and clearer distribution in free running conditions; in particular α_{cell} continued oscillating with some

regularity but more slightly, whereas P^{cell}_{max} time distribution became flat after the first subjective night, dropping to very low values.

4.2.4 Variable fluorescence

The FRRF-derived effective cross section, σ_{PSII}, exhibited clear diel oscillations with maxima during the night and minima in daylight, thus showing 12 hours phase delay with respect to pigment concentrations and the other photosynthetic coefficients. Values decreased during L periods, increased at the onset of the dark, and exhibited rather constant values all over the night (figure 4.10). In continuous light conditions, circadian oscillations persisted but with lower amplitude.

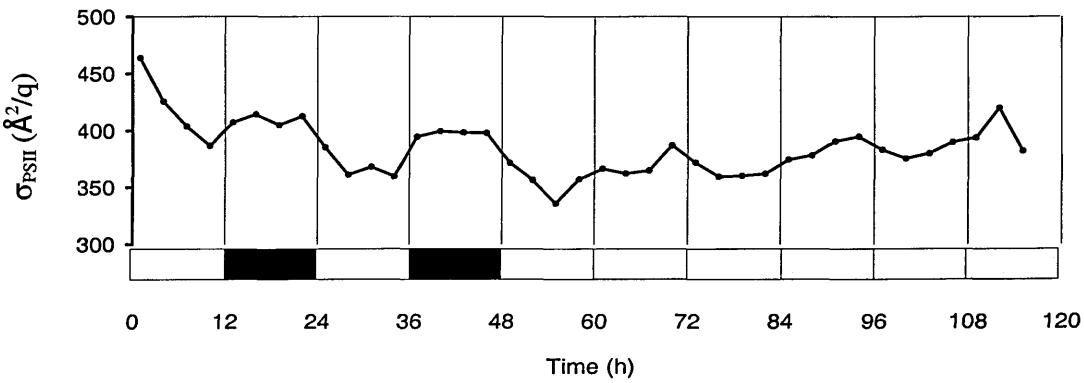

Fig. 4.10. FRRF-derived effective cross section of PSII in artificial LD and LL cycles. (exp INTRO)

In the following I report results from PHYSIO experiment, aimed at verifying and strengthening the information derived from INTRO experiment. In particular variable fluorescence measurements based on the use of Phyto-PAM fluorometer were added. Phyto-PAM is more suited for culture studies than the FRRF profiler, although it produces slightly different information (see section 3.4.5.2).

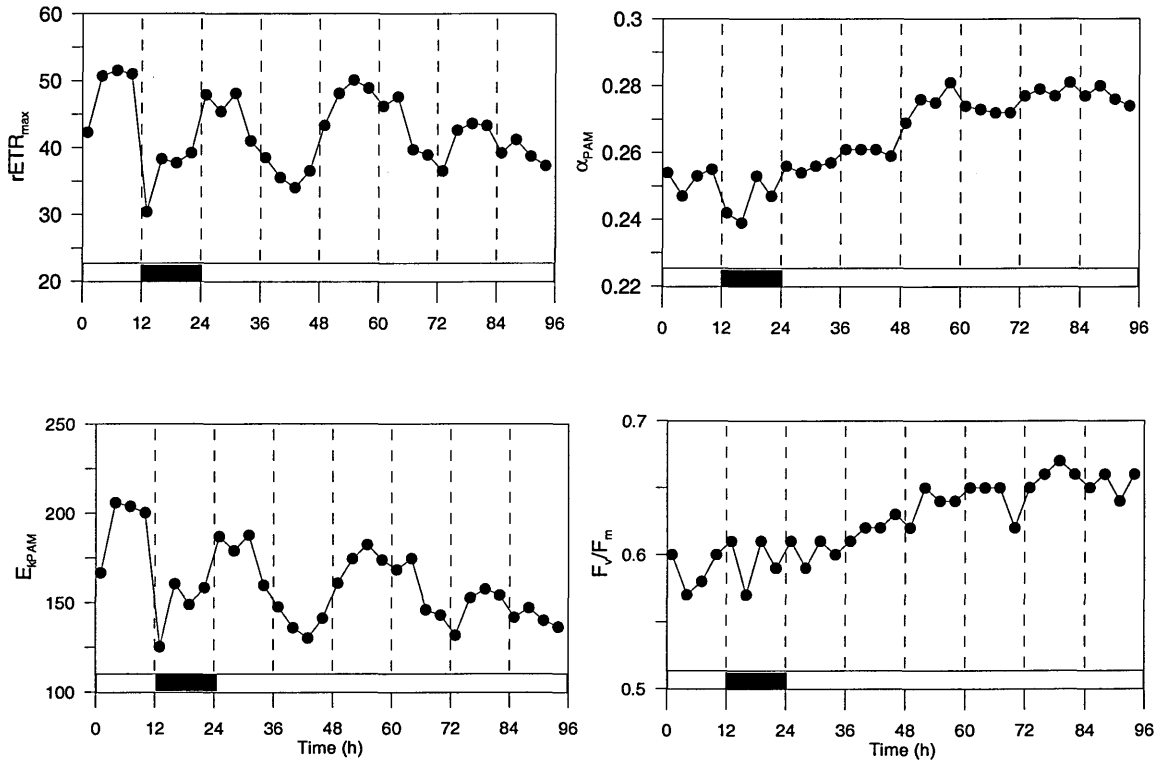

Fig. 4.11 PhytoPAM derived photosynthetic coefficients in artificial LD and LL cycles (exp PHYSIO).

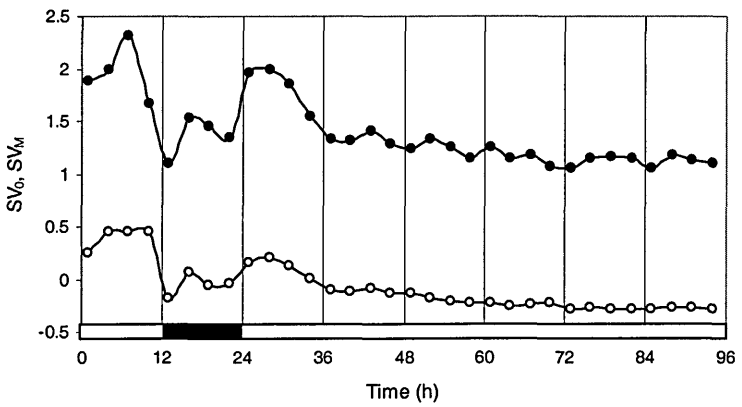

Fig. 4.12. Circadian patterns of NPQ coefficients: SV_0 (open circles) and SV_M (closed circles) measured at 1270 μmolquantam^{-2}s^{-1} by means of PhytoPAM over artificial LD and LL cycles (exp. PHYSIO)

PHYSIO experiment employed the same experimental conditions as INTRO, except for a slightly higher growth irradiance (200 vs 150 μmolquanta·m^{-2}s^{-1}) and a shorter series of measurements over LD period (one cycle vs two). In this part I omit results from

pigments and flow-cytometry since they essentially reproduced the data presented for the exp. INTRO. Phyto-PAM data for the PHYSIO experiment are reported in Fig. 4.11. The relative maximum electron transport rate ($rETR_{MAX}$) showed regular diel oscillations with high values during light periods and lower in the dark. Maxima occurred during the first or central part of the day and minima 12 hours later. Day-night variations were in the order of 30%. On the contrary, α_{PAM} and F_v/F_m exhibited a very noisy distribution. Nevertheless, it was possible to derive general trends conserved throughout all experiments under artificial light, as will be shown for the following experiments: the average diurnal value was higher than the nocturnal one, even though a relative minimum occurred in the central part of the light period. Overall, the time distribution of α_{PAM} reflected the noisy pattern of the maximum quantum yield, F_v/F_m.

The time course of E_{kPAM} (i.e. $rETR_{MAX}/\alpha_{PAM}$) strictly followed that of $rETR_{MAX}$, being less affected by the irregular distribution of α_{PAM}. Oscillations of both $rETR_{MAX}$ and E_{kPAM} strongly persisted in free-running LL, with comparable amplitude in the first two days and decreased (by about the half) in the third. α_{PAM} lost any periodical behaviour in LL displaying a significant increase over the time.

The SV coefficients showed maxima during L periods, indicating the capability of non-photochemical dissipation of light, and minima in the dark. The pattern was completely lost after the first cycle of the LL regime, and values were low and constants, typical of dark periods.

4.2.5 Summary

In synthesis, all the investigated photophysiological properties of *P. tricornutum* showed diel periodicity in artificial "square" wave LD cycles. Pigments maximized their cell

content at the end of the light period or at the beginning of the dark, except for Ddx that anticipated its peak at least by three hours.

With respect to the absorption cross section, cell normalized values reflected variations in the cell pigment content i.e. accumulation throughout the L periods and decrease over the night. This was expected since the most abundant light harvesting pigments (Chl *a* and Fucox) covaried. On the other hand, the time pattern of Chl *a*-normalized absorption coefficients significantly differed as they displayed maxima at the beginning of L periods (exactly at the first sampling point). Photosynthetic coefficients, as derived from both variable fluorescence and C-based measurements, displayed peaks in the central part of the light period. The effective cross section of PSII exhibited the opposite phase with respect to the other coefficients, with maxima at night and minima over light periods.

As for measurements in free running conditions, pigment concentrations kept the same phase and amplitude of circadian oscillation at least for 24 hours, followed by lower amplitude oscillations. P^{cell}_{max} drastically decreased after one cycle in LL, whereas $rETR_{max}$ kept its oscillating behaviour for 2-3 days in LL, driving also E_{kPAM} variability.

All the experiments described above were substantially testing whether an on-off trigger, independent from the diurnal variation of light intensity, was indeed able to entrain a rhythm in the cells. In nature such a light pattern is far from being realistic. In general the on-off trigger is only one aspect because, as analyzed before, light intensity varies according to a quasi-sinusoidal pattern. Therefore, different responses might be superimposed in nature and the regulation of the circadian rhythm, if any, may be tuned to cope with an irradiance varying continuously over the light phase of the day-night cycle. Then, I carried out parallel experiments to determine whether the time distribution of all

pigments and photosynthetic parameters in natural light did resemble the simplified cycle tested before.

4.3 Circadian patterns of pigment concentrations and photosynthetic parameters in PT grown in natural light

The experiment "SPRING" was carried out from March the 21st, i.e. the spring Equinox, therefore the day length was exactly 12 hours. The sky was generally clear, even though PAR intensities measured within the culture displayed some variability (Fig. 4.13).

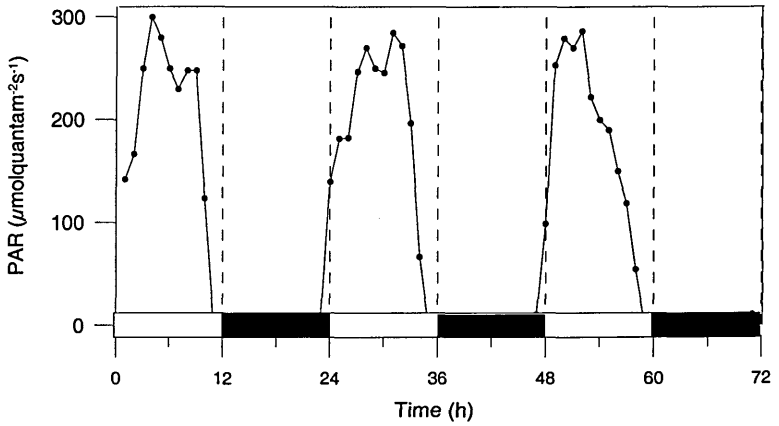

Fig. 4.13. Hourly averages of PAR irradiance measured within the culture during the exp. SPRING

4.3.1 Pigments

The time distribution of PT pigments was less regular than in the ALE experiment, nevertheless it was possible to infer circadian patterns and to point out differences from the results reported above, also with the help of red fluorescence data that displayed regular diel oscillations (Fig 4.14), with maxima around midday (PAR intensity: 200-300 μmolquanta $m^{-2}s^{-1}$), i.e. about 6 hours before that observed in the previous case (ALE), and minima in the late night. The time distribution of cell Chl *a* and RED did not properly match (Fig.4.14) as in the INTRO experiment, even though all cell normalized HPLC pigment concentrations (reported in Fig. 4.15) confirmed the overall occurrence of maxima

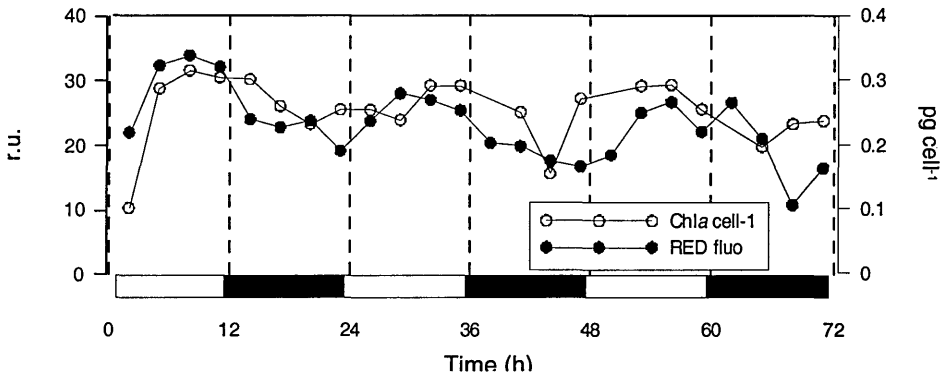

Fig. 4.14. Circadian variability of cellular Chl *a* concentration and red fluorescence over natural LD cycles during the exp. SPRING

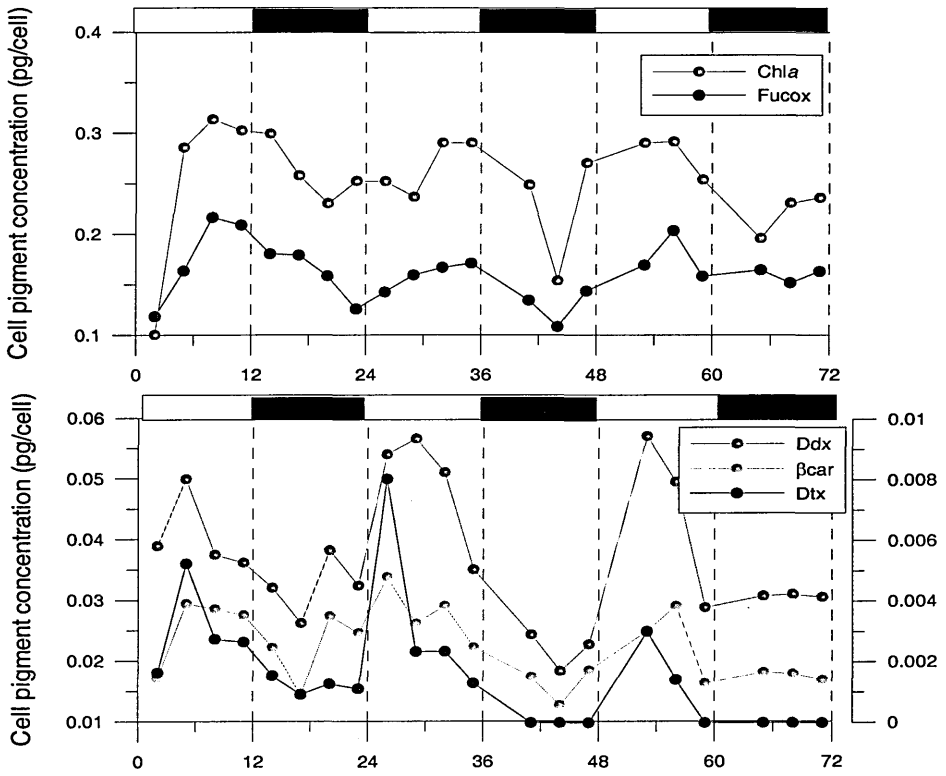

Fig. 4.15. Circadian variability of cellular pigment concentrations over natural LD cycles during the exp. SPRING. Please note the different y axis for Dtx in panel b) (Blue color for both plot and axis)

in the central part of the day and minima in the mid or late night, though with some exceptions (e.g. 2nd day).

Conversely, Ddx distribution was in accordance to what reported above, since its maxima anticipated the ones of the other pigments as demonstrated by Ddx/Chl *a* ratio (Fig 4.16) peaking 3-4 hours after the onset of the light, i.e. at the same time as in the previous case. Large amounts of Dtx were detected in phase with high Ddx concentrations and, as expected, in correspondence of the most intense irradiance values. The time distribution of βcar/Chl *a* did not show the same pattern as in ALE, but on the contrary it matched the distribution of Ddx/Chl *a* (Fig 4.16), as well as that of the PPC/PSP ratio.

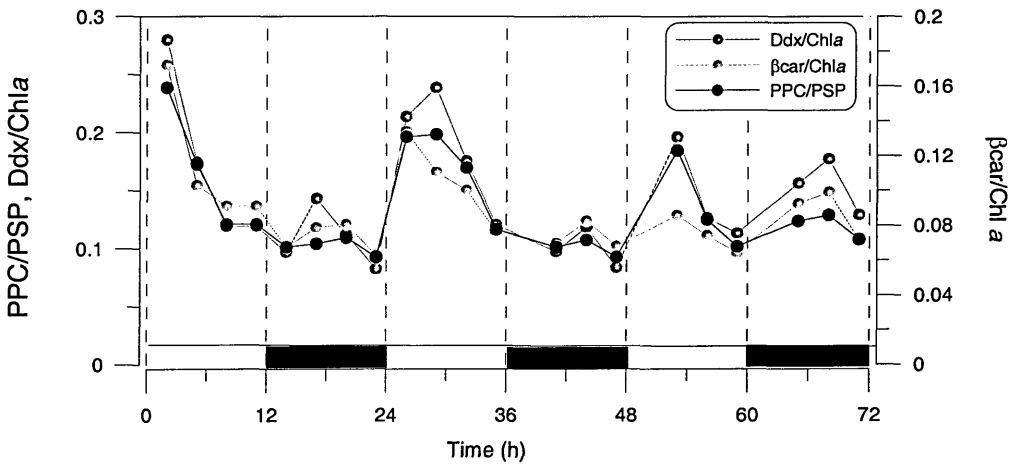

Fig. 4.16. Circadian variability of the indicated pigment ratios over natural LD cycles.(exp SPRING)

4.3.2 PvsE coefficients

In NLE, the resolution of PvsE measurements was reduced due to the difficulty of performing such measurements on the ship, therefore the circadian distribution of the coefficients was not well resolved, as evident in Fig 4.17 and 4.18. Some features were however evident: carbon assimilation rate was maximized during the day and lowered at

dawn, dusk and night. P_{max}^{chl} and α^{chl} covaried displaying maxima during the day and minima at night (Fig 4.18a). A similar day/night distribution was observed in cell normalized data (Fig 4.18b).

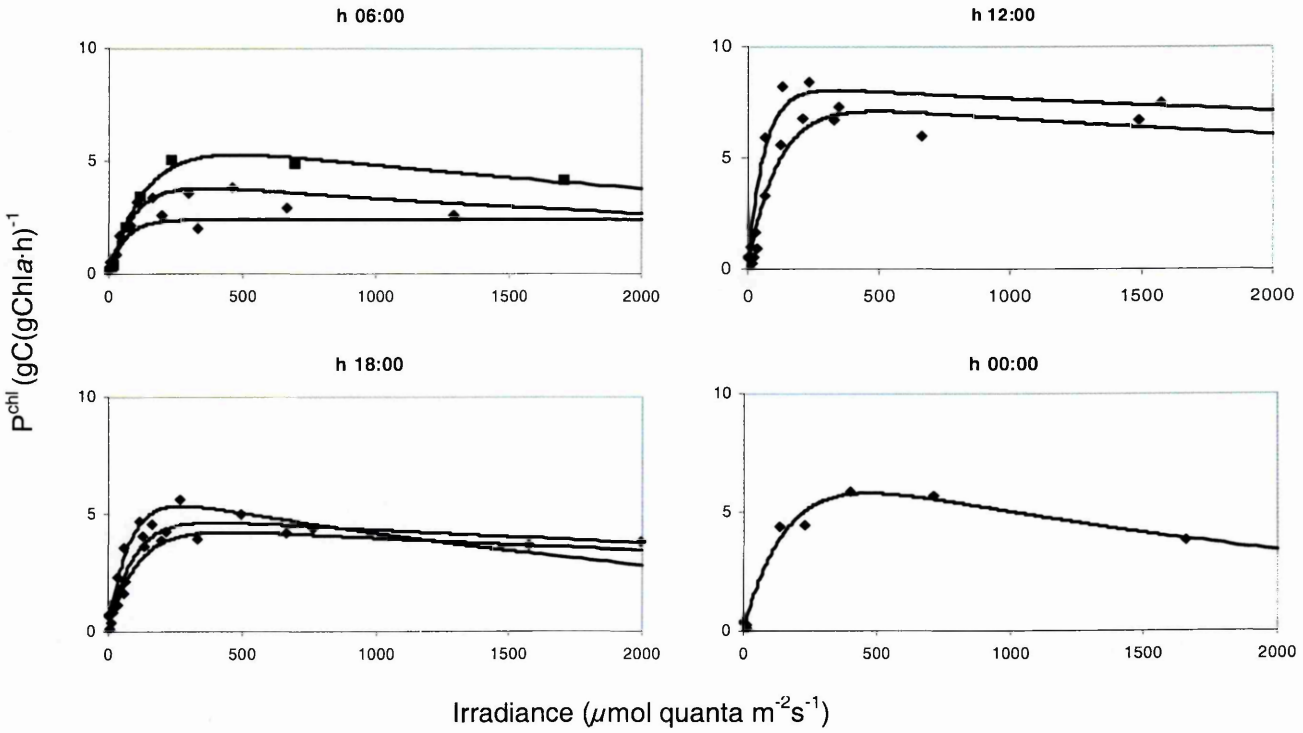

Fig. 4.17. PvsE curves measured over natural LD cycles. Dots represent P^{chl}, i.e., the amount of carbon fixed per Chl *a* unit in the time unit, measured under 9 irradiance levels. Curves were derived by fitting the data with *Eq. 3.1*. Labels indicate local time of the samples, while data from the curves are plotted vs "circadian time" in the following figure

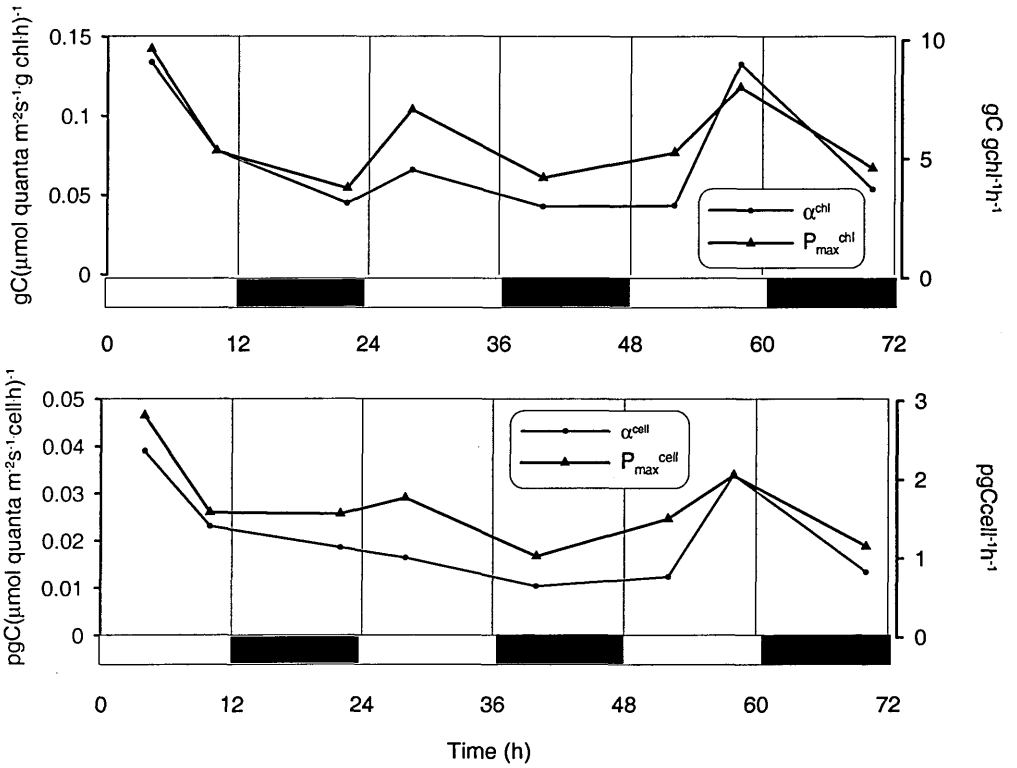

Fig 4.18. Circadian distribution of Chl *a* normalized (a) and cell normalized (b) PvsE coefficients over natural LD cycles (exp. SPRING)

4.3.3 Variable fluorescence

Fluorescence derived parameters, reported in Fig. 4.19, showed clear cyclic patterns, but exhibited some differences with respect to the ALE. The $rETR_{MAX}$ maxima occurred in the first minutes of the morning, while minima appeared at the beginning of the night, thus decreasing values were recorded throughout the day and increasing values during the night.

The α_{PAM} time distribution was characterized by evident drops in the central part of the day, in phase with F_v/F_m. In continuous dark conditions, almost all photosynthetic

coefficients lowered and flattened (not shown), as well as the mean cell pigment content (shown in Fig. 4.20a). Surprisingly, some periodicity was conserved in the $rETR_{max}$ for at least 3 cycles in the dark, but with significantly lower average values (Fig 4.20b). As soon as cells were exposed again to the sunlight, $rETR_{MAX}$ quickly recovered the values typically observed under daylight.

The estimate of NPQ under natural light revealed a quite complicated pattern, reported in Fig. 4.21. SV_0 and SV_M displayed maxima in the first part of the day and minima in the second (sometimes central) half, but additional relative maxima occur at night.

Finally, since the FRR fluorometer was not available during the experiment SPRING I report FRRF data acquired under natural light in the experiment URA,

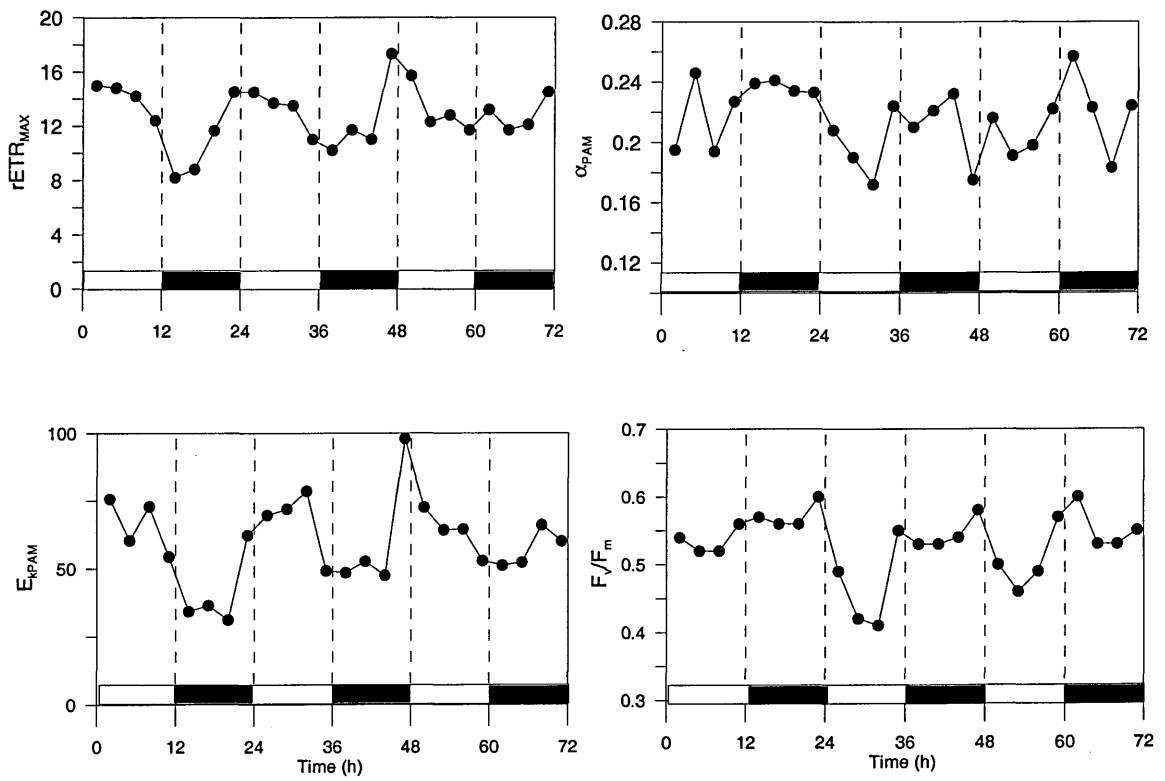

Fig. 4.19. Fluorescence-based (Phyto-Pam) photosynthetic coefficients in natural LD cycles (exp SPRING)

performed on a mixed culture dominated by PT and *Pyramimonas sp.*

The diurnal distribution of σ_{PSII} (Fig 4.22a) was characterized by evident minima corresponding to the highest irradiance intensities (PAR > 500 μmolquanta·m^{-2}s^{-1}, exp. URA). These minima were often accompanied by strong reductions in the absolute values of both F_0 and F_m, and of their values normalized by chlorophyll *a* concentration (F_0^{chl}, F_m^{chl}, reported in Fig. 4.22b), which indicates the occurrence of dissipating processes (i.e. NPQ). Also in this case, the time pattern of σ_{PSII} was in opposite phase with respect to pigment concentrations that were highest during light periods (not shown).

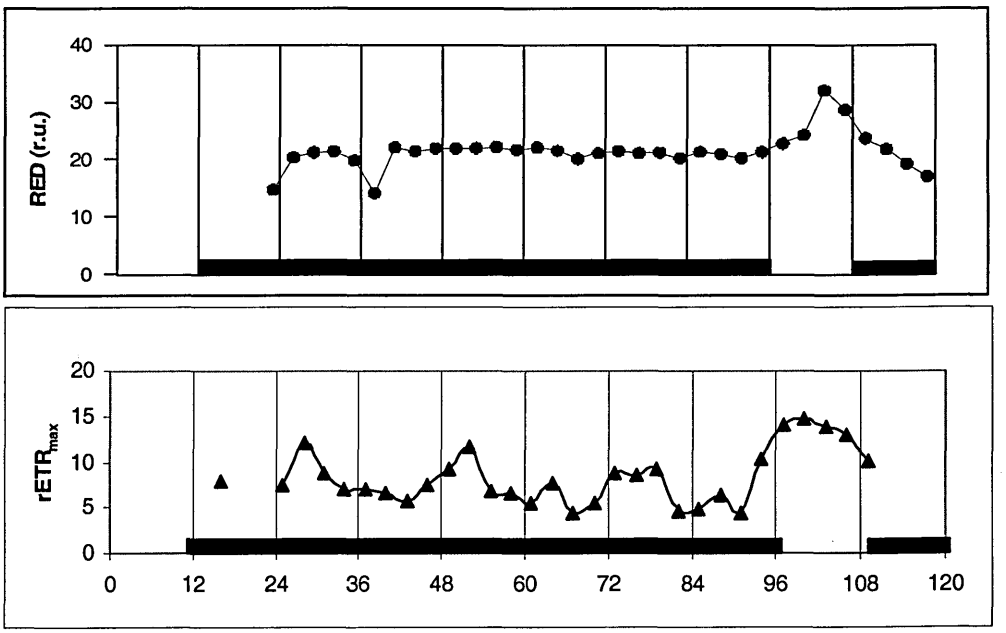

Fig. 4.20 Cell red fluorescence (upper panel) and Phyto-PAM derived $rETR_{MAX}$ (lower panel) in PT cells grown in natural LD and darkened for 84 hours (exp SPRING)

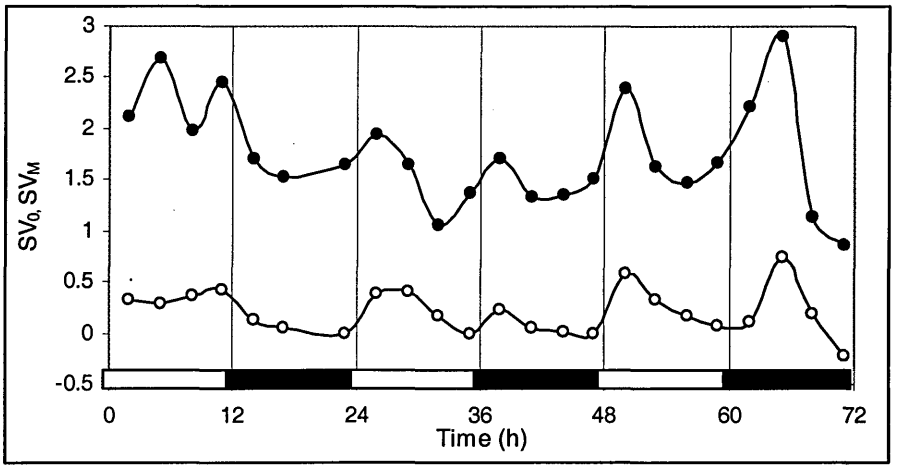

Fig. 4.21. Circadian patterns of NPQ coefficients: SV_0 (open circles) and SV_M (closed circles) measured at 800 μmolquantam^{-2}s^{-1} by means of PhytoPAM over natural LD cycles (exp. SPRING)

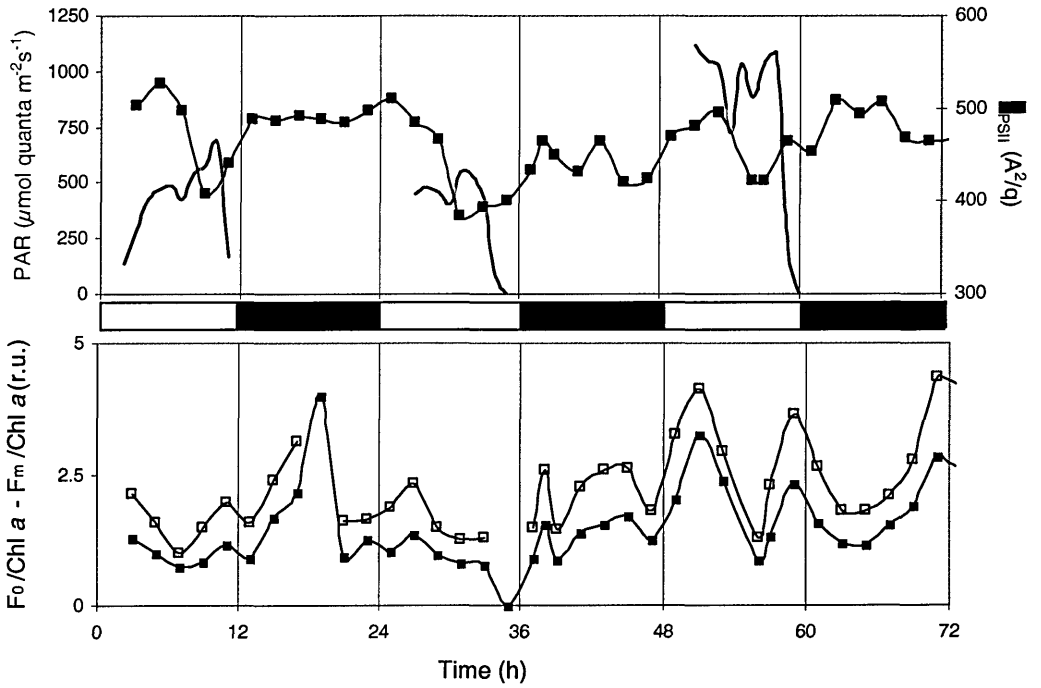

Fig 4.22. FRRF-derived parameters measured on a mixed culture under natural light (exp. URA). Upper panel: σ_{PSII} (squares) and PAR irradiance (red line) measured within the culture. Lower panel: minimal and maximal fluorescence yields normalized by chlorophyll concentration

4.3.4 Summary

Under natural light, all the components of the photosynthetic machinery of PT showed a periodic pattern over the diel cycle. PT cells maximized their pigment content some hours earlier than in the artificial light regime. On the other hand, Ddx still anticipated the occurrence of the other pigments, and Ddx/Chl *a* peaked in the first part of the day, similarly to the ALE.

Fluorescence-based photosynthetic parameters displayed similar or anticipated peaks with respect to what was observed in the ALE. The $rETR_{MAX}$ peaked very early in the morning under very low levels of sun irradiance, while the other fluorescence-derived coefficients displayed quite strong diel patterns, as compared to the ALE results. In particular, concurrent minima were measured in F_v/F_m, α_{PAM} and σ_{PSII} under high irradiance, thus indicating non-photochemical quenching (NPQ) processes both in the antenna and in the RC (Falkowski and Raven, 1997). Hence comparison of the results of ALE and NLE shows that cells adapted to a sinusoidal light pattern tend to anticipate the variation of basic photophysiological parameters and that also the amplitude of the variation is different. The reason for those differences might have resided, apart from the above mentioned difference in the spectral properties, in the different time course of the irradiance, i.e., in the variation of light intensity. Therefore I focused on the relative weight of photoacclimation, short term photoresponses and internal controls in driving the reported circadian patterns to explain the differences observed in NLE vs ALE. In other words, I investigated on the role of light changes in modulating the timing of the photophysiology of PT.

4.4 The effect of changes in light regime on the diel variability of pigment content and fluorescence-derived parameters

This section includes studies on the effect of light variability on the circadian patterns of PT photophysiology. In particular the results I present derive from "short" experiments devoted to discriminate properties and processes strictly related to day-night cycles from those merely driven by light changes *per se*, in terms of either growth irradiance, or duration of photoperiod, or unexpected light transitions. In the following, PTH and PTL refers to PT cultures grown at 200 μmolquanta·m^{-2}s^{-1} and at 40 μmolquanta·m^{-2}s^{-1}, respectively, while PTHH and PTLH are the notations used to indicate the two cultures during their exposition to higher irradiance (i.e. 400 μmolquanta·m^{-2}s^{-1}, experiment CICLAC).

4.4.1 The effect of growth irradiance

4.4.1.1 Pigments

As expected, different growth irradiance induced differences in the mean level of

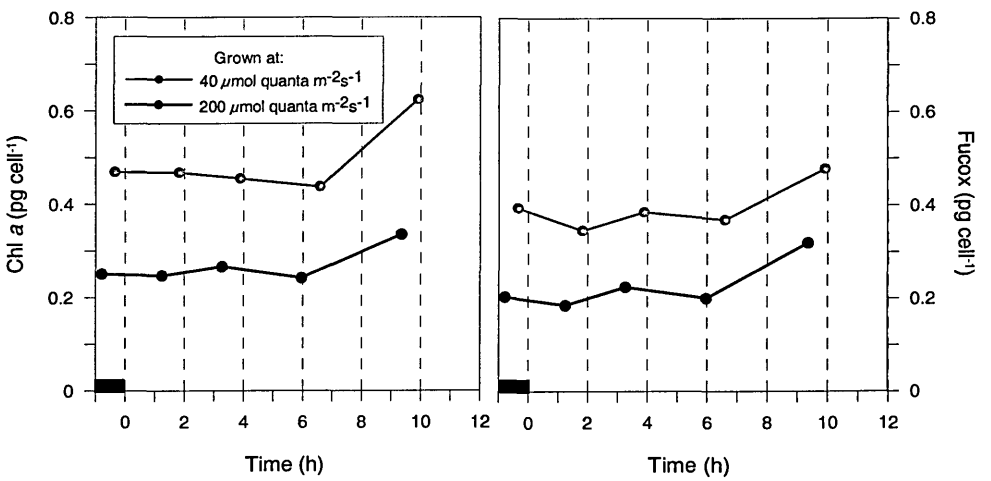

Fig 4.23. Time distribution of cell pigment concentrations in cultures of PT grown under the indicated irradiances (Exp CICLAC)

pigment content. Thus, higher amounts of light harvesting pigments were found in cells exposed to lower light flux, as shown in Fig 4.23. The amount of PPC showed a reversed dependence on growth irradiance, but only under daylight, as evident in the pigment ratios reported in Fig. 4.24.

On the diel scale, the time distribution of light-harvesting pigments was similar in the two light conditions, and in line with the previously reported trends. On the other hand, the time pattern of Ddx to Chl *a* ratio was significantly different in the two cultures: in PTH cells the ratio displayed the lowest value in the dark, the highest at the 3rd circadian hour and high values in the following six hours. On the contrary, in PTL cells the ratio showed a flat time course, and values comparable to those measured at night in both cultures. By contrast, the time pattern of βcar/Chl *a* was similar in the two cases.

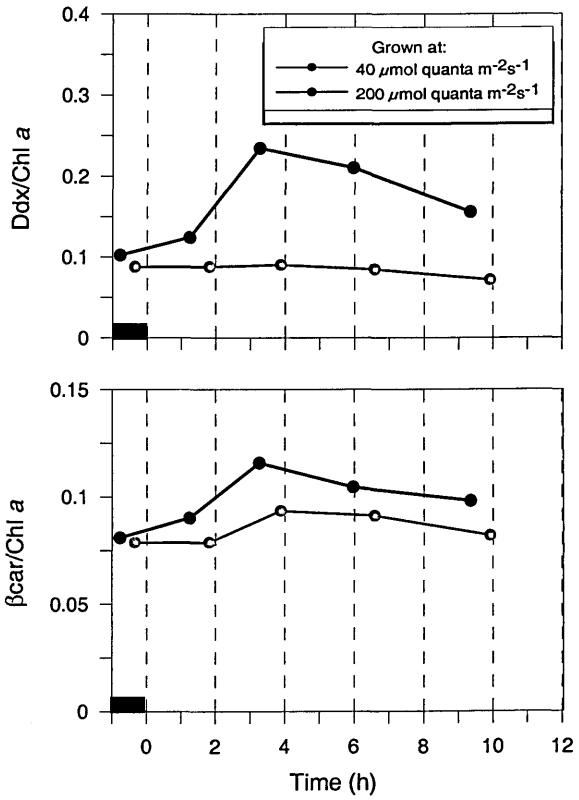

Fig 4.24. Time distribution of pigment ratios in cultures of PT grown under the indicated irradiances (Exp CICLAC)

4.4.1.2 Variable fluorescence

Different growth irradiance induced also different average values of the fluorescence-retrieved coefficients (Fig 4.25). The photoacclimation index E_{kPAM} displayed positive correlation with the growth irradiance, as expected. Also in this case, the

variability in E_{kPAM} was mostly driven by the variability in $rETR_{MAX}$, with α_{PAM} being rather constant over the different growth light levels. SV_M was higher in PTH than in PTL. On the diel basis the time distribution was similar in the two cases, i.e. the maximal variability in photosynthetic coefficients occurred corresponding to the light-dark transitions.

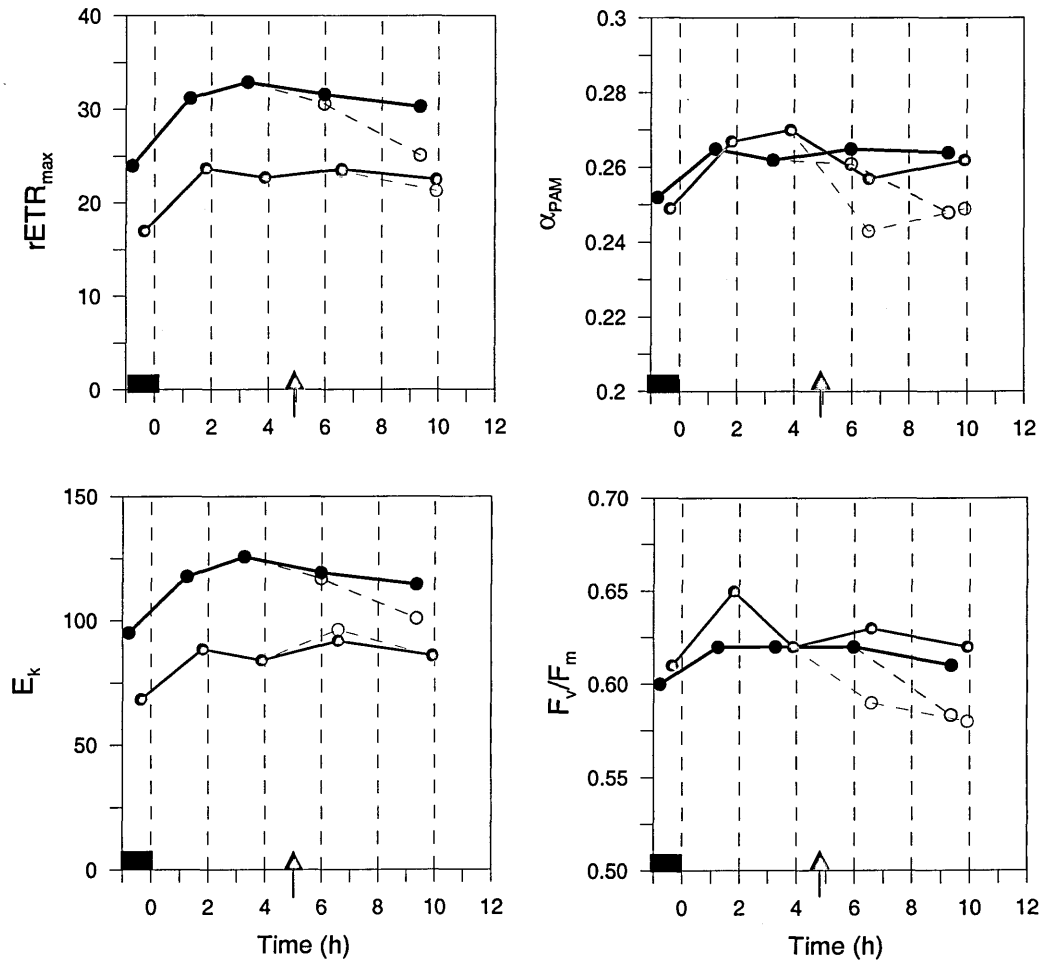

Fig 4.25. Time variability of Phyto-PAM photosynthetic coefficients in two growth irradiance conditions: 40 μmolquanta $m^{-2}s^{-1}$ (red line) and 200 μmolquanta $m^{-2}s^{-1}$ (black line) and the effect of a shift to 400 μmolquanta $m^{-2}s^{-1}$. Dashed lines refer to the cultures during the exposition to high light. The time of the light transition is indicated by the arrow (exp. CICLAC)

4.4.2 The effect of light shifts

4.4.2.1 Pigments

The 5 hrs exposure to 400 μmolquanta·m^{-2}s^{-1} did not induce any significant change in light harvesting pigments in both cultures (~5% variation in cell Chl *a* content, not shown). On the other hand the photoprotectant pool rapidly and considerably enhanced in both cases. In particular, PTHH cells showed 40 and 60% higher Ddx concentration than PTH, 1 and 5 hours after the light shift, respectively. Even more drastic increases were found in PTLH that exhibited up to 138% larger Ddx content than control. βcar displayed the highest increase after 1 hour (about 37% in both cases). Dtx was detected only after the

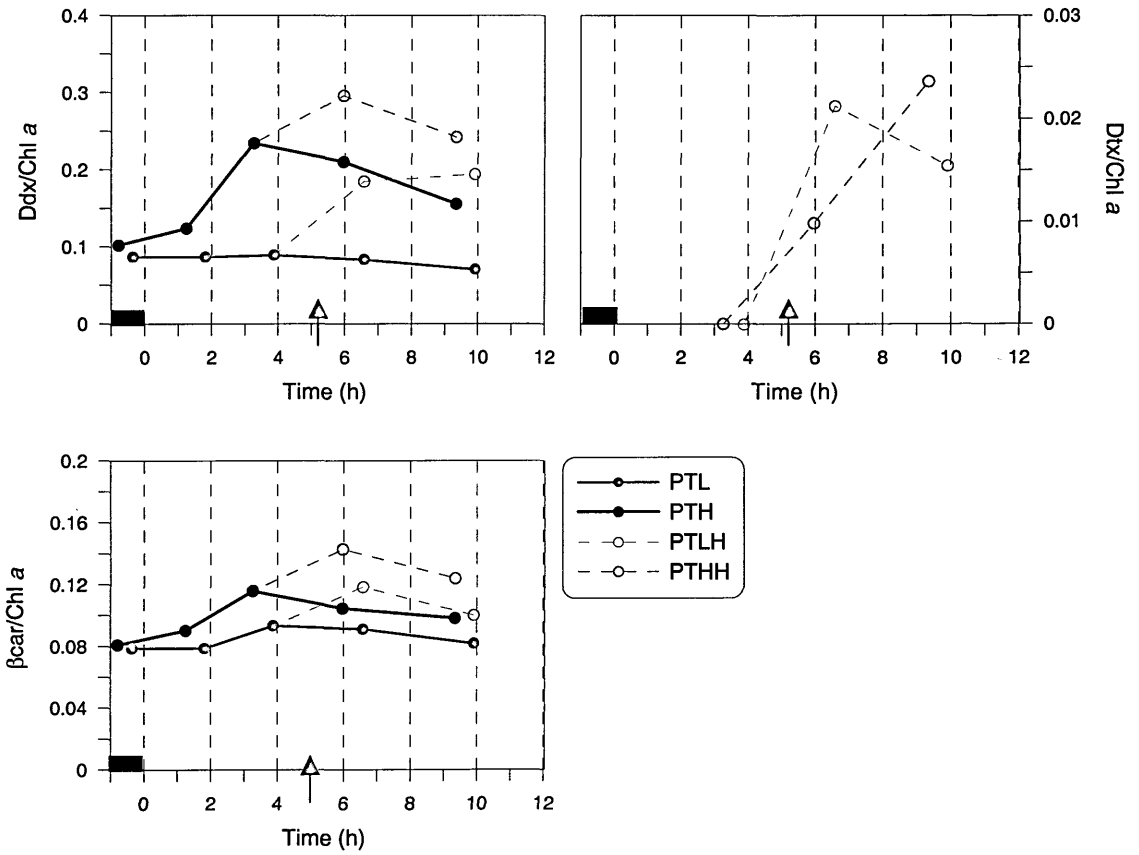

Fig 4.26. The effect of a shift to high light (400 μmolquanta m^{-2}s^{-1}) on the time variability of the indicated pigment ratios on PT cultures grown under two irradiance levels: 40 (red line) and 200 μmolquanta m^{-2}s^{-1} (black line). Dashed lines refer to measuremnt performed during the exposition to high light, solid lines indicate the control. The time of the light transition is indicated by the arrow (exp. CICLAC)

light shift. Its rise was quicker in low light acclimated cells, so that after one hour Dtx was higher in PTLH than in PTHH, whereas after 5 hours PTHH displayed slightly higher content.

More information can be derived by from the study of the pigment ratios. Normalizing each pigment concentration by the amount of chlorophyll *a* it was possible to better discern relative variations within the whole pigment pool. The data reported in fig 4.26 revealed that in both cases the ratios between any of the PPC and Chl *a* increased in high light. Moreover the level of accumulation of each pigment was comparable in the two cases. This was true also for Ddx whose concentration before the light shift was very low and constant in PTL cells, as pointed out above.

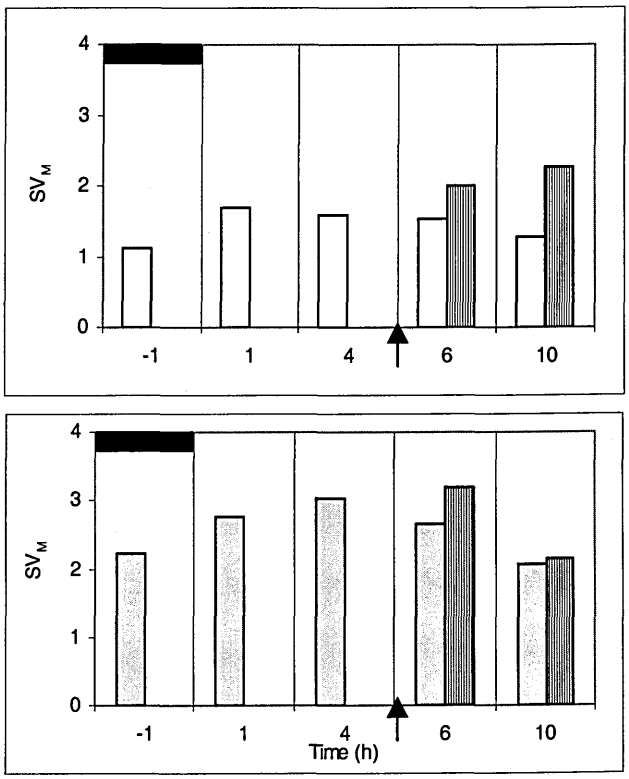

Fig. 4.27. (Exp. CICLAC). Circadian variability of SV_M for two PT cultures grown at different light levels: 40 μmolquanta $m^{-2}s^{-1}$, (PTL, white bars) and 200 μmolquanta $m^{-2}s^{-1}$, PTH, grey bars) and the effect of an unexpected transition to high light (400 μmol quanta $m^{-2}s^{-1}$). Vertical lined-bars refer to cultures exposed to high light. The time of the light transition is indicated by the arrow. SV_M coefficients were determined at 1350 μmol quanta $m^{-2}s^{-1}$ by means of Phyto-PAM

4.4.2.2 Variable fluorescence

The shift to higher irradiance induced reductions in both $rETR_{MAX}$ and α_{PAM} (Fig 4.25). Variations were greater and quicker in α_{PAM} than in $rETR_{MAX}$ in low light acclimated cells, whereas the opposite occurred in high light acclimated cells that responded to high

light with a faster and stronger reduction in $rETR_{MAX}$ than in α_{PAM}. E_{kPAM} remained rather constant in both cases. The SV_M coefficient increased in response to the light stress. The major changes occurred in the culture grown in the lowest light regime (4.27), starting from lower levels. Moreover, while the culture grown in low light showed the level of quenching linearly increased with the time elapsed under stress, in the other case the effect of the light shift was more evident after 1 hour of incubation than after 5 hours. It can be noticed that day-night transition induced comparable or higher variation in SV_M.

4.4.3 The effect of the duration of photoperiod

4.4.3.1 16:8LD cycles

PT cells adapted to 16L:8D cycles showed a continuous increase in cellular pigment content throughout the whole light period, followed by a more rapid decrease in the (shorter) dark phase, as evident from red fluorescence flow cytometry data, reported in Fig. 4.28a (red line). On the other hand, cells grown in 12L:12D, when brought to 4 hours longer photoperiod (i.e. 16L:8D), showed the expected pigment peak around the 12th hour, while only

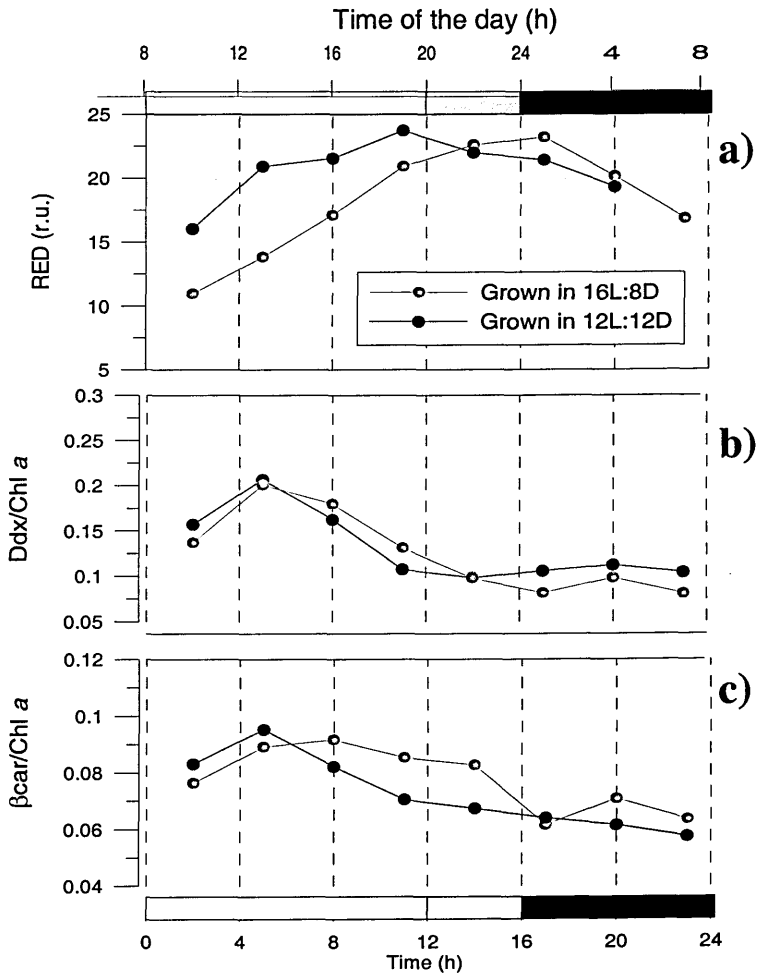

Fig. 4.28. Pigment time distribution over a 16:8 LD cycle (exp. C36). PT cells were grown under the indicated photoperiods. Grey boxes refer to subjective night for cells grown in 12:12 (black line). a) cell red fluorescence; b) Ddx/Chl *a*; c) βcar/Chl *a*

slightly decreasing values were measured in the following 12 hours. Ddx content still anticipated the occurrence of the other pigments, and a Ddx/Chl *a* maximum occurred in both cases at the 4th hour of the light period (Fig. 4.28b). Finally βcar/Chl *a* displayed some hours delay and a more flat distribution in 16:8-grown cells with respect to the culture adapted to 12:12 LD (Fig. 4.28c).

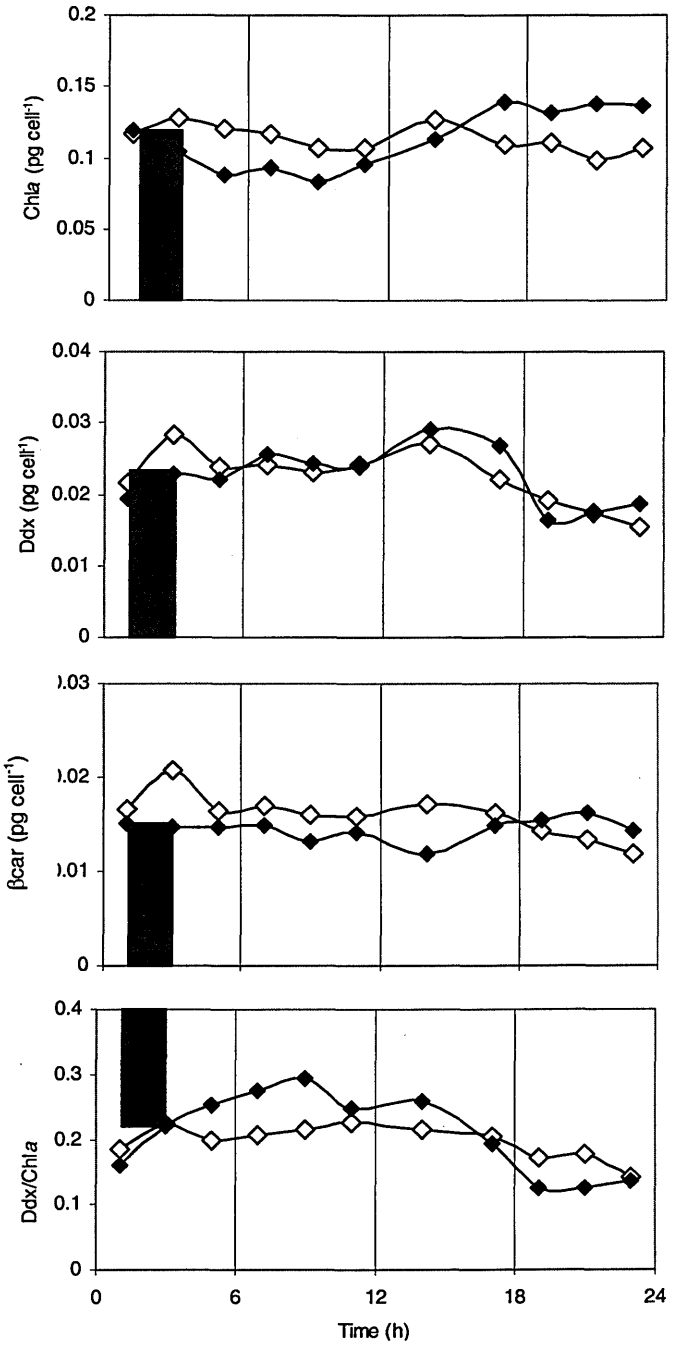

Fig. 4.29. Time distribution of PT pigments in LL conditions (open diamonds). Effect of a short (2h) dark period (indicated by the shaded box) on the same pigments (closed diamonds). The culture was grown under LL cycles for two weeks.

4.4.3.2 24 : 0 LD cycles

Pigments

Cells grown for two weeks in continuous light conditions more than tripled their number every 24 hours. Cell pigment content did not vary over the day. On the other hand, the imposition of a short (2h) dark period affected the pigment concentrations, as shown in Fig. 4.29. Chl *a* concentration decreased with respect to the control (culture exposed to LL) displaying 10-27% lower values for about 12 hours from the restoring of the light.

Afterwards chlorophyll *a* cell content increased up to values 39% higher than in the control cells not exposed to a dark period.

Ddx/cell and βcar/cell did not significantly change (Fig. 4.29b and c), except for a decrease just after the short dark period. As a consequence, Ddx/Chl *a* (Fig. 4.29d) and βcar/Chl *a* (not shown) changed accordingly, with high values in the first 6-8 hours after the dark period, lower afterwards.

Variable fluorescence

Fluorescence derived photosynthetic parameters did not show any particular diel pattern, although α_{PAM} exhibited some variability over the experiment duration, even in the control culture (Fig. 4.30). In the darkened culture the value of α_{PAM} dropped just after the dark period, then it rose up to (the hypothetical) midday, afterwards it declined, thus

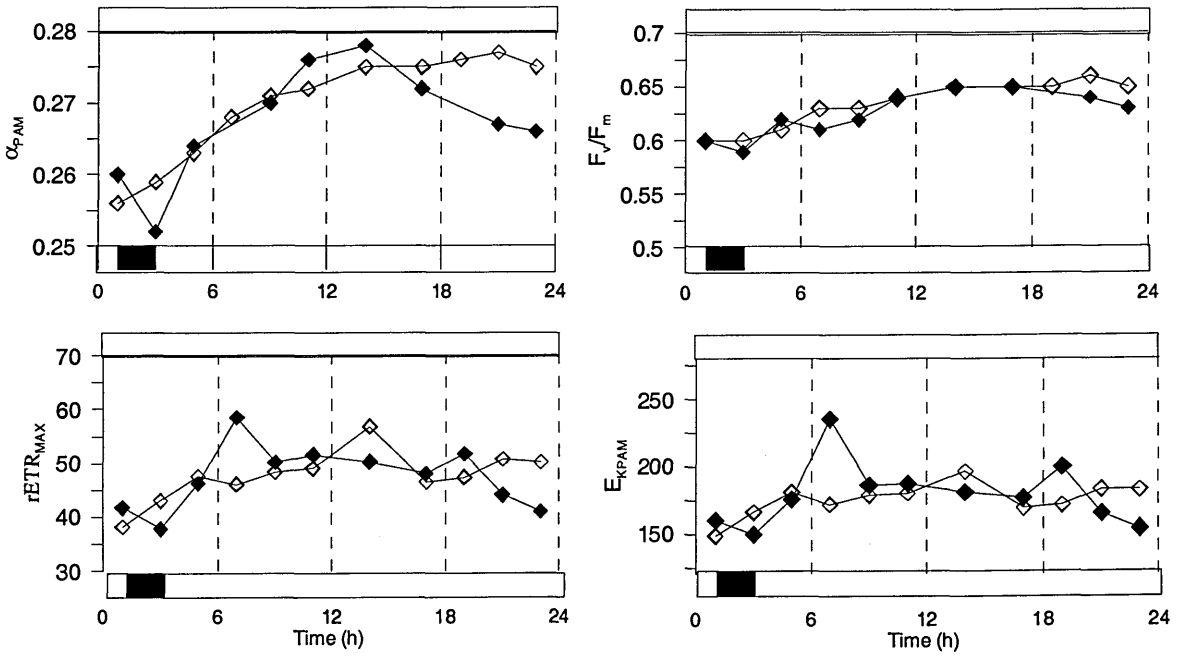

Fig. 4.30. Time distribution of fluorescence-derived photosynthetic coefficients of PT cells in continuous light conditions (open diamonds). Effect of a short (2h) dark period (indicated by the black box) on the same parameters (closed diamonds). The culture was grown under LL cycles for two weeks

significantly differing from the culture not exposed to dark. F_v/F_m was flat over time and not at all affected by the dark period. $rETR_{MAX}$ and E_k did not display strong diel variations, but the dark period induced immediately a slight decrease of both parameters, followed by a steep increase, resulting in a peak 6 hours later, resembling in some way the distribution usually observed after the onset of light in LD regime.

4.4.4 Summary

Growth intensity affects both pigment levels and photosynthetic performance according to expected schemes: low light acclimated cells exhibit high concentration of light harvesting pigments, reduced photoprotectant pool, low $rETR_{MAX}$ and E_{kPAM}. The reversed pattern is observed in high light acclimated cells.

With respect to diel cycles, similar time variability was found under two growth irradiance conditions (cultures PTL and PTH) for all investigated parameters, with the exception of Ddx/Chl *a* ratio which exhibited no diel periodicity in low light acclimated cells. On the other hand, the unexpected exposure to HL induced rapid synthesis of Ddx, with kinetics comparable to that shown by high light acclimated cells.

The light shift modified to a major extent photoprotectants rather than light harvesting pigments in both cases, according to the patterns outlined for acclimation to the growth irradiance. On the contrary, variations on the functional level were in some way opposite to what was observed for growth irradiance, at least for $rETR_{MAX}$ that decreased along with increasing light, as well as α_{PAM}. However, since in both cases (high and low light acclimated cells) $rETR_{MAX}$ and α_{PAM} varied in parallel, E_{kPAM} did not significantly change, and therefore the overall effect was the maintenance of the photoacclimation index.

A photoperiod extended by 4 hours (16:8LD) did not change some of the persistent features of the pigment distribution over 12:12 LD, the anticipated accumulation of Ddx within PT cells, and the occurrence of the Ddx/Chl*a* in the first part of the L period (around the 4th hour). On the other hand, the time distribution of the remaining cell pigment pool followed the LD (16:8) cycle. On the contrary, algae grown in the absence of dark periods still recover a certain degree of variability after the imposition of a dark period, even if short.

Since all the experiments described so far were performed on algal cultures, I investigated whether similar patterns in photophysiological parameters would occur in natural plankton populations *in situ*. It is worth noting that the responses observed in natural assemblages reflect the average behaviour of the components. If a circadian regulation of photophysiology did evolve in phytoplankton communities as an adaptive advantage, then it should manifest as a widespread feature in nature and therefore the average response should mimic what I observed in monospecific cell suspensions. For this reason I made a specific experiment *in situ*.

4.5 Circadian patterns of pigment concentrations and photosynthetic parameters in situ

The experiment TRICICLO was carried out in spring (April 2003) in a coastal site of the Mediterranean Sea. Samples were collected from two depths, 5 and 45 m, roughly corresponding to the first optical depth and the bottom of the euphotic zone, respectively. At 5 m, irradiance varied over the day from 0 to 600 μmol quanta·m^{-2}s^{-1} (ca 35% of the incident PAR), whereas at 45 m, the midday value was about 15 μmol quanta·m^{-2}s^{-1} (ca 1% of PAR at the sea surface).

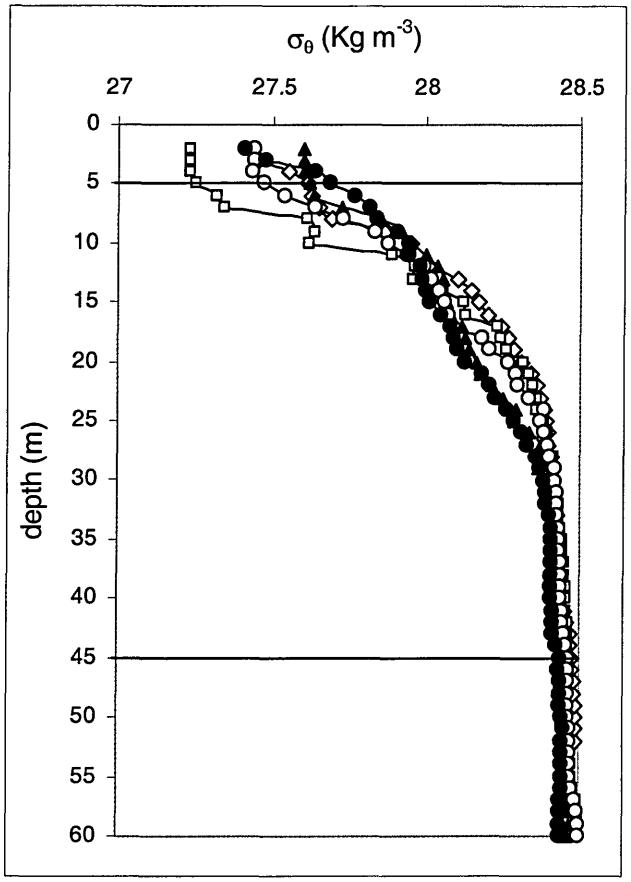

Fig. 4.31. Density profiles acquired during the experiment TRICICLO at different times. Open symbols refer to measurements performed in the daytime: 7.00 (circles), 15.00 (diamonds), 17.00 (squares). Closed symbols indicate nocturnal profiles: 00.00 (circles), 5.00 (triangles). Horizontal lines indicate the two sampling depths

The physical structure of the water column was characterized by a mixed layer depth varying between 5 and 10 meters depending on the time of the day (Fig. 4.31), due to the effect of heat exchanges between air and sea. This resulted in lower surface density values during the afternoon. A seasonal pycnocline was evident between 10 and 30 meters and a homogeneous stratum occupied the bottom layer below 30 m (the bottom depth was about 70 m). Thus, the population sampled at 5 m was likely to experience conditions varying between 0 and 10 m, whereas the population sampled at 45 m may be considered representative of the layer below 30 m.

4.5.1 Pigments

Chlorophyll *a* concentration was similar in the two populations, since it ranged between 0.17 and 0.36 μg/l in the surface and between 0.23 and 0.31 μg/l at 45 m. In both stations the size class smaller than 5 μm was dominant (about 80% of the total).

As reported in Fig 4.32, the pigment composition of the surface and deep population revealed the dominance of golden-brown microalgae, as indicated by the high concentration of the pigments 19'hexanoiloxyfucoxanthin (~25% of the accessory pigments at 5m, ~30% at 45m), 19'butanoyloxifucoxanthin and fucoxanthin (around 9 % in both populations) and

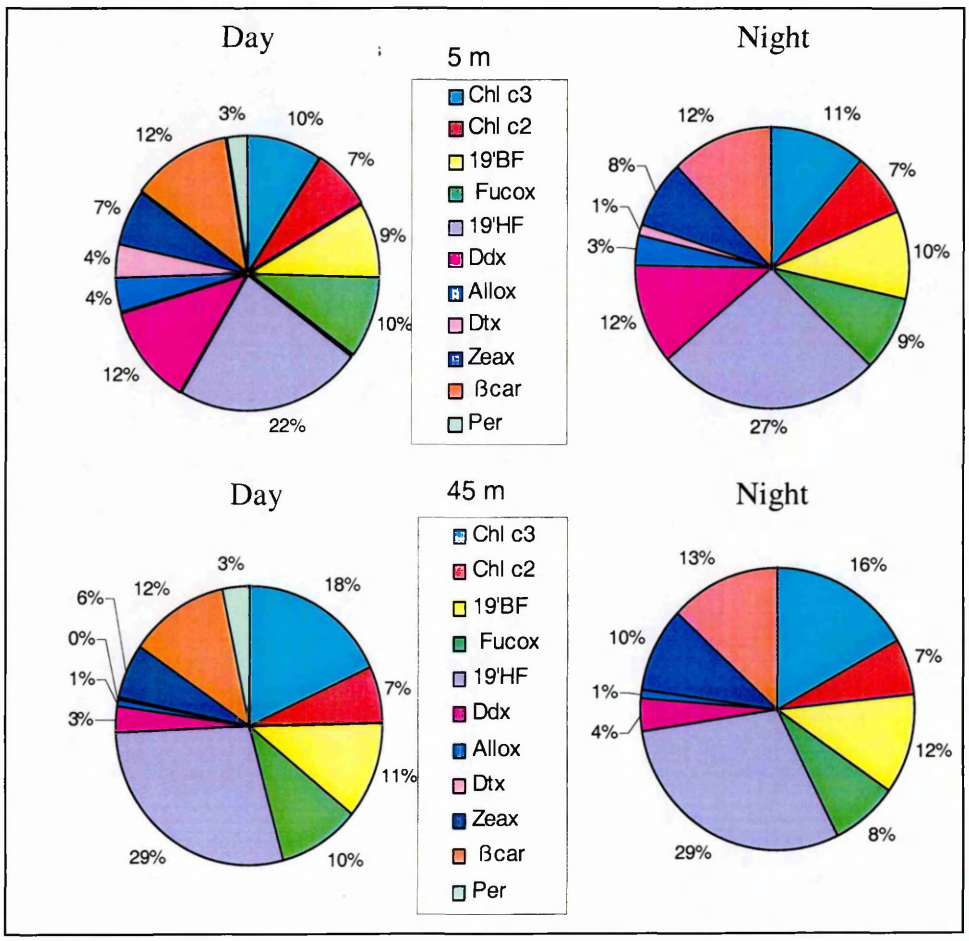

Fig 4.32. Diurnal and nocturnal averages of the relative percentages of pigments (excluding Chl *a*) detected at the indicated sampling depths of a South Tyrrenian Site (exp. TRICICLO). Chl *a* represented about 40 % of the total in both cases

diadinoxanthin (12% in surface and 3% below), which indicated the presence of prymnesiophyceae, crysophyceae and diatoms.

The detection of zeaxanthin (7-8%) and peridinin (3-2%) revealed the presence of cyanophyceae and dinoflagellates, respectively.

Chlorophyll *c* was present as c_3 with 10% in surface and 17% at depth, whereas chlorophyll c_2 concentration was similar (7%) in both populations, as well as βcarotene (12%). Note that the reported relative percentages refer to daily averages of all the detected pigments excluding chlorophyll *a*, which represented 38-40% in both classes of samples.

Dtx was detected in all surface samples, where the average diurnal (12 h) concentration accounted for 4% of the total pigment pool on average, and for 8% at the maximum measured level (at 10:00 h, not

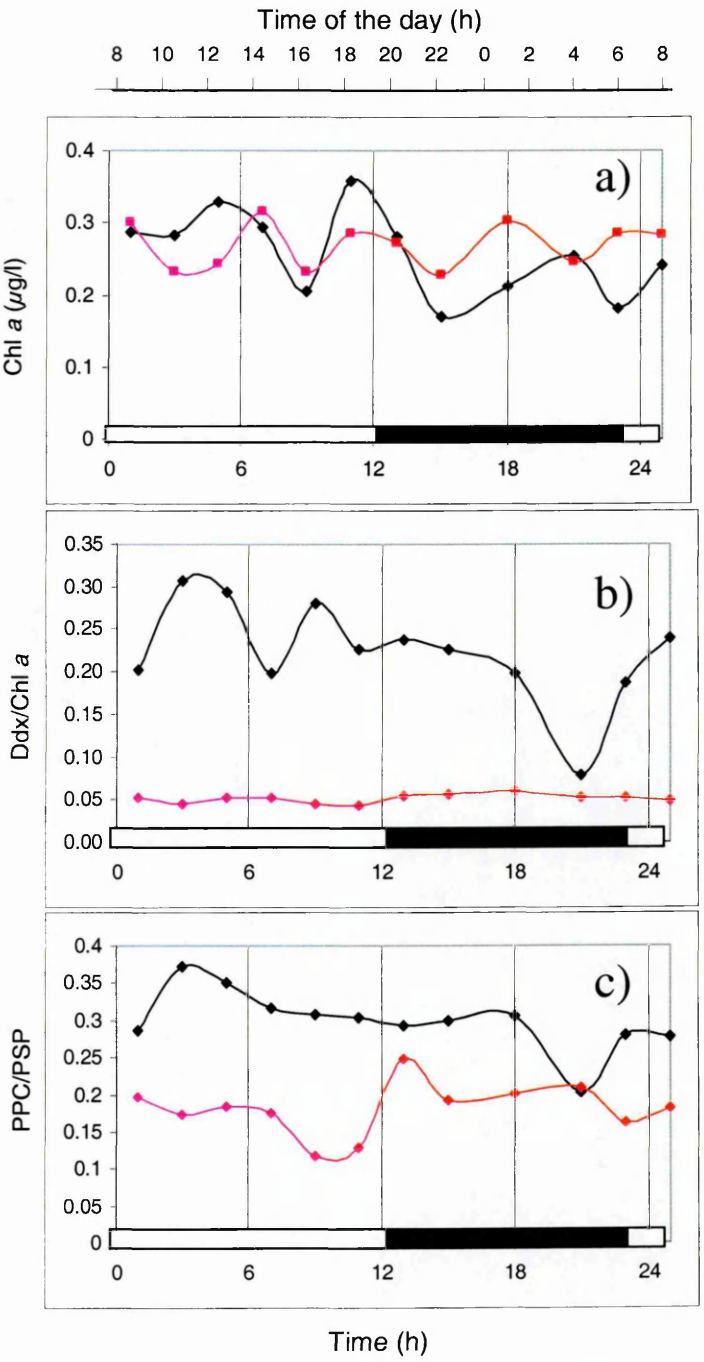

Fig 4.33. Circadian distribution of pigments at at 5m (black line) and 45 m (red line) of a South Tyrrenian site (exp. TRICICLO) a) chlorophyll *a*. b): (Ddx+Dtx)/Chl *a* c) PPC/PSP

shown). Very small amounts of Dtx were detected at depth only at midday.

In Fig. 4.32 the relative percentage of accessory pigments detected in the two classes of samples was averaged over the diurnal and nocturnal period. The comparison revealed that greater differences occurred between the two depths than in the same population due to the day-night cycle. On the other hand, the time and vertical distribution of the (Ddx+Dtx)/Chl *a* reflected what was observed in PT cultures: under high irradiance the ratio displayed some circadian variability with high values in the first part of the day, while in light limited conditions low values and flat time distributions were observed (Fig 4.33). The pattern was basically driven by differences in Ddx, since the Chl *a* content did not show any significant difference in either the vertical, or over the diel time scale. The same is true for the ratio between PPC and PSP, which revealed the expected differences between the surface and the deep populations with higher values in the former throughout the day (Fig. 4.33).

Differences in the PPC/PSP ratio were found in the two populations also on the diel scale: in the surface layer the ratio was high in the first part of the day (8.00-12.00 h), and decreasing afterwards. On the contrary 45m values were lower during the day than over the night.

4.5.2 PvsE parameters

PvsE experiments were performed on both populations at four sampling points: dawn, midday, dusk, night (Fig 4.34 and 4.35). The duration of the incubations was 1 hour.

Also in this case the coarse resolution of the measurements did not allow the detailed reconstruction of the circadian variability, even though some interesting features emerged.

The families of curves from the two populations displayed macroscopic differences reflecting photoacclimation to different light levels: photosynthetic efficiency was significantly higher at depth than in the surface layer, and P^{chl}_{max} capacity was higher in surface. On the other hand, the time distribution of PvsE parameters was similar in the two populations, i.e. maxima at midday, minima at night and intermediate, and practically identical, values at dawn and dusk. Some differences among coefficients emerged: in surface samples P^{chl}_{max} varied by a factor of ca 5 over 24 hours (1.9-10.5 gC(gChl*a* h)$^{-1}$), while in samples from 45m, the same coefficient varied over a more narrow range (1.5 –3.7 gC(gChl*a* h)$^{-1}$). On the contrary, α^{chl} did not show any circadian variability at 5m, while at 45 m it displayed excursions at of the same extent as those of P^{chl}_{max}. Consequently, in the surface layer, the time distribution of E_k strictly followed that of P^{chl}_{max}, spanning from 70

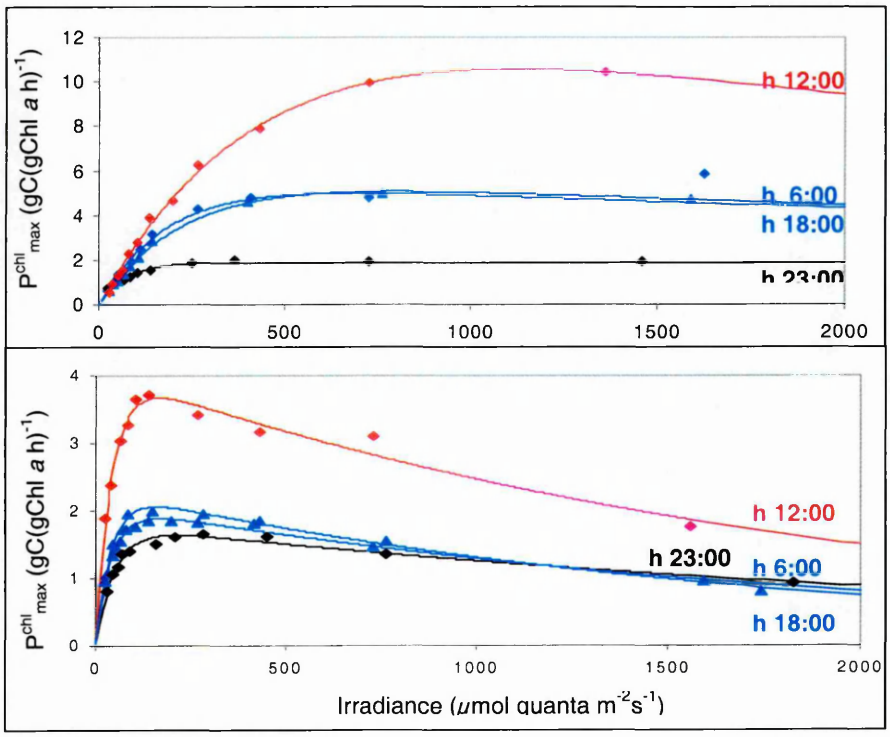

Fig 4.34. PvsE curves measured on natural samples at different times over a diel cycle on two sampling depths (exp. TRICICLO): 5 m (panel a) and 45 m (panel b). Please note the different scales on y axis

to 350 μmol quanta·m^{-2}s^{-1}, while at depth, because of the parallel (and similar) variations of P^{chl}_{max} and α^{chl}, E_k was quite constant over the experiment.

4.5.3 Variable fluorescence

The time distribution of Phyto-PAM derived coefficients over the two sampling depths are reported in Fig 4.36. The E_{kPAM} coefficient was definitively higher at 5m than at 45 m under daylight, whereas quite similar values were measured at night at the two sampling depths. Despite the large differences in irradiance conditions, and in opposition to what was previously reported (exp. CICLAC), $rETR_{MAX}$ varied over very similar ranges in the two cases, whereas α_{PAM} displayed the greatest dissimilarity.

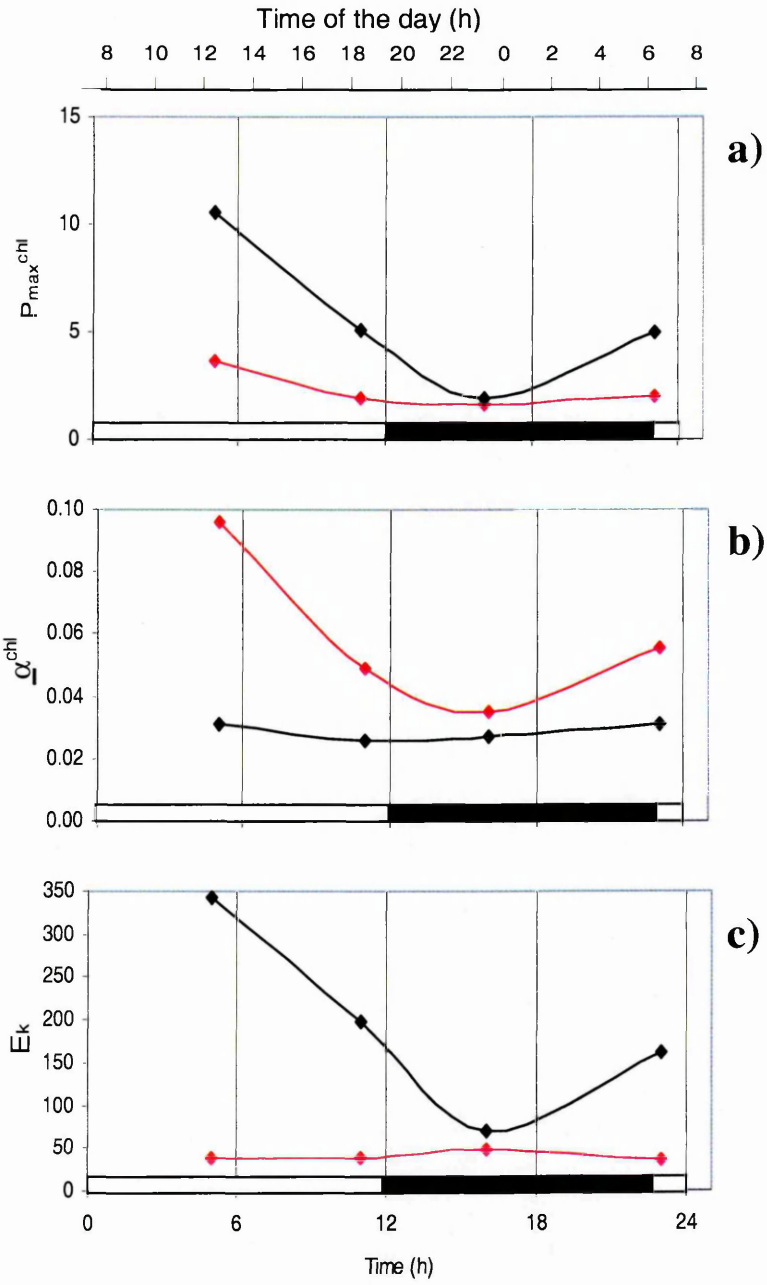

Fig 4.35. Circadian distribution of PvsE coefficients measured on natural samples from 5m (black line) and 45 m (red line) of a South Tyrrenian site during the exp. TRICICLO. a) α^{chl} (gC(gChl *a*·h·μmolquantam^{-2}s^{-1})$^{-1}$) b) P^{chl}_{max} (gC(gChl*a*·h)$^{-1}$) c) E_k(μmolquantam^{-2}s^{-1}). Note that the last measurement reported was performed at dawn (h 6:00)

In fact, in the surface it exhibited a strong decrease in the central part of the day, which did not appear at 45 m. Therefore α_{PAM} changes were mostly responsible for differences in

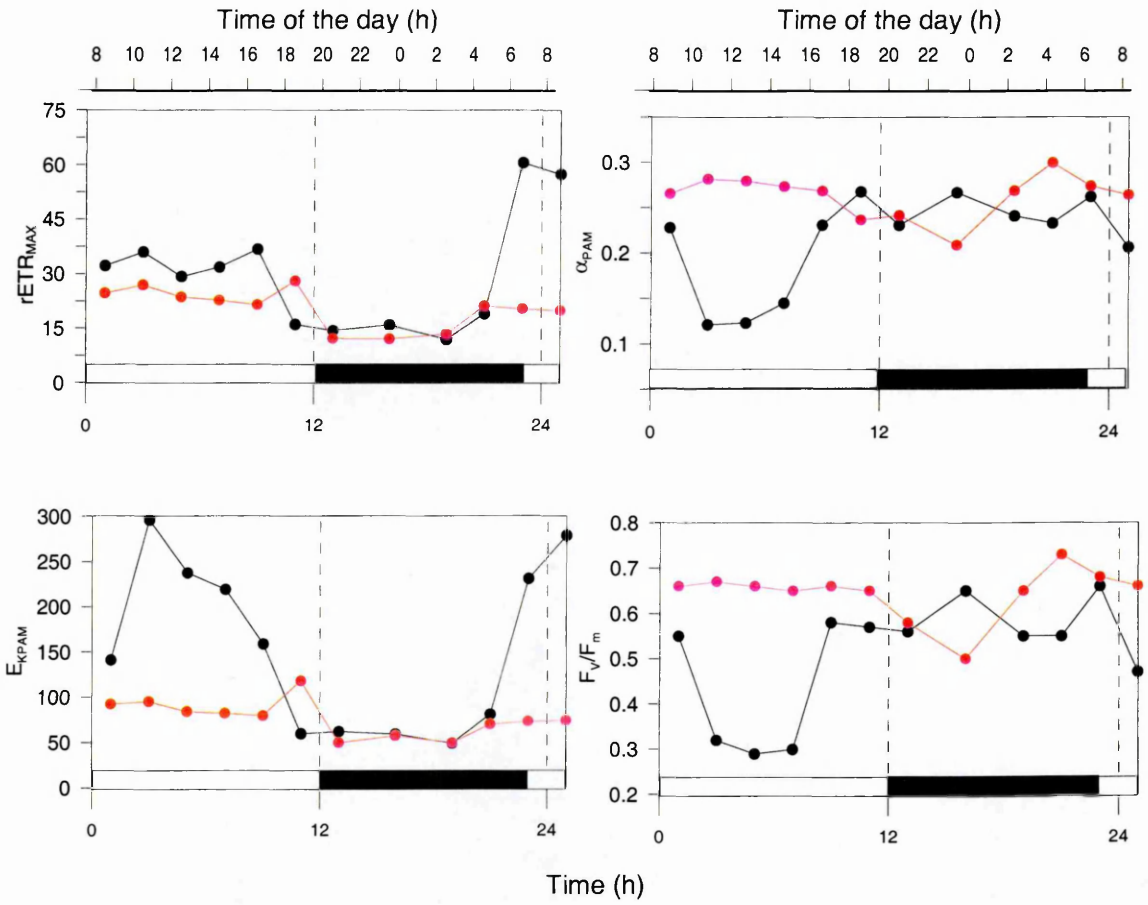

Fig 4.36. Circadian distribution of PhytoPAM-derived photosynthetic coefficients measured on natural samples collected at 5m (black line) and at 45 m (red line) during the exp. TRICICLO. Note that the last two measurements were carried out in daylight (6:00 and 8:00)

E_{kPAM}. σ_{PSII} displayed a pattern similar to α_{PAM}: definitively higher at depth under daylight whereas similar to the surface at night.

On the diel scale, all the Phyto-PAM coefficients, F_v/F_m, α_{PAM}, $rETR_{MAX}$, E_{kPAM} displayed high variability in samples from 5 m and little variations in phytoplankton living at 45 m.

In particular, α_{PAM} displayed its minima under maximal sun irradiance and high and constant values at night in the surface layer. The same time distribution was observed in F_v/F_m, whereas $rETR_{MAX}$ displayed the opposite behaviour, with the highest values under daylight. On the other hand, samples from 45 m showed the reversed pattern both in α_{PAM}

and F_v/F_m, since they exhibited the highest values during the day and decreasing values in the first part of the night even if, as already mentioned, the excursions were not as significant as in samples from 5m. On the contrary, $rETR_{MAX}$ had the same phase in both classes of samples, even if the day-night variability was much more evident for surface samples.

σ_{PSII} showed a diurnal depression in both cases, but much stronger in surface (Fig 4.37), where it was to a certain extent in phase with α_{PAM} and F_v/F_m. As already mentioned, the concurrency of strong reductions both in σ_{PSII} and in F_v/F_m indicates NPQ occurred both in the antenna and in the RC. Conversely, the pattern observed at 45 m seems to resemble the one reported from the AL experiments, where NPQ was mainly due to antenna quenching. Finally, the typical nocturnal recovery of σ_{PSII} reported in the ALE seemed to commence during the second part of the day for these natural populations.

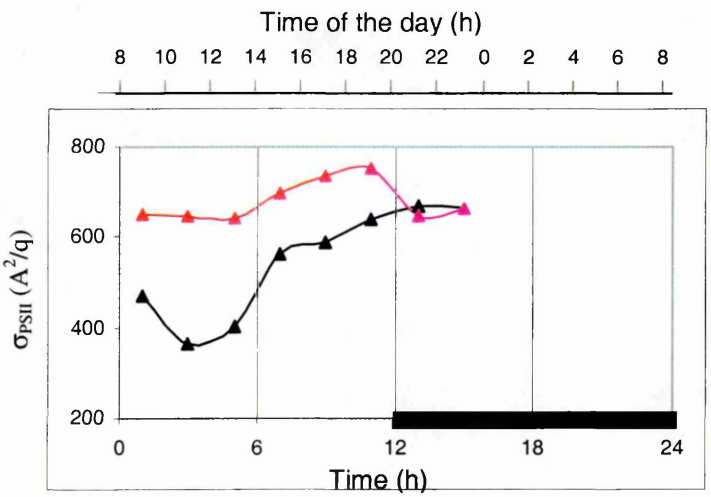

Fig 4.37. Circadian distribution of the functional cross section of PSII measured *in situ* at 5m (black line) and at 45 m (red line) by means of FRRF during the exp TRICICLO

4.5.4 Summary

The HPLC analysis revealed the dominance of golden-brown microalgae smaller than 5μm at both sampling depths.

Diel variations of the quality of the pigment pool were less important than those due to the vertical location of the two populations.

The opposite is true for fluorescence derived parameters that vary more on the diel scale than on the vertical one, even if the circadian variability was much more evident in surface samples. Here, $rETR_{MAX}$ drastically increased at dawn, as was observed in the PT cultures exposed to natural light, suggesting that just the presence of light, even at very low levels, acts as a signal for the "wake up" of the photosynthetic machinery.

PvsE derived parameters exhibited both circadian and vertical variability, with similar values at dawn and dusk, maxima in daylight and minima at night. Variations in P^{chl}_{max} were more pronounced in the surface population, whereas α^{chl} was more variable at depth. In addition, the patterns observed in the surface clearly reflected also the action of light dissipation processes, as confirmed by the depression of some photosynthetic parameters in the central part of the day, i.e. under the maximal irradiance.

4.6 Synthesis of the chapter

Most of the investigated photophysiological properties of *P. tricornutum* showed strong diel periodicity both in artificial "square" wave and natural LD cycles. The circadian patterns observed for different parameters were often similar under the two light regimes with major differences occurring in the phase. For example light harvesting pigments

maximized their cell content at the end of the light period or at the beginning of the dark in artificial light -both in 12:12 and 16:8 LD cycles- and few hours before in natural light.

In both artificial and natural light regimes Ddx cell concentration anticipated its peak at least by three hours. This feature was also observed when the photoperiod length was set at 16 hours and was confirmed in a natural population of phytoplankton dominated by golden-brown microalgae (including diatoms) living in the surface layer of a Mediterranean site, which maximizes Ddx/Chl *a* ratio in the first part of the day.

On the other hand, the cyclic accumulation of Ddx is prevented at low irradiance in *Phaeodactylum* (40 μmolquanta·$m^{-2}s^{-1}$), which was also observed in natural phytoplankton living at the base of the photic zone (midday irradiance 15 μmolquanta·$m^{-2}s^{-1}$).
Finally, unpredictable transitions to high light modify to a major extent photoprotectants (synthesis) rather than light harvesting pigments (reduction).

Many photosynthetic coefficients measured on PT cultures, both using variable fluorescence ($rETR_{MAX}$) and C-based techniques (P^B_{MAX}, α^B), displayed peaks in the first or central part of the light period in artificial light. On the other hand, σ_{PSII} showed maxima at night and minima over light periods reflecting changes in the size of the antenna due to the circadian variability of the PPC/PSP ratio.

The time distribution of $rETR_{MAX}$ observed in PT cultures grown under natural light was not symmetrical over the day, i.e., did not match the curve of solar irradiance, thus indicating that cells use light for photosynthesis with different efficiency over the day not depending only on its intensity.

The diurnal minima in σ_{PSII} were more pronounced under high intensities (around midday under natural light both in culture and *in situ*) where they were accompanied by

strong reductions of F_v/F_m indicating the occurrence of strong processes of light dissipation (NPQ).

Finally, the patterns observed in free running conditions were different depending on the considered parameter: pigment concentrations kept the same phase and amplitude of circadian oscillation at least for 24 hours, followed by lower amplitude oscillations; P^B_{max} drastically decreased after one cycle in LL, whereas σ_{PSII} and $rETR_{max}$ kept their oscillating behaviour for 2-3 days in LL indicating the uncoupling of different components of the photosynthetic machinery and the existence of different mechanisms of control.

Chapter 5

The time course of the cell cycle of *P. tricornutum* in different light regimes

5.1 Background

The "scope" of every cell is duplication. The cell cycle is the sequence of events occurring from the birth of a cell to its division into two genetically identical daughter cells. Details of cell cycle vary from organism to organism, nevertheless, some aspects are universal. In fact, every cell has to replicate the DNA in each chromosome, and separate the chromosomes into the daughter cells, thus transmitting to them all the genetic information. In both prokaryotes and eukaryotes, the cell cycle is classically divided into four phases named G_1, S, G_2, M. The former three constitute the interphase; the DNA is replicated during the S phase (synthesis). The notations G_1 and G_2 refer to "gaps" of the synthesis, and are phases during which most of the somatic growth occurs. Finally, M stands for mitosis, i.e. the segregation of chromosomes, followed by cell division, or cytokinesis. In the classical book "The Biology of the Cell Cycle" (Mitchison, 1971), the author distinguished between the "DNA division cycle", characterized by discontinuities due to DNA replication, segregation and division, and the "growth cycle" characterized by relatively continuous processes e.g. protein synthesis and volume increase, occurring during the G phases.

The major difference between the cell cycle of prokaryotes and eukaryotes resides in the structure of genome: in eukaryotes the genome is distributed over a number of

different chromosomes where the replicated strands remain aligned until their division, while prokaryotes have generally a single chromosome from which the daughter strands immediately separate and become segregated. In both cases, the main events of the cell cycle occur in a strict sequential order, therefore mechanisms of regulation, coordination and error correction are required. The transition from one cell cycle stage to another is regulated by different cellular proteins (Vermeulen *et al.*, 2003). Key regulatory proteins are the cyclin-dependent-kinases (CDK). They are activated by another class of proteins, the cyclins, whose level periodically rises and falls during the cell cycle, thus cyclically activating the CDKs, which are responsible for driving the cell from one phase to the next. CDKs are targets of checkpoints that control the entry into the following phase (Crews and Shotwell, 2003). Indeed, both internal and external controls are involved in the cell cycle progression throughout the different phases. Crucial checks take place at fixed times of the cell cycle called "restriction points". Once cells pass a restriction point they are committed to progress through the cell cycle phases even in absence of a factor critical for the growth. In general, if the continuous processes of growth are inhibited for some particular reason (unfavourable conditions, e.g. the lack of light in photoautotrophs), the ongoing discontinuous processes will continue and terminate but no new discontinuous processes (i.e. DNA synthesis) will start. On the other hand, if a discontinuous process is inhibited there is no effect on the cell growth: protein synthesis and cell size increase will continue (for some time) even in absence of DNA replication and mitosis.

In diatoms, the cell cycle exhibits typically two restriction points. The first is located in mid-G_1. It is a light-dependent point, but also nutrients (mainly nitrogen, table I in Vaulot (1995)) are required to overcome it, thus light limitation and nutrient starvation induce the cell arrest in G_1. The second check point, located in the late G_2, is related to

frustule formation before cell division. Both light and silicon are required at this time. This light-dependency late in the cell cycle may be related to the energetic requirements for silicon transport and deposition during valve formation (Brzezinski *et al.*, 1990). In this paper, they characterized the cell cycle of 7 diatoms, including PT, determining also the duration of each stage (see their table 1). They found that the longest phases are G_1 (from 4.5 to 12.9 hours), and G_2 (1.9-7.6 h) whereas S and M are generally shorter (0.3 to 1.7h). Only one species (*T. weissflogii*) showed unusually long S and M (about 3 h each) whereas two (*C. simplex* and *M. polymorphus*) displayed very short G_2 (0.3-0.7 h). No silicate-dependent segments were observed within the cell cycle of *P. tricornutum*, or any light-dependent arrest point in G_2. This was in some way expected, since PT is an atypical diatom in that it does not have a silicon frustule in its most abundant morphotypes (as already mentioned in section 3.1), and does not require silicon for growth. Nevertheless, in spite of the lack of any restriction point in G_2, PT is the diatom (among those taken into account by Brzezinski *et al.* (1990) exhibiting the longest G_2, without any evident reason.

Both culture and *in situ* studies show that phytoplankton division is phased to the LD cycle (Chisholm, 1981; Chisholm *et al.*, 1980). In a recent paper Jacquet *et al.* (2001) studied the effect of 12:12 LD cycles in a variety of marine picophytoplanktonic strains including both prokaryotes and eukaryotes. They demonstrated that there is little variability in growth and division patterns among picophytoplankton, despite the large phylogenetic range examined spanning from cyanobacteria to Prasinophytes, Pelagophytes and Bolidophyceae.

In particular, cell size and pigment content are reported to increase almost only during the light period, triggered by the light onset, whereas division is observed in the initial part of the dark period. Larger sized groups are reported to display the highest

percentage of dividing cells at night, even though more variability is observed (Chisholm, 1981).

This widespread time pattern might reflect the need to efficiently organize cellular activities over the day, e.g. phasing light requiring processes (i.e. photosynthesis) with the photoperiod, and consequently performing other processes (e.g. cell division) at night. Whether this differentiation in the physiological activities exists and how it is realized is not clear. In particular, it is not well established whether the cell cycle is directly entrained by light or through an endogenous clock. This directly connects to the questions of the previous chapter: whether and to what extent is photosynthesis synchronized to the diel cycle through the cell cycle, or independently? In particular, it has to be clarified which components of the photosynthetic machinery (e.g. Chl *a*, ETR) are directly controlled by the cell cycle, and which are more strictly or exclusively related to the light regime.

The intrinsic problem emerging from the studies I mentioned above is that since both the cell cycle and photosynthesis are entrained by the day/night cycle, then what is observed in LD regimes might not be conclusive for determining the interdependence of the two classes of processes, since periodicity may be entrained independently. Indeed, for a better comprehension of the relationships between cell cycle and photosynthesis and of their temporal organization, it is necessary to consider the latter as a process not uniquely devoted to carbon fixation. Actually, as recently remarked by Behrenfeld *et al.* (2004), photosynthesis should be seen as a process producing energy (ATP) and photoreductant molecules (e.g NADPH, ferredoxin) used in all metabolic pathways downstream from the PSII, of which C-fixation is only one, the others being nutrient uptake/reduction, photorespiration, inorganic carbon accumulation, respiratory phosphorylation, etc. From this point of view, a closer link with the cell cycle emerges, where the diel modulation of

photosynthesis might in fact reflect changes in energy and carbon requirements during each phase of the cell cycle. Hence every metabolic pathway prevails on the others depending on specific needs, (e.g. balance between growth -high reductant demand- and maintenance -high ATP demand-), but also on the temporal separation of metabolic events, thus affecting the size of the pools of ATP and reductants, and in turn generating feedback requirements.

The results presented in this chapter attempt to characterize the circadian patterns of the cell cycle of PT under different light regimes (photoperiod, light intensity), with special attention to the relationships between cell cycle stages and cell properties related to somatic growth, i.e. cell geometrical properties, biochemical components (pigments) and their synthesis. As for the former, FCM FALS and RALS will be used as proxies for cell size and shape, respectively.

5.2 Results

5.2.1 Circadian patterns of growth, geometrical parameters and cell cycle stages of PT cells grown in artificial light

5.2.1.1 Size/shape dependent properties of PT cells

Flow cytometry data revealed a close coupling of cell geometrical properties with the LD cycle: FALS and RALS displayed a parallel time variation, increasing during light periods and decreasing over night (Fig 5.1), indicating an enlargement of the average cell size during the day followed by a nocturnal reduction. Maxima were displayed just before or after the onset of the dark while minima occurred always before the end of the night. In continuous light conditions, geometrical parameters lost their periodicity after the first subjective night, exhibiting intermediate and rather constant values in the following two LL cycles. This pattern is similar to that already reported for cell pigment content and red

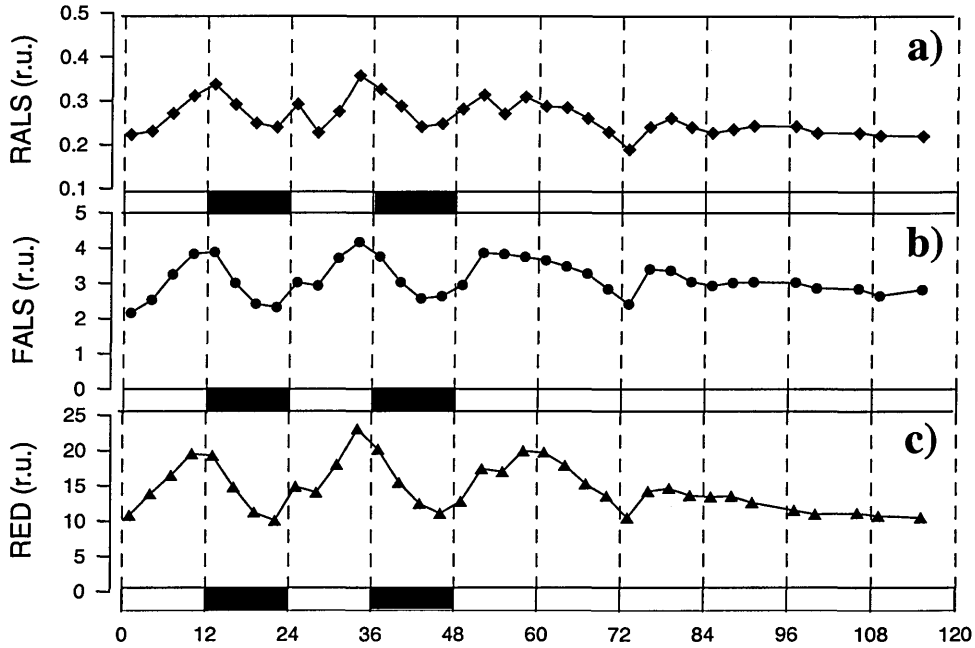

Fig. 5.1. Circadian distribution of flow cytometric parameters, a) RALS, b) FALS, c) red fluorescence over LD and LL cycles (exp. INTRO).

fluorescence (Fig. 4.4 and 5.1c) suggesting a strict relationship between cell size and pigment accumulation.

5.2.1.2 Cell cycle stages and growth rates

The temporal variation of cell cycle stages revealed strong circadian periodicity (Fig 5.2) under the imposed LD regime. The percentage of cells in G_1 displayed maxima (87-92%) between the middle of the night and the beginning of the following day, with steep increases during the night. The values decreased during the day down to minima (25-35%) at the end of the L period or in the first hour of D. At the same time, the percentage of cells exhibiting double DNA content (i.e. cells in G_2 phase or in mitosis) showed maxima corresponding to G_1 minima; peaks were sharp and did not exceed 50%. Finally, the

percentage of cells performing DNA synthesis generally showed two peaks within 24 hours, one in the L period and the other in the dark, separated by 6 or 9 hours from each other. The abundance of cells in S was never higher than 50%. In continuous light regime (LL) the regular phasing of G_1 and G_2 abundances disappeared since the first subjective night, when G_2 cells did not completely disappear, i.e. division apparently did not occur to the same extent as before. This is not confirmed by the hourly growth rate, which indeed peaked at the expected time (i.e. at the beginning of the subjective night) displaying a value comparable with those observed in the previous days at that time (Fig. 5.3d). In addition, while the time distribution of all the stages became quite flat in the following LL cycles,

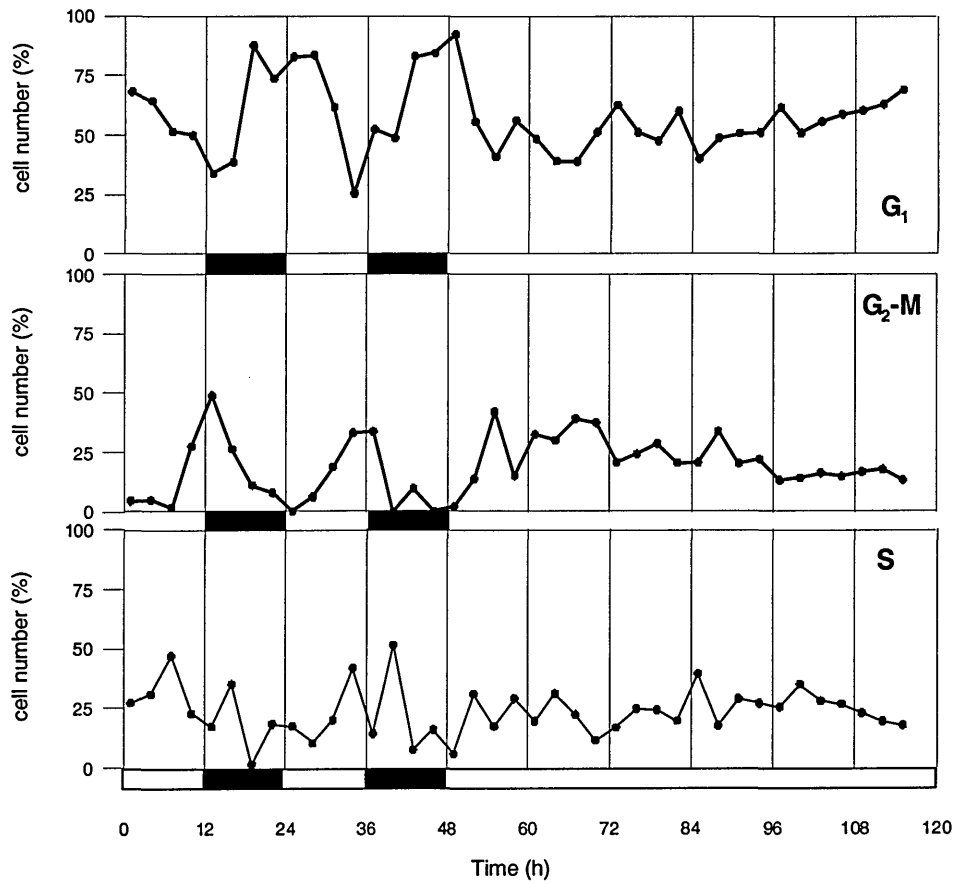

Fig. 5.2. Circadian distribution of the relative percentage of cells in different stages of the cell cycle (G_1, G_2-M, S) over artificial LD and LL cycles (exp. INTRO)

cell division continued to be in some way phased to the entraining light-dark cycle, in that peaks kept similar height but anticipated their occurrence by three hours at each cycle. Secondary peaks appeared at intermediate times.

The study of the rate of variation of the abundance of cells in the different cell cycle stages may help the interpretation of the above reported results. As shown in Fig. 5.3, under LD cycles the transition to the G_2 phase was particularly favoured (positive $\Delta G_2/\Delta T$) at the end of light periods (maximal increases of between 4.8 and 9.4% per hour) and dropped (by 7.5 –11.2% per hour) in the night due to division, i.e. formation of G_1 cells, as evident from the occurrence of sharp peaks of growth rate followed by maxima of $\Delta G_1/\Delta T$ (up to 16.3% h^{-1}). Conversely, negative $\Delta G_1/\Delta T$ occurred in most of the light points, with particularly drastic minima in the second and third day of experiment (hourly variation of about -12%). Finally, $\Delta S/\Delta t$ showed a noisy distribution with frequent maxima and minima, phased by 6-9 hours among each other.

ALE			NLE		
Day	Light regime	μ (d^{-1})	Day	Light regime	μ (d^{-1})
EXP. INTRO			EXP. SPRING		
1	LD 12:12	1.05	1	LD 12:12	0.68
2	LD 12:12	0.89	2	LD 12:12	0.41
3	LL 12:12	0.97	3	LD 12:12	0.49
4	LL 24:0	1.06	4	LD 12:12	0.79
5	LL 24:0	1.18			
EXP. C24					
1	LD 12:12	1.04			
EXP. C36					
1	LD 16:8	1.17			

Table 5.1. Daily growth rates (from cell counts) of PT during the indicated experiments in artificial light (ALE) and natural light (NLE)

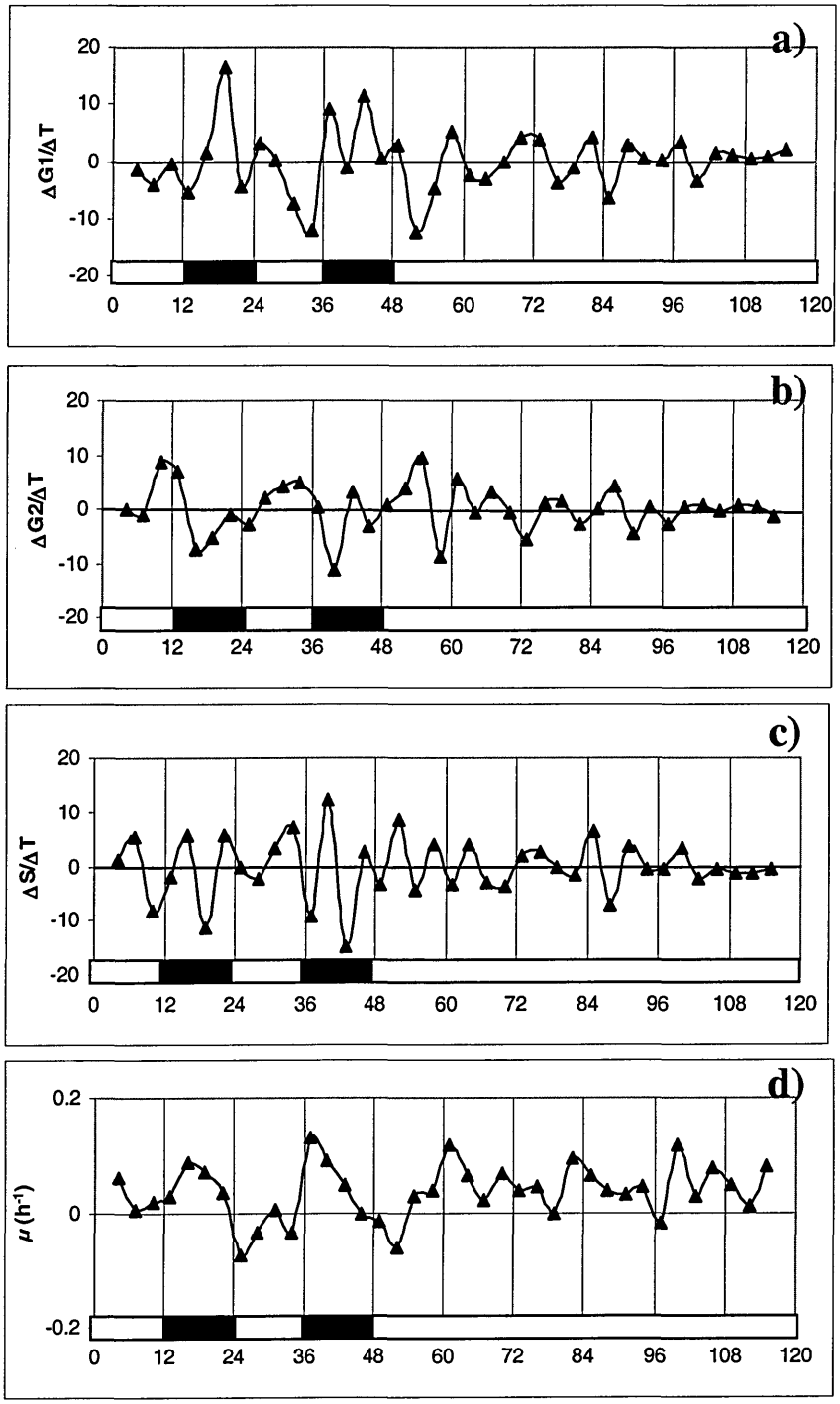

Fig 5.3. Circadian distribution of the hourly rate of variability of the percentage of cells in different cell cycle stages in artificial LD and LL cycles (a, b, c). d) hourly growth rate derived from cell counts (exp. INTRO)

As already mentioned, the onset of LL regime caused the rapid disappearance of any circadian pattern in cell cycle stages, hence both negative and positive variations of cells in the different phases decreased in their absolute value and exhibited a confused pattern. Finally, the daily growth rates derived from cell counts and reported in table 5.1 showed a progressive but slow increase during LL cycles

5.2.1.3 Summary

All the investigated cell parameters (FALS, RALS, Red fluorescence) increased rather continuously and linearly over time during the light periods and decreased over the night, resulting from a close coupling between cell growth and pigment accumulation.
In addition, the match between maxima in the abundance of G_2 cells and cell fluorescence (or Chl *a*/cell) suggested that the observed diel oscillations in cell pigment content may merely result from the intense growth associated with G_2 phase and preceding cell division. This pattern was particularly evident under LD cycles.

Such results do not solve the question whether cell cycle or light regime (or both) directly drive pigment synthesis. In addition, the experiment reported above was carried out in a light regime far from the natural one. In fact, the diurnal variation of light intensity may be a critical factor, more for pigment content than for cell cycle progression, in which LD alternation *per se* is likely to be the relevant forcing. Then, in the following section I report the results deriving from a parallel experiment conducted in natural light.

5.2.2 Circadian patterns of growth, geometrical parameters and cell cycle stages of PT cells grown in natural light

5.2.2.1 Size/shape dependent properties of PT cells

Under natural light, cell geometrical properties of PT exhibited evident circadian periodicity. As a general pattern, size-dependent properties showed high diurnal values and low nocturnal ones (Fig 5.4a and b, black line). On the other hand they displayed different phases: RALS increased during the day, peaking in the late afternoon (h 18:00) or in the early night (h 21:00) and decreased during dark periods (except in the first night), while FALS generally peaked 3-6 hours before. Red fluorescence maximum were prior to midday, as already showed in the previous chapter (Fig. 4.14). In continuous dark

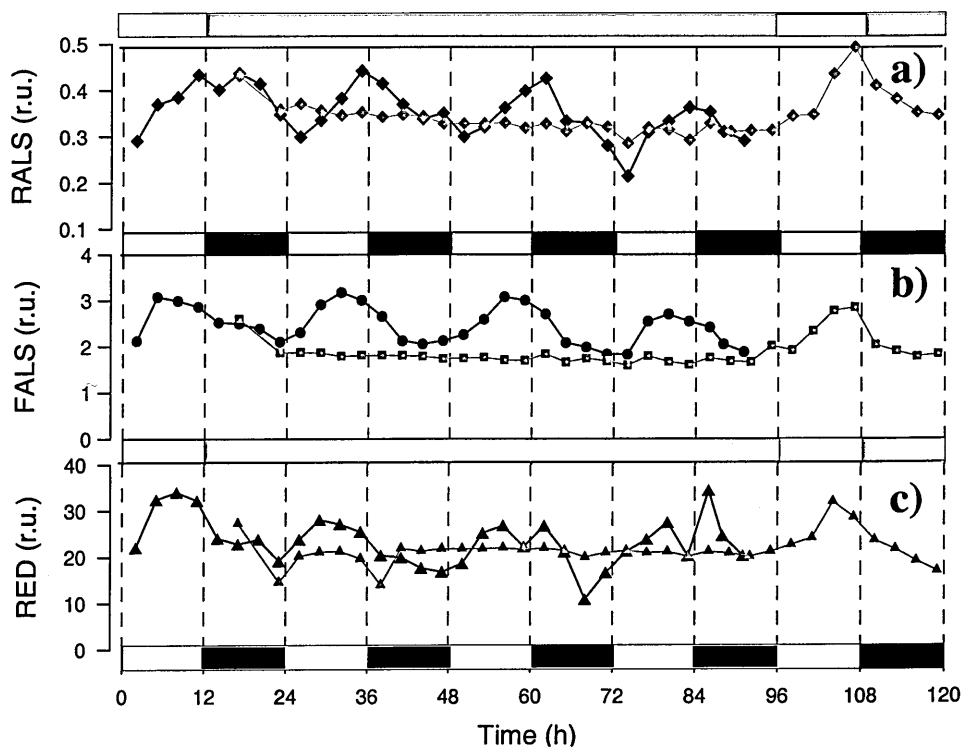

Fig. 5.4. Circadian distribution of flow cytometric parameters (RALS, FALS, red fluorescence) over natural LD cycles (exp SPRING). Red refers to a culture exposed to dark conditions for 84 hours (light regime indicated in red)

conditions (Fig 5.4 red line), periodicity disappeared immediately and the two geometrical parameters exhibited constant low values, equal to those displayed at the end of night, indicating small cells with low chlorophyll content. Once the light was restored, all the parameters recovered their diurnal values, or even higher, in some case with a time delay (i,e. FALS).

5.2.2.2 Cell cycle stages and growth rates

The cell cycle of PT displays periodical variability also under natural light (fig 5.5): the time pattern of G_1 cells was similar as in the previous case (ALE), except for a more continuous and regular increase during D periods. Maxima were always observed after

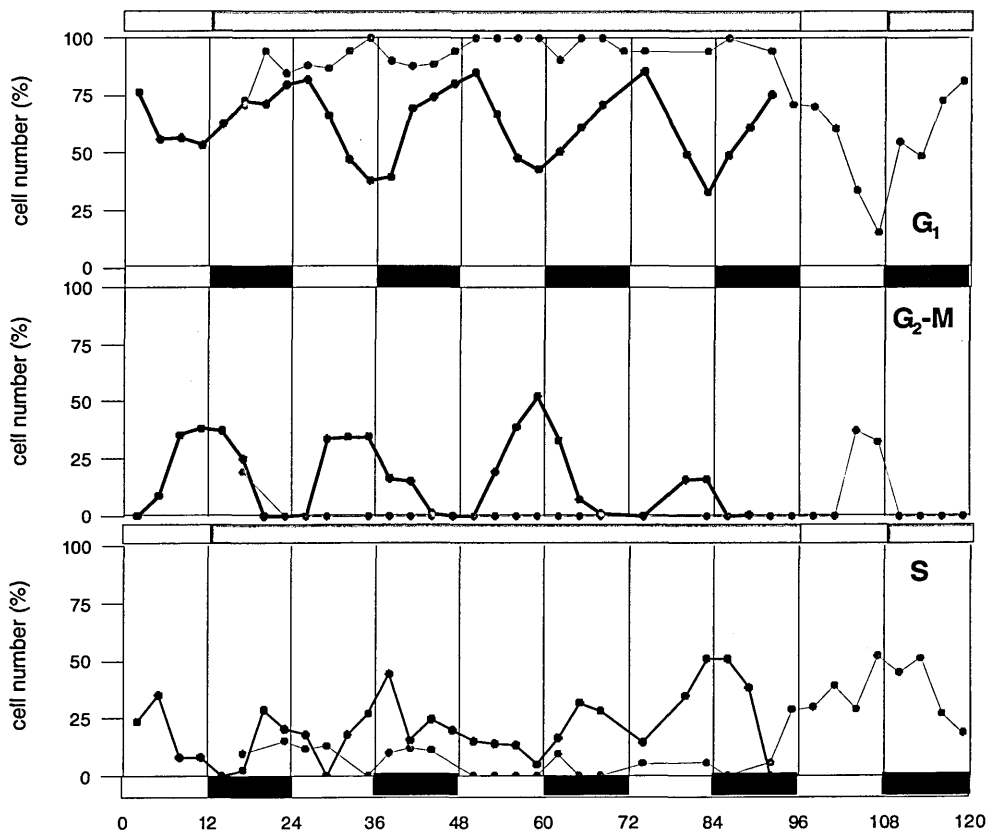

Fig 5.5. Circadian distribution of the relative percentage of cells in different stages of the cell cycle in natural light (exp. SPRING). Red refers to a culture exposed to dark conditions for 84 hours (light regime indicated in red)

dawn and minima at dusk (please note that in figure 5.5 the last sampling point of dark periods actually refers to the last minutes before sunrise, i.e. under some very low diffuse light). Peaks of G_2-M cells were generally observed immediately after midday or three hours later, i.e. 3-9 hours before than in the above reported experiment. In addition, differently from what reported above, high percentages of G_2 cells persisted for 6-9 hours, which is consistent with the lower daily growth rates observed during the experiment SPRING (Table 5.1). Cells performing DNA synthesis did not show any circadian distribution, even though some variability was observed with major peaks at night. $\Delta G_2/\Delta T$ was positive for 1-3 points under sunlight (Fig. 5.6), with maxima generally under the highest irradiance, while negative or null variations were observed at night, due to cell division.

Hence, positive, small and rather constant variations of the number of G_1 cells ($\Delta G_1/\Delta T$) were measured throughout all the dark periods and negative rates occurred during light periods, indicating that the birth of new cells occurs in a continuous (i.e. not synchronized) way over the night as confirmed by the irregular pattern of μ. $\Delta S/\Delta t$ showed a confused distribution with both diurnal and nocturnal maxima (Fig. 5.6).

Finally, at the onset of continuous dark conditions, cells being in the G_2-M phase (20%) divided at the expected time, while G_1 cells were prevented to go through DNA synthesis and hence blocked in that phase until the restoration of the light that entrained again the phasing to the day-night cycle.

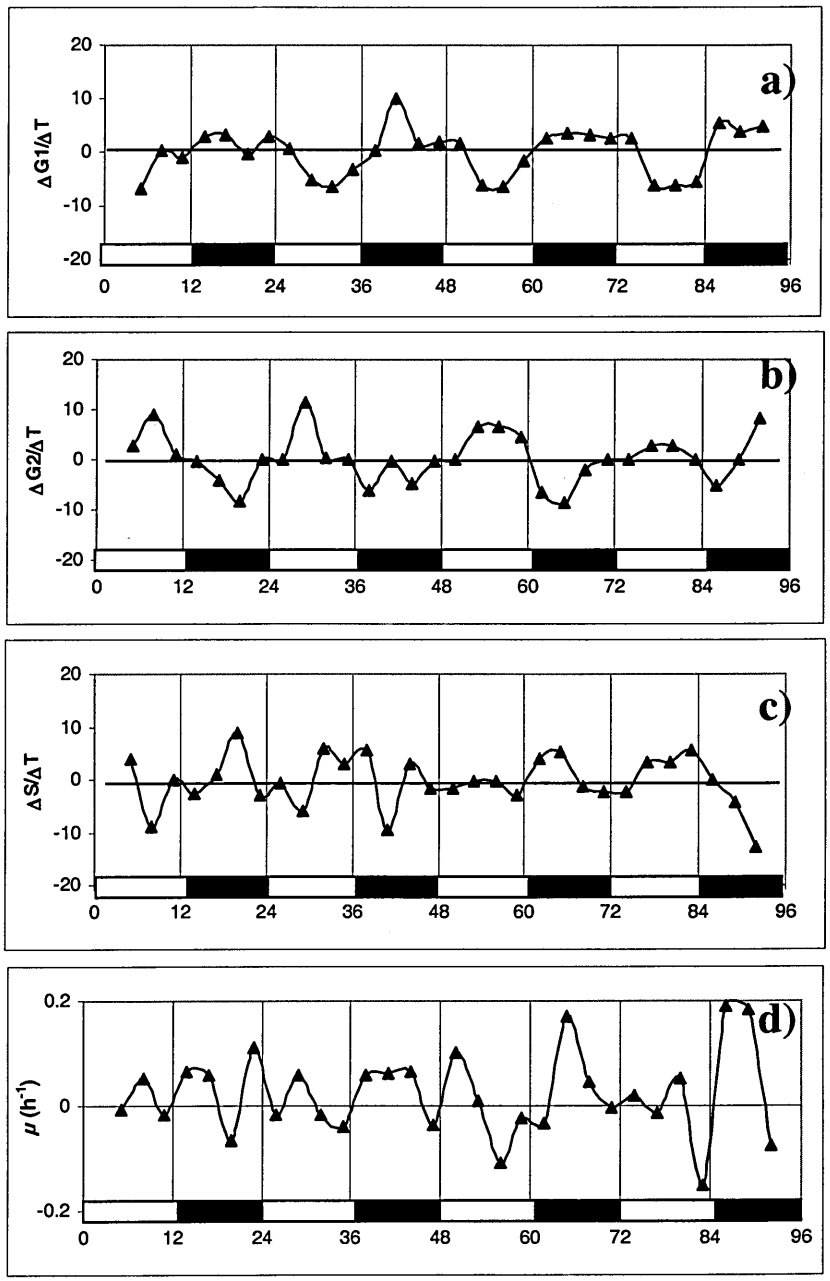

Fig 5.6. (exp. SPRING) Circadian distribution of the rate of variability of the percentage of cells in different cell cycle stages in natural LD cycles (a, b, c). d) hourly growth rate derived from cell counts

5.2.2.3 Summary

In natural light regimes all the parameters relative to cell growth displayed strong circadian periodicity. Differences were observed among their timing: indeed only RALS displayed the same phase as in the previously reported experiment, FALS anticipated its phase by about 3 hours, while red fluorescence (and chlorophyll cell content) generally peaked in advance respect to the size-dependent parameters (or in phase with FALS), matching the maximal solar irradiance.

The abundance of G_2 increased since the central part of the day. In addition, high concentrations of G_2 were observed all through the second part of light periods, thus differentiating these observations from the previously reported pattern where sharper peaks occurred at the end of the day or the beginning of night. This suggest, either a really longer duration of G_2 phase in SPRING experiment due to the lower growth rate, or, alternatively, a not perfect synchronization of the cell cycle within the population, which would result in an apparently longer G_2.

The results of cell cycle measurements performed in DD confirmed the presence of a light restriction point during the G_1 phase, typical of all diatoms, and the absence of any light dependent restriction in G_2, peculiar to PT.

In conclusion, also under natural light, the diel variability of the chlorophyll cell content seemed to vary in parallel with the cell cycle. This would mean either that it is directly controlled by the cell cycle, or that it is synchronized with the same phase as the cell cycle. However, in order to better understand and interpret these data I decided to perform one day experiments in batch cultures of rapidly dividing PT cells under different photoperiods, in order to decouple the cell cycle phase from the synthesis of pigments, which is likely to be phased with the LD cycle.

5.2.3 Circadian patterns of growth, geometrical parameters and cell cycle stages of rapidly dividing PT cells grown in artificial light

Rapidly dividing PT cells (almost 3 divisions per day) were obtained by providing optimal conditions (in terms of both light and nutrients) by means of frequent dilutions that allowed low cell density levels during the adaptation period preceding the experiments C24 and C36 conducted in batch mode. In cultures grown in 12:12 LD cycles, the highest cell number enhancement was observed at night (Fig. 5.7, upper panel). In particular, in the first 12 hours (L period) cell concentration increased by about 50%, whereas during the following 12 hours (D period) the cell number doubled. On the contrary, chlorophyll accumulation in the suspension was faster than growth over the photoperiod and proximal to zero at night. The increase in cell concentration was more homogeneous through the 24 hours in a 16:8 LD cycle (Fig 5.7, lower panel) and Chl *a* accumulation proceeded almost on parallel over the light period and showed an arrest in the dark.

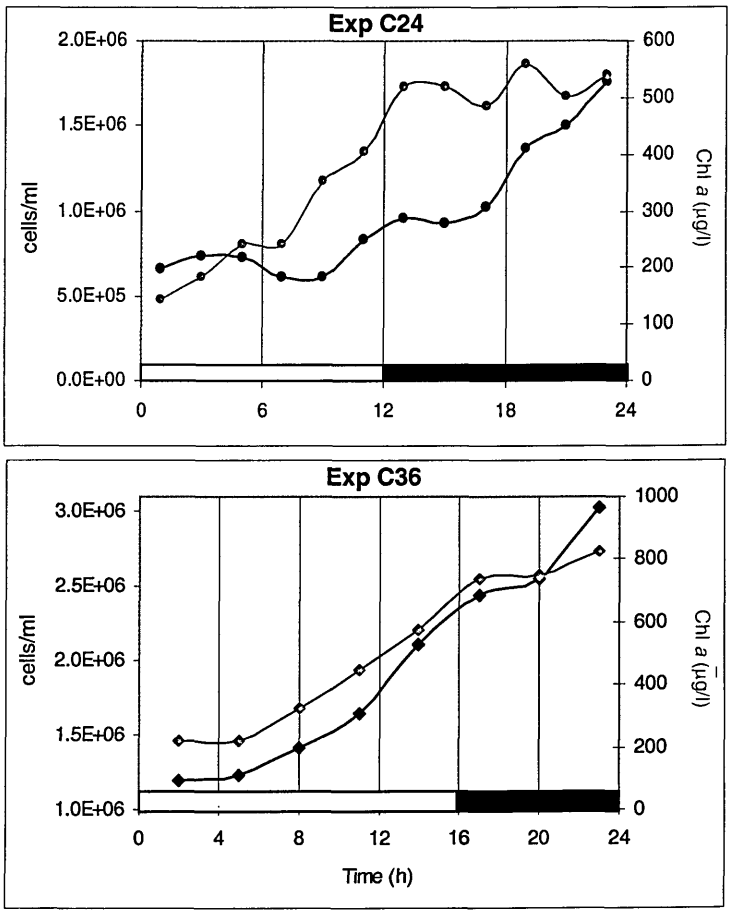

Fig. 5.7. Diel variability of cell (black line) and Chl *a* (red line) concentration in PT cultures during the exp. C24 (12:12 LD, upper panel) and C36 (16:8 LD, lower panel) conducted in batch mode. Please note different scales on y axes

Single cell based measurements substantiated the "desynchronisation" of the processes of cell growth and pigment accumulation (results presented in Fig 5.8). In both experiments, FALS, RALS and RED displayed single or multiple peaks almost never in phase to each other. In particular, in the exp. C24 cell, Chl *a* content (i.e. RED) increased until the 15th circadian hour (3 hrs after the onset of the dark) and decreased afterwards, apparently in contrast with the chlorophyll data of Fig.5.7. On the contrary, the nocturnal decrease of RED in the exp. C36 was coherent with the pattern already observed in the experiments reported above, and with the absence of Chl *a* synthesis in the dark.

The time pattern of the cell cycle stages reported in Fig. 5.9 did not support the distribution of the cell pigment content, since cell red fluorescence did not match the

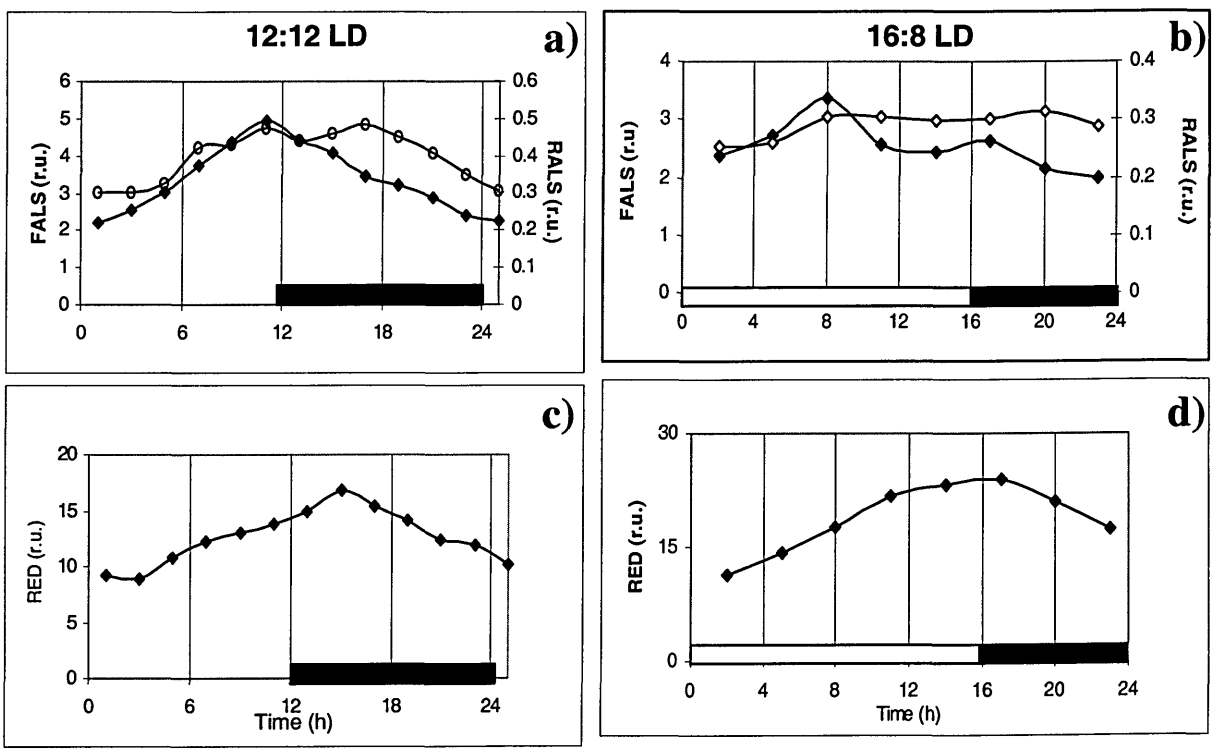

Fig 5.8. Diel variability of FCM parameters in PT cells during the experiments C24 (left) and C36 (right) conducted in batch mode over two different photoperiods: 12:12LD and 16:8LD. a-b) cell geometrical properties: RALS (open circles), FALS (closed circles). c-d) RED. Note different scales on y scales in the two experiments

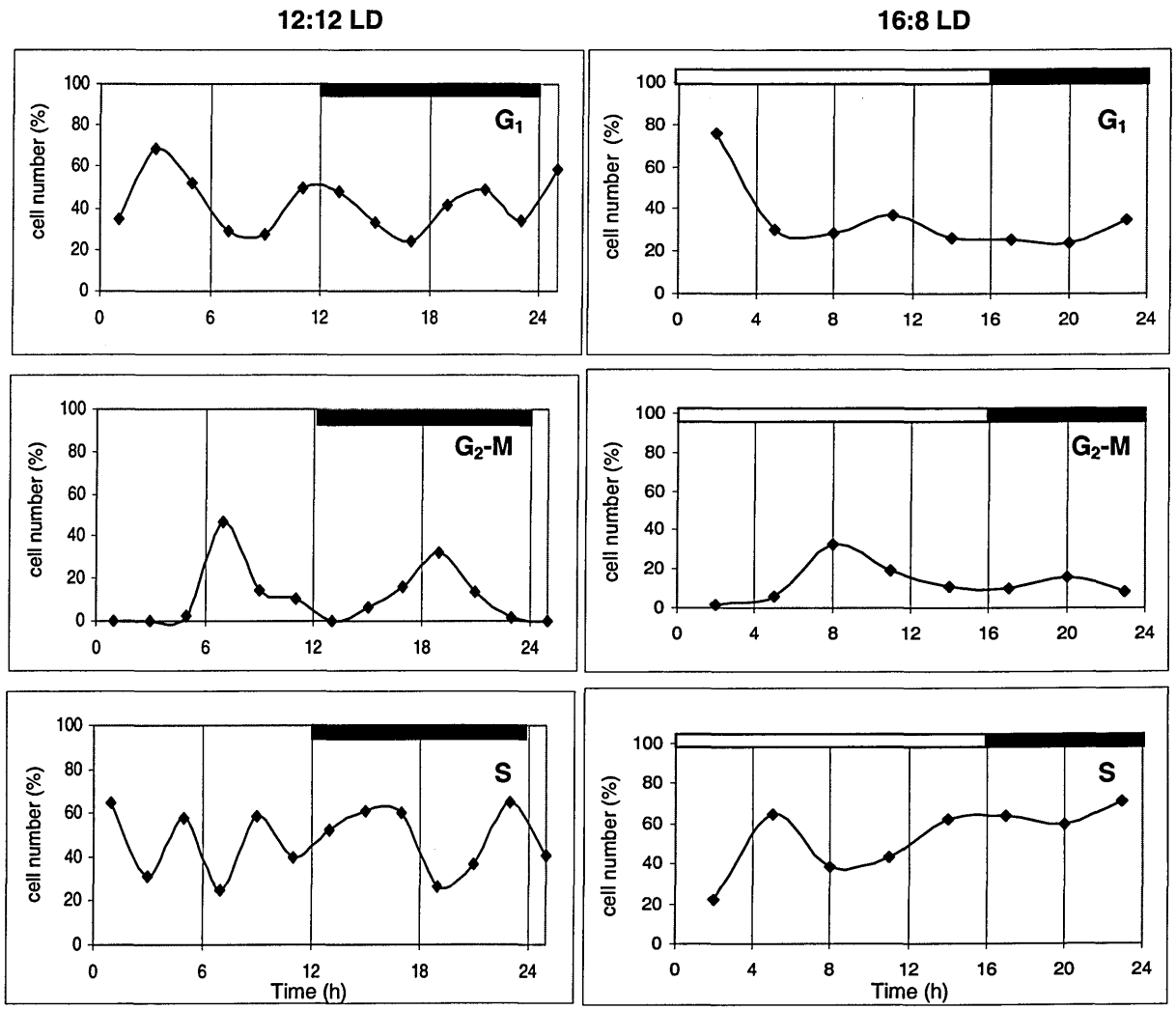

Fig. 5.9. Circadian distribution of the percentage of cells in the different cell cycle stages during the experiments C24 (left) and C36 (right)

distribution of G_2 cells, characterized by two peaks, at the 7-8th and 19-20th hour in both cases. The percentage of G_1 cells displayed several oscillations, more regular in C24 where the highest resolution of measurements (2 hours) allowed also a better characterization. In this case, maxima were equidistant: the first during the L period, the second around the L-D transition, the third at night. The distribution of the cells in the S-phase was quite irregular and characterized by average values higher than in the above experiments.

5.2.3.1 Summary

Experiments with fast growing cells evidenced the possibility of easily decoupling the processes of cell growth, pigment accumulation and cell division, which resulted in the loss of time covariation of cell size/shape properties and pigment content. Nevertheless, the LD cycle imposes a constraint for some processes like Chl *a* synthesis.

5.2.4 Size/shape dependent properties and pigment composition of the three different morphotypes of PT

In this section I report the results of a study devoted to characterize the diel patterns of cell geometrical properties and related pigment content of the three different morphotypes of PT, with the aim of finding out whether differences in the average PT cell parameters and pigment content may be due to different morphotype composition of the culture. Monoclonal cultures of each morphotypes were grown in 12:12 LD cycles. As detailed in section 3.3.2.2, oval cells (O) were intentionally kept in disadvantageous growth conditions (75% lower growth irradiance and scarce nutrient replenish) in order to prevent their transformation into different shapes (generally in the fusiform type). As a consequence the growth rate was very low (proximal to 0) as compared to the other two clones (fusiform, F, and triradiate, T), that exhibited similar values (~0.025 h^{-1}, data not shown).

FCM analysis revealed some difficulties in the interpretation of data from the oval clone, due to the formation of cell aggregates resulting in highly scattered data. Nevertheless, it was however possible to infer some general information.

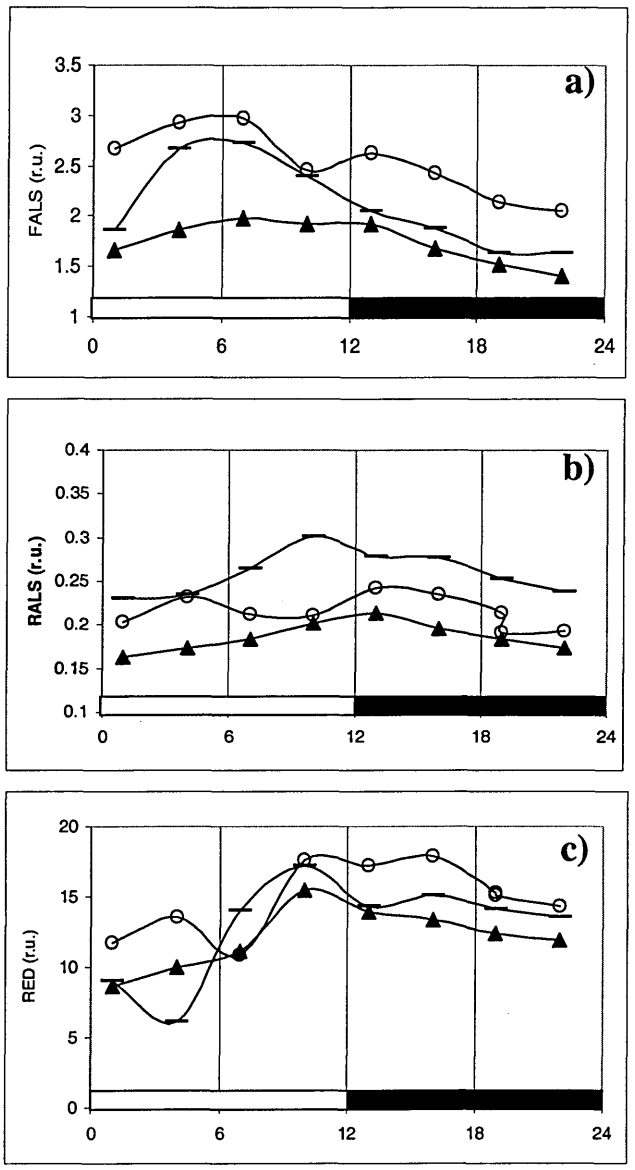

Fig. 5.10. Circadian variability of FCM parameters for the three morphotypes of *P. tricornutum*. a) FALS (forward angle light scattering). b) RALS (right angle light scattering). c) RED (red fluorescence). Triangles refer to triradiate shape, short lines to fusiform type, circles to oval cells.

As expected, the three morphotypes exhibited different geometrical properties, with the highest FALS for O and F shapes and the lowest for T cells (Fig 5.10). In all three cases FALS peaked in the central part of the L period, even if this was less evident for the triradiate clone. RALS was higher in fusiform cells and lower for triradiates, whereas intermediate values were recorded for the oval ones. On the other hand, the mean cell pigment level, as estimated by red fluorescence (Fig. 5.10c), was similar in all the morphotypes, as well as the circadian distribution, in spite of the different growth rate of oval cells. RED increased over the day and became quite flat or slightly decreased over night. Only minor discrepancies were observed between the second and the third sampling points. HPLC analysis was performed only on the midday sampling point. Results of the analysis are reported in Fig. 5.11 and 5.12. All pigment concentrations

were practically identical in F and T cells, while dramatic differences were found in oval cells.

Cell chlorophyll *a* was significantly higher (4 fold) in O than in the other two clones, as well as all the other pigments, showing concentrations from 3 (Ddx) to 5 (Fucox) folds higher. This may result from two factors: the underestimation of the number of oval cells, due to the above mentioned formation of aggregates, the photoacclimation to low irradiance. When normalized to the Chl *a* content (Fig. 5.12), pigment concentrations from oval cells differed by 20-25% with respect to the other two clones. Differences were negative for non-photosynthetic carotenoids (Ddx/Chl *a*, βcar/Chl *a*), and positive for Fucox/Chl *a*, accordingly to the photoacclimation pattern.

In conclusion, the most abundant morphotypes of PT in the commonly used experimental conditions, i.e. F and T, did not reveal any significant difference neither in growth nor in pigmentation. Therefore one cannot attribute to different morphotype composition possible phase delays of geometrical parameters. The oval form is confirmed to be present only in "non physiological" conditions, with very low growth rates, mainly in form of aggregates.

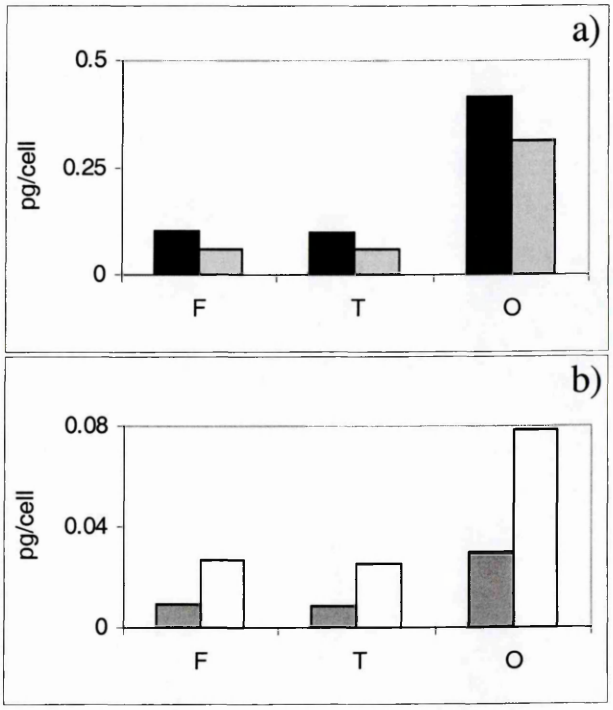

Fig. 5.11. Cell pigment concentrations of the three morphotypes of PT (fusiform: F, triradiate: T, oval: O) at the 4th circadian hour (i.e. h 12:00) of the exp. "MORPHO". a) Chl *a* (black) and Fucox (light grey) b) Ddx (white) and βcar (dark grey)

Chapter 6

Towards an integrated view of the diel biological activities of a marine phytoplankter

The central question of this work was about the existence and the significance of circadian rhythms in marine diatoms, a successful phytoplankton group that for its biological traits appears better suited to highly dynamic environments - where unpredictable short term variability usually prevails on the circadian one - than to less energetic environments, where diel variations may be more important. Diel cycles of key features and components of diatoms physiology have been reported since the 60's, and, as remarked in the first chapter, day-night alternation is a persistent feature of almost all environments on the Earth. Even in the regions where the photoperiod spans over 24 hours, a periodicity in the amplitude of irradiance still exists. This occurs at any depth of the photic zone. Hence a phytoplankton cell might have selective advantages in phasing its activities (e.g. pigment synthesis, photosynthesis, nutrient uptake, cell division) to the light dark cycle. Nevertheless, the full comprehension of factors and mechanisms, both internal and external, driving such diel variability has not been obtained. Therefore the effort addressed in the present study was devoted to better understand and clarify:

- to what extent light bands, and band ratios, may be active underwater in eliciting algal photoreceptors (results presented and discussed in Chapter 2)
- which are the responses of the photosynthetic machinery to different patterns of LD transitions (Chapter 4)

- which is the interplay between the cell cycle and the circadian variability of different cell properties and rates in different light regimes (Chapter 5).

6.1 Rationale of the experiments

Most of the studies have been conducted on the marine diatom *P. tricornutm*, but two experiments have been carried out on natural populations. The experimental activity has been organized according to the sequential-logical scheme reported in Chapter 3 (pag. 32).

Long experiments in artificial light were conducted on cultures of PT both over LD and sequential LL cycles for 4-5 days. The observations in free running conditions are an important aspect of circadian studies. As self-sustainability is a feature of circadian rhythms (see section 1.2), the persistence of cyclic oscillations in absence of external light cues would support the existence of endogenous clocks. At the same time, the absence of oscillations over LL cycles following LD cycles may also be misleading, due to the possibility of periodic signals which overlap with a different phase. This could be the case for unicellular organisms that divide once a day or more frequently and may easily lose the phase in absence of an entraining signal.

There are several limitations in the experimental approach I used, which make my inferences less robust than one would hope for. In particular:

- notwithstanding the care I took to homogenize the suspension during the experiments and to dilute it, when working in turbidostat-like mode, I cannot rule out errors in the estimates of pigment content and cell concentrations due to an inefficient mixing or inexact dilution; at the same time I verified

that the general conditions of nutrient and illumination were substantially preserved all through the experiments.

However, in some experiments I took replicate samples of HPLC and FCM, getting relatively low variance in pigments and cytometric data, so that I can at least exclude large errors due to sampling or analytical procedures.

- most of the parameters I monitored were averages over the bulk of the algal suspension and could have reflected either the most probable value as in a Gaussian distribution or the average among subgroups with different properties and/or phases;

I tried to mitigate their impact on the interpretation of results either integrating the bulk measurements with a careful analysis of FCM data (proposed in the following sections), which derive from single cell measurements, or fitting the data with interpolating curves.

- the experiments with the sinusoidal illumination were carried out in natural light and on a ship, and were therefore affected by the light variability due to the cloud coverage and/or the relative position of the sun and the ship's deck. Occasional fluctuations of irradiance may have affected the normal time course of biosynthesis.

This, from one hand, explains the major noise observed in NLE, which sometimes prevented clear conclusions, and from the other reproduced an environment closer to the reality, which may make the same conclusions stronger. Moreover I used statistics to verify the robustness of the patterns described in the previous chapters. In particular I performed the cross-correlation analysis to quantitatively assess the degree of correlation between couples of parameters and, more important, to identify the time delay between their

periodicities. I could perform the analysis only on the experiments which had sufficient data to make the test statistically meaningful, i.e., "long" experiments.

6.2 Cell growth and pigments

A recurrent pattern observed in the experiments presented in this work is the parallel accumulation of cell pigment content and the increase in cell size preceding cell division. In particular, Chl *a* increases along with the somatic growth until the division distributes the pigment content in the two daughter cells, with the chloroplast division at the end of the cell cycle.

This is obviously due to the fact that somatic growth is a prerequisite for cell division. In Fig. 6.1 I report the time variability of hourly growth rates (μ) and average cell red fluorescence for the experiments INTRO and SPRING. In both cases the highest values of RED precede the highest hourly growth rates. The absence of sharp peaks in the curve of μ (especially in SPRING experiment) indicates that the cells are not fully synchronized and, therefore, that they reach the maximum of somatic growth and, likely, of chlorophyll

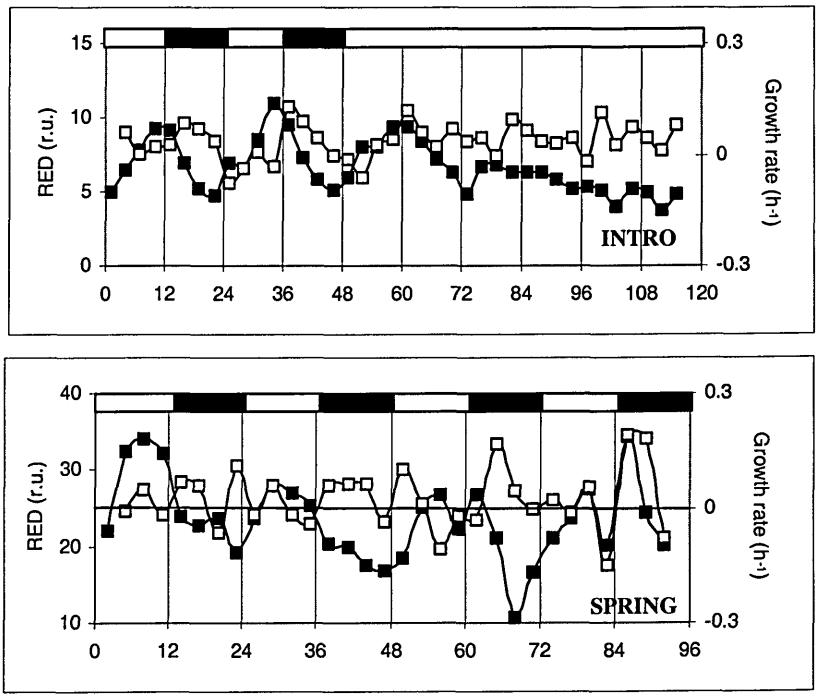

Fig. 6.1. Time distribution of cell red fluorescence (closed squares) and hourly growth rates (open squares) during the indicated experiments

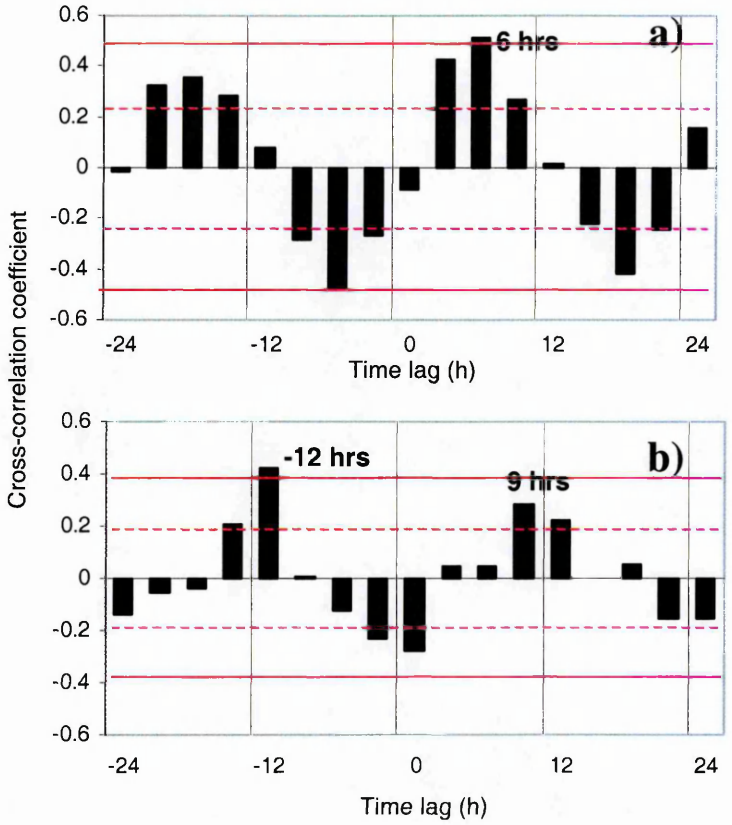

Fig. 6.2. Cross-correlation analysis between RED and hourly growth rate (μ) over LD cycles of INTRO (a) and SPRING experiments (b). Red lines indicate confidence bounds (dashed: 0.67, solid: 0.95)

content at different times. The conclusion is that while a subgroup is dividing, halving their cell chlorophyll content, another subgroup is reaching the maximum content and is going to divide successively. This pattern is partially paralleled by that of the cell size (see Fig. 5.1 and 5.4), of which FALS can be considered the most appropriate proxy (Bouvier *et al.*, 2001). The time lag corresponding to the maxima of correlation between RED and μ over artificial LD cycles is 6 hours ($p<0.05$), but also time lags of 3 and 9 hours are statistically significant ($p< 0.33$), as shown in Fig. 6.2a. The above results imply that cell division may occur with different amounts of cell chlorophyll *a*, with the fraction of cells that divide later in the night having presumably smaller amount of chlorophyll than cells dividing earlier.

In natural light, the highest level of chlorophyll content occurs around midday (Fig. 6.1 and 4.14), i.e., under the maximal ambient irradiance (Fig 4.13), while the maximum in division rate still occurs during the night, i.e. with a 9-12 hrs. time lag between the two maxima (Fig. 6.2b). This means that many cells divide having a smaller amount of

chlorophyll for the daughter cells; in other words, pigment synthesis, somatic growth and cell divisions are only weakly phased. I will return on this point later.

The time pattern described for chlorophyll *a* is followed by the other light harvesting pigments plus βcarotene, which display maximum cross-correlation coefficients with Chl *a* at a time lag = 0 ($p<0.01$), as shown in Fig. 6.3 for the pigment Fucox, in INTRO and SPRING experiments. On the other hand, as already pointed out in Chapter 4, the photoprotectant pigment Ddx displays the highest values since the first hours of the day, anticipating Chl *a* by three-six hours in artificial LD regime (see Fig. 6.4a, black bars) and by three hours in natural light (though this result is statistically less significant, as shown in Fig. 6.4b). This is also clear from the pattern of Ddx/Chl *a* reported in Fig. 4.5 and 4.16. This means that cells accumulate Ddx earlier and faster than the rest of the pigment pool and that this accumulation, at least beyond a threshold in Ddx cell concentration, is decoupled from the somatic growth. Therefore, Ddx synthesis is not modulated (only) by the somatic growth. In INTRO, it is not even modulated by variations in light intensity since it is constant.

My interpretation is that *de novo* synthesis is triggered by the D-L transition independently from that of FCP pigments, while its maximum cell content is regulated by light intensity as it has been shown in previous studies (Casper-Lindley and Bjorkman, 1998) and confirmed by experiment CICLAC, showing that the content of Ddx, as of the other PPC, is maximized in high light grown cells, while the opposite is true for PSP. Other data substantiate this interpretation. Algae grown in 16:8 LD cycles (exp. C36) display a peak of the Ddx to Chl *a* ratio at the same time as in algae grown in 12:12 LD (i.e. four hours after the onset of light), while their cell chlorophyll content peaks four-six hours later

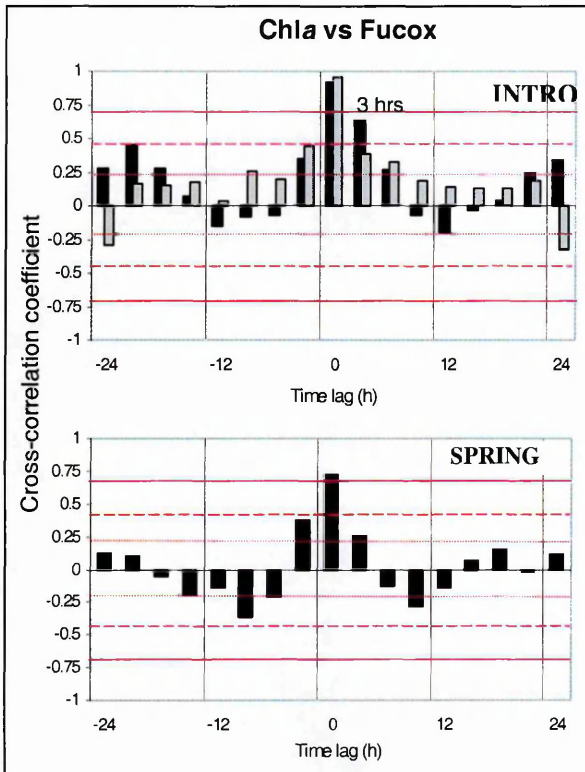

Fig. 6.3. Cross-correlation analysis of Chl *a* vs Fucox in LD (black bars) of INTRO and SPRING exp. Grey bars refer to cross correlation in LL cycles. Red lines indicate confidence bounds (dotted: 0.67, dashed: 0.95, solid: 0.99)

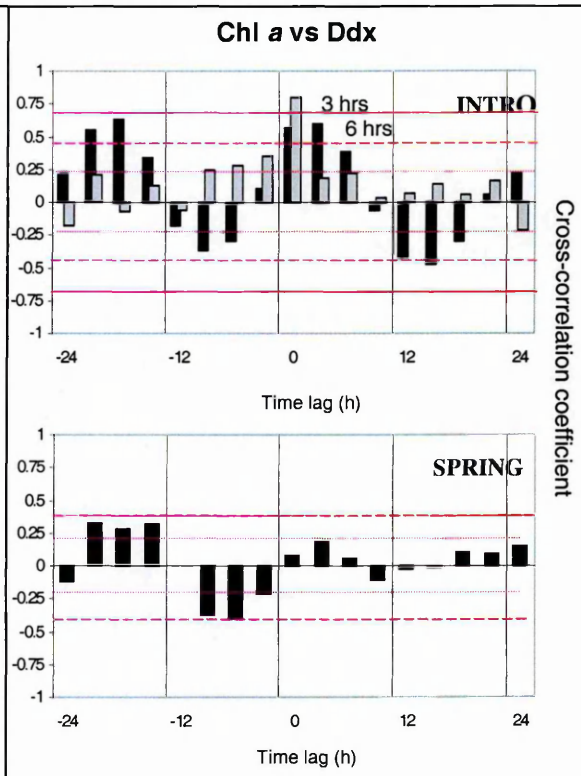

Fig. 6.4. Cross-correlation analysis of Chl *a* vs Ddx in LD (black bars) of INTRO and SPRING exp. Grey bars refer to cross correlation in LL cycles. Red lines indicate confidence bounds (dotted: 0.67, dashed: 0.95, solid: 0.99)

than in algae adapted to 12:12 LD cycle (i.e. around the beginning of night -17th circadian hour).

Moreover, even in natural populations, the diel cycle of Ddx roughly follows the pattern reported for PT, at least in the upper layer of the water column where the highest levels of Ddx, and of the whole PPC pool is higher in the first part of the photoperiod (exp. TRICICLO, Fig. 4.33). The only exceptions to the pattern described above were PT cultures grown under low light intensities (~ 40 μmolquanta·m^{-2}·s^{-1}, Fig. 4.24) and natural populations living at the base of the euphotic layer (maximal PAR ~ 15 μmolquanta·m^{-2}·s^{-1},

Fig. 4.33b). In both cases no diel variability was detected in Ddx content which showed values comparable to the nocturnal levels usually observed in intermediate-high light conditions. It can be concluded that Ddx concentration is not raised above the background level when PAR is below a threshold value.

The significance of the time distribution of Ddx and its peculiarity versus the other pigments has to reside in its function. Ddx is one of the two pigments responsible for the main photoprotection cycle of xanthophylls in diatoms (Olaizola *et al.*, 1994), which is based on the conversion of Ddx to Dtx, the latter being a pigment that efficiently dissipates energy and protects the reaction centers from photodamage. In this view, the availability of a large Ddx pool allows the cell to face possible stressing irradiance intensities, particularly those around midday.

It is worth noting that the described pattern has been observed also in conditions that did not activate the xanthophyll cycle, i.e. when Dtx was not detected (i.e. produced) at all. Therefore the *de novo* synthesis of Ddx appears as a (circadian) preparation of the cell to probable stressing conditions even if they have not, and will never, experience them (the experiments were conducted on cells grown in non-saturating conditions).

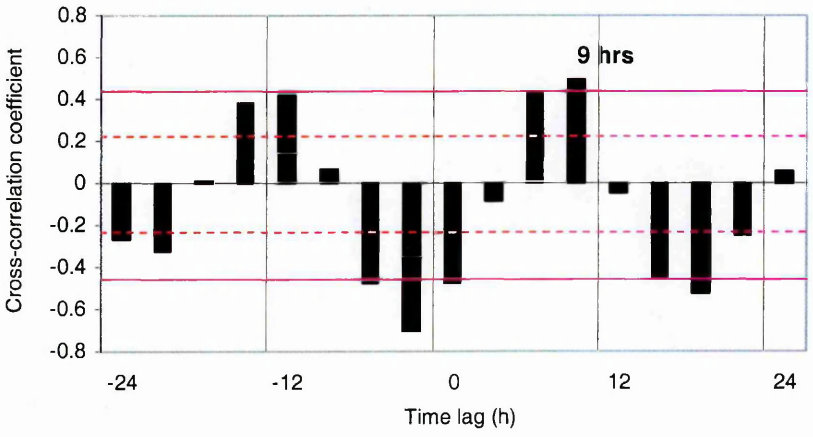

Fig. 6.5. Cross-correlation analysis between a^*_{cell} and a^*_{chl} in LD cycles of INTRO exp. Horizontal lines indicate confidence bounds (dashed: 0.95, solid: 0.99)

Another interesting feature about the modulation of light capture and dissipation emerges from the analysis of the absorption data: while the time distribution of the cell optical cross-section basically reflects that of pigment content, a decrease in Chl *a*-specific cross section is observed along with the diurnal increase of cell pigment concentration. This is more evident in ALE (exp. INTRO) than in NLE (exp. SPRING) where data were noisier (not shown). As shown in Fig. 4.6, a^*_{chl} reaches its maximum at the beginning of L periods (exactly at the first sampling point, i.e. one hour after the D-L transition), differently from a^*_{cell}, which peaks in the second part of L periods (time delay between the two absorption coefficients: 6-9 hrs, Fig. 6.5). The pattern reported for a^*_{chl} may be driven either by a major contribution of accessory pigments in the first part of the day (increasing a^*_{chl}), or by Chl *a* packaging, which would increase through L periods (thus lowering a^*_{chl}) – see section 4.1. Since the contribution to a^*_{chl} by PPS other than Chl *a* (i.e. Chl c_2 and Fucox) is flat over time, and since the absorption of PPC, even displaying a circadian pattern (Fig. 4.7), accounts at most for 19.5 % of the absorption capability of PT, I conclude that it is just chlorophyll accumulation within the cell which decreases the specific absorption efficiency, due to the packaging effect. This is also demonstrated

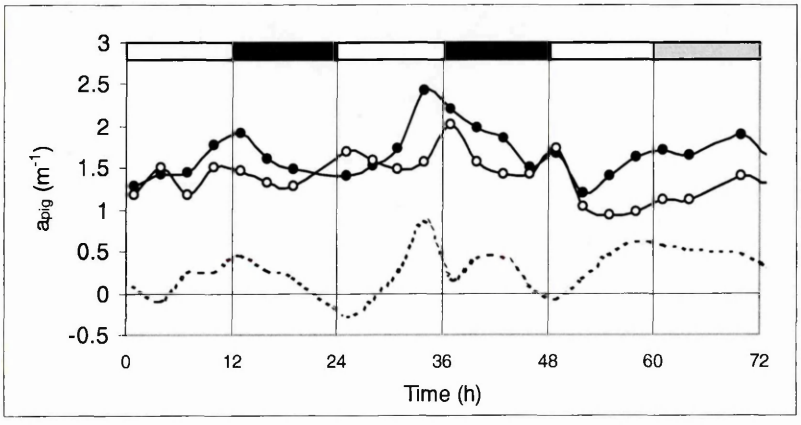

Fig. 6.6. Time distribution of the absorption coefficient due to pigments, a_{pig}, as measured on samples (open circles) and computed from HPLC data (closed circles) over the first 3 days of INTRO exp. Dotted line indicates the difference between the two estimates, as proxy of pigment packaging (see sections 4.1 and 4.22)

by the time course of the difference between the estimated absorption coefficient and the one measured on samples (Fig. 6.6). Hence the packaging is minimum in the early morning, when the size spectrum is dominated by small, young cells resulting from cell division during the night, which have low chlorophyll - and in general low pigment - content. Then, packaging increases over the day and peaks (up to 39%) in the late day or early night.

A third relevant aspect that emerges from the observations is that pigment content and somatic growth decouple during dark periods. Because of the concurrence of cell division and cell biosynthesis, this is not clearly shown by previous plots and analyses. In fact, while cell chlorophyll *a* estimated from RED-FCM is more robust than HPLC-derived Chl *a,* being based on a good statistics of single cell measurements, it does not give absolute rate of Chl *a* synthesis. Thus I merged the information of HPLC, FCM and dilution rates, to obtain the curve of the progressive accumulation of cells and pigment content in the suspension, in absence of dilution. I did this for all HPLC-derived pigments and RED over the experiment duration (Fig. 4.1 and 6.7). In the latter case I multiplied the average value of cell red fluorescence by the number of cells to obtain an estimate of the "total RED" in the culture, as a proxy for the total Chl *a* concentration. The comparison between the two curves confirms that RED and Chl *a* are interchangeable. To determine the cell size, I conducted on FALS data an analysis similar to that described for RED, computing the "total" FALS as the closest proxy for the total biovolume of the suspension (blue curve in Fig. 6.7).

Then the curves of cell number, "total RED" and "total FALS" accumulation were fitted with the growth exponential function (R^2=0.99), as shown in Fig. 6.7, while in Fig. 6.8 the same curves have been calculated and shown for each day of the LD regime, separately. The total biovolume of the suspension strictly follows the pattern of cell concentration, i.e. quite stationary over L periods and increasing over night, while total

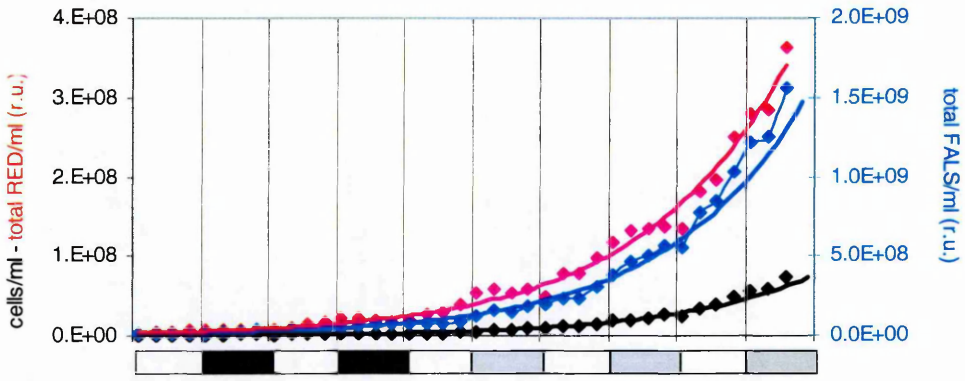

Fig 6.7. Curves of theoretical accumulation of the concentration of cells (black diamonds), total RED (red diamonds), total FALS (blue diamonds) in the suspension during the exp. INTRO, in absence of dilution. See text for details. Solid lines are exponential curves fitting the data (R^2=0.99).

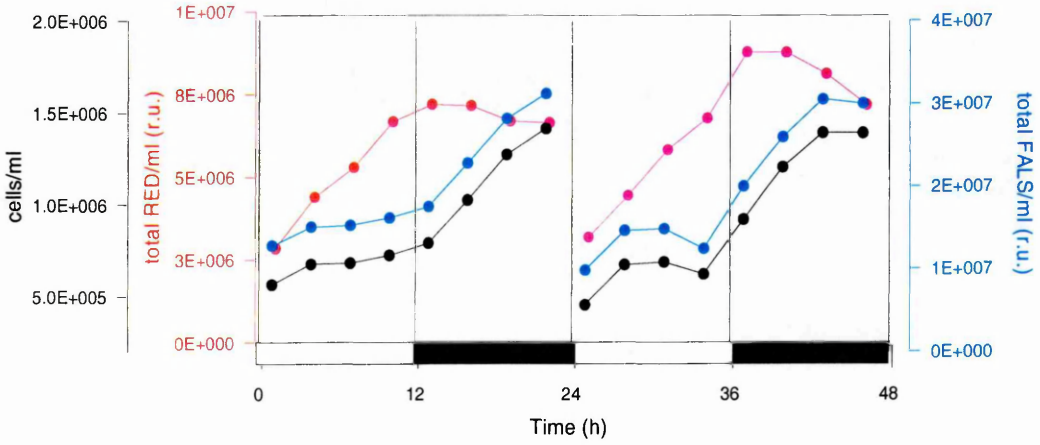

Fig. 6.8. Curves of theoretical daily accumulation of the concentration of cells (black), total RED (red), total FALS (blue) in the suspension for the two LD cycles of the exp. INTRO, in absence of dilution

chlorophyll concentration displays the reversed pattern, i.e. accumulation over L periods and constant values over night.

Thus, while Chl *a* synthesis stops at the LD transition, cells continue to grow and divide. It is important to highlight that the drastic difference between the patterns of RED and FALS did not emerge from just looking at FCM data of INTRO experiment, which would rather suggest a covariation between the two parameters (Fig. 5.1). Subtracting the exponential trend from the curves of Fig. 6.7 and 6.8, I inferred the circadian component of cells, biovolume and pigment accumulation in the culture. In Figure 6.9 the residuals over the exponential are reported. They have been again calculated separately for each day of LD regime (i.e. from curves in Fig 6.8), in order to better visualize the data and to be able to compare the anomalies. As expected cell number and total FALS exhibit parallel variations, nil or negative (respect to the average exponential increase) during the day and positive (i.e. increases exceeding the average growth) over dark periods.

On the contrary, the anomaly of chlorophyll *a* over the exponential increases during the L period, being positive in the second half, and decreases during the dark down to significantly negative values.

Overall the following synthetic pattern emerges. Somatic growth leading to cell division is, to a large extent, regulated by the light intensity and duration of photoperiod (i.e. the the total photo dose), but it continues during the dark period presumably at the expenses of the energy stored during the light period, as shown by the increase of biovolume (i.e., FALS) during the night.

By contrast, the synthesis of both PPC and PSP is strictly controlled by the presence of light, which suggests that during the dark period, the biosynthetic machinery for pigments is either inactivated or its components are diverted to the other activities aimed at concluding the cell cycle. In addition, the synthesis of Ddx proceeds much faster than the synthesis of Chl *a*, stopping even before the onset of the dark.

Therefore the periodicity in the pigment pool of the suspension is certainly related to the L-D alternation, as confirmed by the chlorophyll increase observed during the 4 hours-subjective night in a suspension adapted to the 12:12 LD cycle, when shifted to the 16:8 LD cycle (Fig. 6.10, from exp. C36). On the other hand, the evident decrease in the rate of Chl *a* synthesis suggests that the internal nocturnal rearrangement of biosynthetic machinery, hypothesized above, was already ongoing. This in turn suggests the presence of an overall coordination of the cell activity. In NLE, the analysis of FCM data did not give as robust results as in ALE, but the curve of accumulation of Chl *a* in the suspension (i.e. "total" RED) confirms and supports the conclusion that pigment concentration highly increases in the first part of the day and

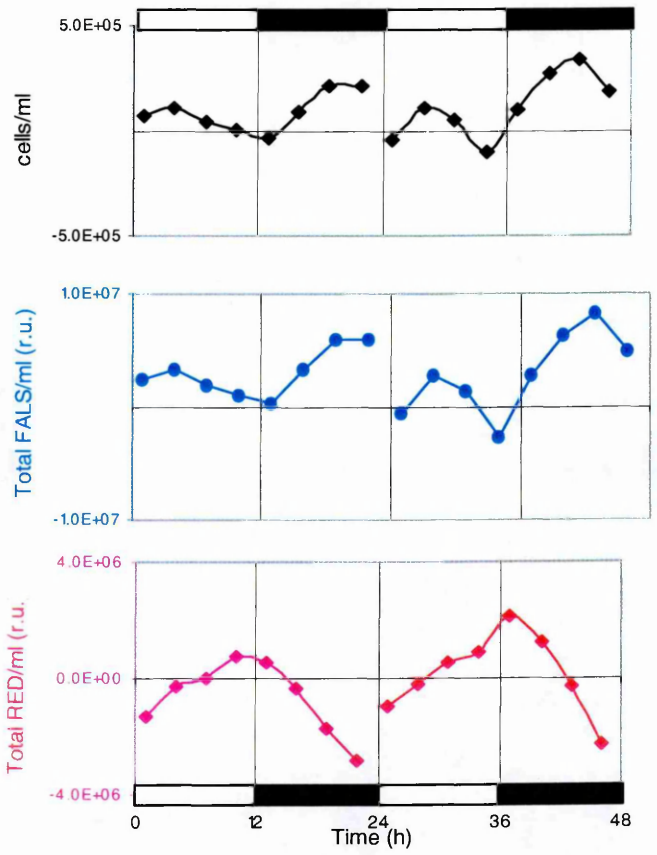

Fig. 6.9. Anomaly of the curves reported in Fig.6.8 with respect to the exponential trends of Fig. 6.7 (exp. INTRO)

becomes stationary or even lower during the second one (Fig. 6.11c), thus earlier than in ALE. Another difference is in the coupling between somatic growth and pigment content. In this case the two parameters used as proxies for biovolume (i.e. "total" FALS) and Chl *a* ("total" RED) are in phase. The curve of growth (Fig. 6.11a) only partially matches this distribution, displaying additional nocturnal maxima, confirming that the culture was not synchronized during the experiment SPRING. Hence, pigment synthesis goes along with growth, and both processes follow the sinusoidal shape of natural irradiance.

However most of the cells divide at night, as evident from the occurrence of the highest growth rates (Fig. 6.1) and of positive values of $\Delta G_1/\Delta T$ (indicating cell division, Fig. 5.6 ($\Delta G1/\Delta T$)) during dark periods, thus they did not reach cell division in an active phase of biosynthesis, as in ALE. In addition, also photosynthetic performance is lowered in this part of the day, as will be discussed in the following section.

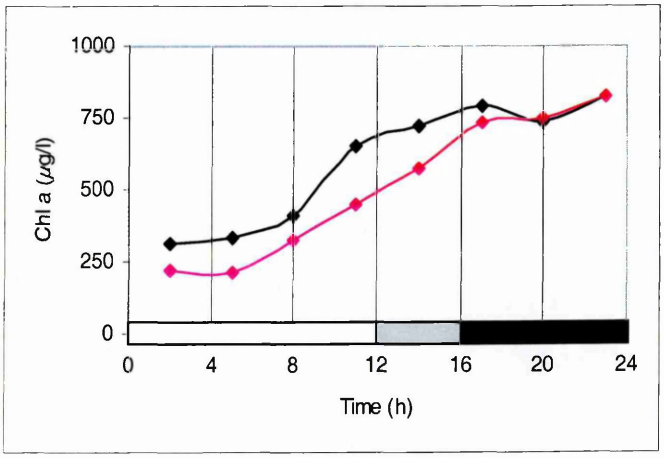

Fig. 6.10. Time course of Chl *a* concentration in a 16:8 LD cycle. Black line: culture of PT adapted to 12:12 LD regime; red line: culture of PT adapted to 16:8 LD regime (exp. C36). Grey box represent subjective night for the cells adapted to 12:12.

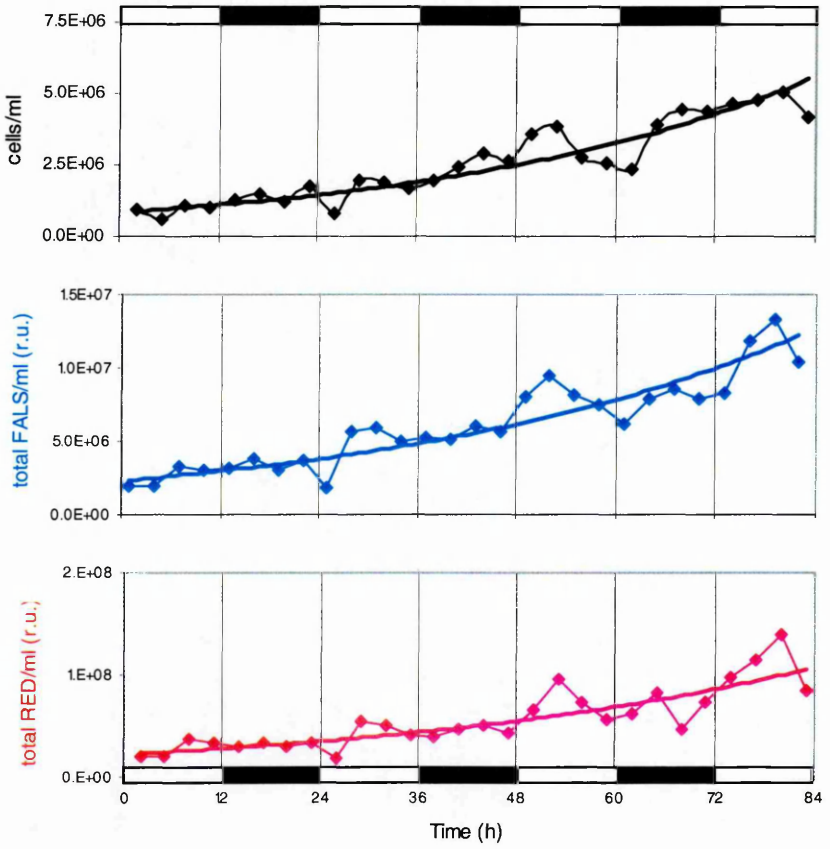

Fig 6.11. Curves of theoretical accumulation of the concentration of cells (black diamonds), total RED (red diamonds), total FALS (blue diamonds) in the suspension during the exp. SPRING, in absence of dilution. Solid lines are exponential curves fitting the data (R^2=0.77-0.87).

6.3 Photosynthetic machinery

Pigment content and the functioning of the photosynthetic machinery often show different time patterns. In particular, the effective cross-section of PSII, σ_{PSII} exhibits, as a general feature, maxima during the dark period and minima over the light period, but with differences due to light intensity. In fact, drastic diurnal minima are observed under intense natural light, both in culture (exp. URA) and *in situ* (exp. TRICICLO, surface samples).

They are accompanied by the depression of the fluorescence yields (F_0, F_m), of the maximum photochemical yield (F_v/F_m) and of the initial slope of rETR curves, α_{PAM}, which indicates non-photochemical dissipation events occurring in the antenna and in the RC to prevent photodamage. On the other hand, also in square wave light regime or at very low levels of sun irradiance (i.e. at the basis of the photic zone) σ_{PSII} displays the same circadian variability, but with smaller oscillations. I relate low values of σ_{PSII} to high concentrations of non-photosynthetic pigments in the antenna, that in fact reduce the transfer of absorbed light to the RC, thus lowering σ_{PSII} during L periods. This is confirmed by the inverted distribution of PPC/PSP and σ_{PSII} in all the conditions investigated in the present work, and by the cross-correlation analysis performed between the two parameters over long experiments, which indicates that 12 hrs is the time lag of the highest correlation i.e., in opposition of phase (not shown).

The photosynthetic efficiency (α^{chl}) is, by definition (Sakshaug *et al.*, 1997), linearly proportional to the optical cross section (a^*_{chl}), even though the two parameters appear not always coupled in my data, in that α^{chl} displays high levels all through the photoperiod, while a^*_{chl} drops in the second part of the day. On the other hand, the cross-correlation coefficient between the two time series under LD cycles is maximum (0.46, $p<0.05$) for time lag = 0 indicating that they are in phase. A better correspondence is found between α^{chl} and P^{chl}_{max} (cross-correlation coefficient = 0.77, $p<0.01$). The two photosynthetic parameters covary over LD cycles, showing high values in L periods and low at night, as also reported in literature (see Behrenfeld *et al.*, 2004 for a review).

$rETR_{MAX}$ and P^{chl}_{max} display similar circadian patterns under artificial LD cycles (Fig. 4.9 and 4.11) conversely the switch to LL condition causes different responses in the two parameters, as will be discussed in the following section.

The low resolution in ^{14}C-based measurements during the exp. SPRING prevents a detailed characterization of the circadian variability of photosynthetic coefficients in natural light regime. Phyto-PAM and FRRF measurements partially compensate for the lack of PvsE data in that they easily provide several photosynthetic parameters (see section 3.3.5.2 for a detailed description) allowing a better resolution of data over natural light-dark cycles, however with the *caveat* that fluorescence and carbon-based parameters measure different processes.

$rETR_{MAX}$ peaks very early in the morning, which implies that very few photons are required to activate the photosynthetic machinery by steeply increasing the electron transport rate, or, alternatively, that during the last hours of the dark period, the electron transport chain is prepared to optimally function from dawn. $rETR_{MAX}$ decreases all through the light period displaying minima in the early night (in one case in the late afternoon). Such a diurnal pattern cannot be related to variations in light intensity, since the time distribution of $rETR_{MAX}$ over the L period is not sinusoidal (i.e. symmetric around midday). Hence my interpretation is that changes in photosynthetic performance reflect different needs of the cell over the day. For example, high electron transport rates in the morning may satisfy the need of new cells to grow; vice versa, low rates may be associated with critical steps of the cell cycle, like cytokinesis. Thus the gradual reduction under daylight may reflect a progressive structural or functional change in the electron transport chain rate along with the somatic growth, until cells are sufficiently large in size to divide in the early night. This idea also agrees with the conclusions of Behrenfeld *et al.* (2004) who

highlighted that some components of the electron transport chain, as well as the electrons themselves, are required and used for other metabolic pathways than the linear electron transport. Consequently, the diel modulation of photosynthesis reflects changes in energy and carbon requirements during each phase of the cell cycle.

I do not exclude a close dependence of $rETR_{MAX}$ on light intensity. In fact the results of the experiment CICLAC confirms the importance of light intensity in terms of growth irradiance, from one hand, and of light changes, from the other, in driving the variability of $rETR_{MAX}$. As a result of the photoacclimation status, the higher the growth irradiance, the higher are $rETR_{MAX}$ and the related coefficient E_{kPAM}, while no significant differences are found in α_{PAM}. Growth irradiance does not affect the circadian distribution of fluorescence-derived coefficients, differently from what is observed for PPC pigments. A transition to high light however, implies a decrease in all Phyto-PAM coefficients, as a first response to stressing conditions. This is only partially true for low-light acclimated cells that are less efficient in adjusting $rETR_{MAX}$ but that rapidly reduce α_{PAM} and F_v/F_m.

The in situ experiment (TRICICLO) overall confirms the patterns reported from the experiment CICLAC concerning the dependence of photosynthetic parameters on the light regime (the study was conducted on natural populations living at ca 35% and 1% of the incident PAR) and responses to high light. Both in the surface layer and at the euphotic depth, almost all photosynthetic parameters display day-night variations; these are much more evident in the first case. Under daylight $rETR_{MAX}$ displays a rather flat distribution in both cases, the only significant variations being at dusk and dawn. This pattern differs from the one observed in culture, especially in NLE. I relate this feature to the light conditions, in two different ways. As for the population living at depth, it is worth noting that the

observed diel variability was actually entrained by a natural light dark cycle characterized by very low light intensity (max PAR irradiance ~ 15 μmolquanta $m^{-2}s^{-1}$), thus low day-night excursions. Hence, constant values during the day are likely to reflect the small excursions of the light field. Conversely in the surface layer of the water column, the steadiness of the coefficient may result from the coaction of two factors leading to opposite variations of $rETR_{MAX}$: the optimization of the photosynthetic machinery during the light period (enhancement of the transport rate) and the response to high light (decrease of rETR). Moreover, the occurrence, in the surface, of mechanisms of dissipation/photoprotection during the central hours of the day is confirmed by the concurrent depression of the other fluorescence-derived coefficients, i.e. F_v/F_m, α_{PAM}, σ_{PSII}. In particular, the latter parameter displays parallel, but less pronounced, circadian variability also at depth, in full accordance with the results of culture studies, showing similar day-night variations under non-saturating irradiance (experiment INTRO), and exceptionally low σ_{PSII} values under high natural light intensities (exp. URA). P^Bmax exhibits major excursions in surface samples, while the opposite is true for α^B. However in both cases the same time pattern occurs: the highest values at midday, intermediate values at dawn and dusk, and the lowest at night. The scant resolution of the measurements prevents, again, a careful characterization of the circadian distribution as well as any consideration on the response to high light (P^B depression, etc.), but the overall distribution of parameters substantiate the periodical pattern obtained on PT cultures.

6.4 Time patterns in free running regimes

LL experiments were carried out on cells pre-adapted to LD cycles, which, as extensively discussed above, display circadian oscillations in key parameters, e.g., pigment

concentrations, photosynthetic parameters. The oscillations of cell pigment content progressively dampen out during the LL phase, paralleled by the steadiness of cell cycle parameters, which would suggest a loss of synchronicity among the cells and, as a consequence, the disappearance of any circadian periodicity. In particular, the persistence of a diel rhythm during the first day in LL could be interpreted as the persistence of the same periodical pattern as under LD cycles after the synchronization due to the last DL transition.

Accordingly, the subsequent loss of oscillations, mostly in Chl *a*, may result from the desynchronization of the cells which would increase the number of subgroups of cells with different pigment levels, whose average would remain constant. Indeed, this is not at all the case. In fact a careful analysis of FCM data excludes the hypothesis that the observed differences in the mean cell pigment content result from the spread of the data, since their coefficient of variation displays very similar values in both phases of the experiment.

In addition to the loss of periodicity, both FCM and HPLC data show a significant decrease in the average cell Chl *a* content as well as in the other pigments, including photoprotectants. A similar pattern is observed in size/shape cell parameters (FALS and RALS), which means that LL cells accumulate less Chl *a* and that they are smaller in size. Indeed, the parallel lowering of the RED to FALS ratio (not shown) clearly indicates that the reduction in pigment concentration is more important than that occurring in size.

The growth rate increases only slightly during the LL phase and definitely less than one would expect after doubling the available light. In addition, the consequent decrease of the mean cell lifetime (from ca 18 to 14 hrs) does not justify the extent of the decrease in Chl *a* accumulation, especially considering that the removal of dark cycles should instead enhance Chl *a* synthesis.

All the above suggests that significant changes occurred in the biosynthetic machinery. I postpone the analysis of the photosynthetic activity, to discuss some

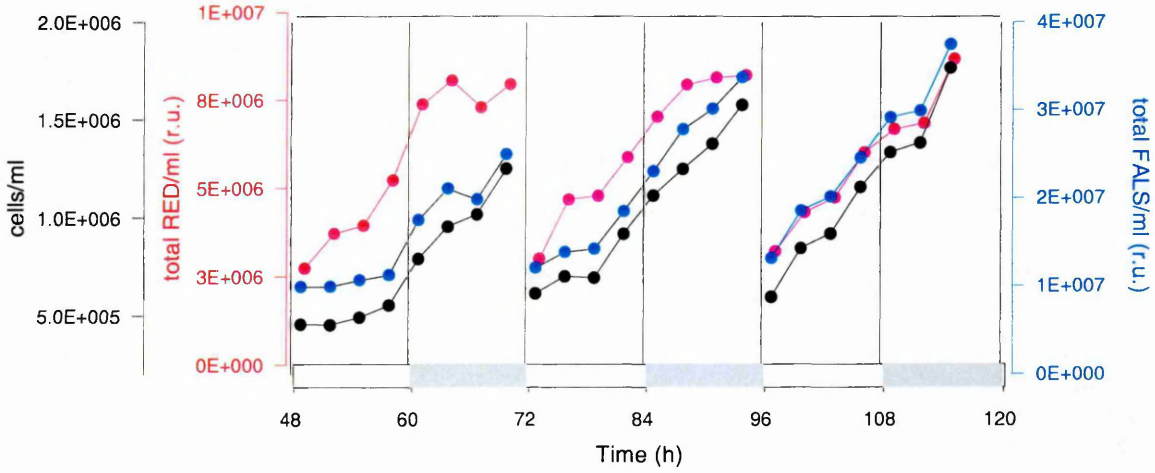

Fig. 6.12. Curves of theoretical daily accumulation of the concentration of cells (black), total RED (red), total FALS (blue) in the suspension for the three LL cycles of the exp. INTRO, in absence of dilution. (See text for details)

additional relevant aspects related to pigments and the light regime.

In Fig.6.12 and 6.13 I show the results of the analysis conducted on FALS, RED and cell number data over LL days, similar to what was shown in section 6.2 for LD cycles.

It is clear that an oscillating pattern in pigment synthesis is preserved at least for two LL cycles, while weaker periodicity is observed in the division rate. Pigment synthesis and cell division are decoupled and pigment concentration keeps its maxima in the whole suspension at the end of the subjective day or in the early subjective night as during LD cycles.

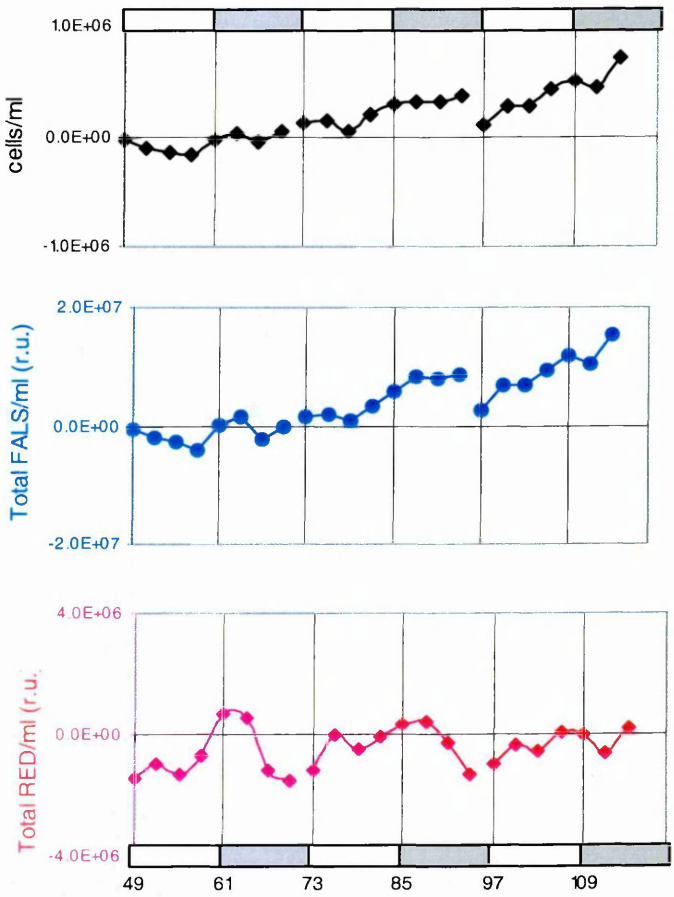

Fig. 6.13. Anomaly of the curves reported in Fig.6.12 with respect to the exponential trends of Fig. 6.7 (exp. INTRO)

By contrast Ddx suddenly loses its phase and since the second LL day exactly matches the oscillation in Chl *a* synthesis (Fig. 4.2). This is statistically relevant, as shown in the cross-correlogram in Fig. 6.4a (grey bars) referring to LL days (maximum cross-correlation coefficient at time lag 0), when compared to LD days (black bars). On the

contrary, PSP pigments and βcarotene do not significantly change their time dependence on Chl *a*, as shown in Fig. 6.2a for Fucox (grey bars).

I interpret those patterns as a residue of circadian oscillations of pigment synthesis in the whole suspension, while Ddx starts covarying with PSP because of the removal of the trigger represented by the D-L shift. This point has been tested in the experiment LL24 showing that cells grown in continuous light conditions significantly increase (up to 38% respect to the control) the Ddx/Chl *a* ratio after imposing a dark period for a short time (2 hours). Though, it is important to notice that the ratio is driven more by a reduction in chlorophyll *a* content than by an increase in the Ddx pool.

I mentioned above that while the division rate increased, cell size as well as cell pigment content and (synthesis) decreased. This is paralleled by a change in the performance of the photosynthetic machinery. As shown in Chapter 4 and in Fig. 6.14, the maximum photosynthetic rate drastically drops during the LL phase. In addition, another interesting difference emerges. During L periods of LD cycles P^B_{max}[1] is significantly higher (by up to 69%) than the rate actually achieved under the irradiance used in the experiment INTRO (i.e., $P^B_{max} > P^B(E_g)$, where E_g stands for growth irradiance). On the contrary, LL regime was characterized by much larger decrease of P^B_{max} than of $P^B(E_g)$, which resulted in the convergence of the two coefficients ($P^B_{max} \sim P^B(E_g)$). This is true both for cell and chlorophyll-normalized coefficients.

[1] I use the notation P^B_{max} to indicate generically both P^{chl}_{max} and P^{cell}_{max}

Thus in LL regime cells lower any potentiality to exceed the actual level of photosynthesis. Estimates of C fixation (either per unit chlorophyll or cell) integrated over 24 hours (Fig. 6.15) are quite similar in LD and LL -excluding the first day in continuous light when the highest C fixation level was achieved- in spite of the doubled light availability. I interpret such a decrease in the photosynthetic performance as a consequence of stressing conditions represented by the removal of dark periods. In fact the absence of the night impedes the temporal organization of all the cell metabolic pathways that are phased with day/night cycle. In other words, the alternation of different metabolic activities during the light and dark periods would be unpaired by the continuous light regime, thus depressing the rates of many metabolic processes. I also hypothesize that the stress is specifically due to the transition from a DL to a LL regime, since cells adapted to grow in LL for long time easily reach growth rates up to 1.6 d^{-1} (not shown). As already mentioned, $rETR_{MAX}$ does not follow the same pattern as P^B_{max} in LL, but keeps its diel oscillations, displaying same values for 36 hours and slightly lowers only in the last 24 h.

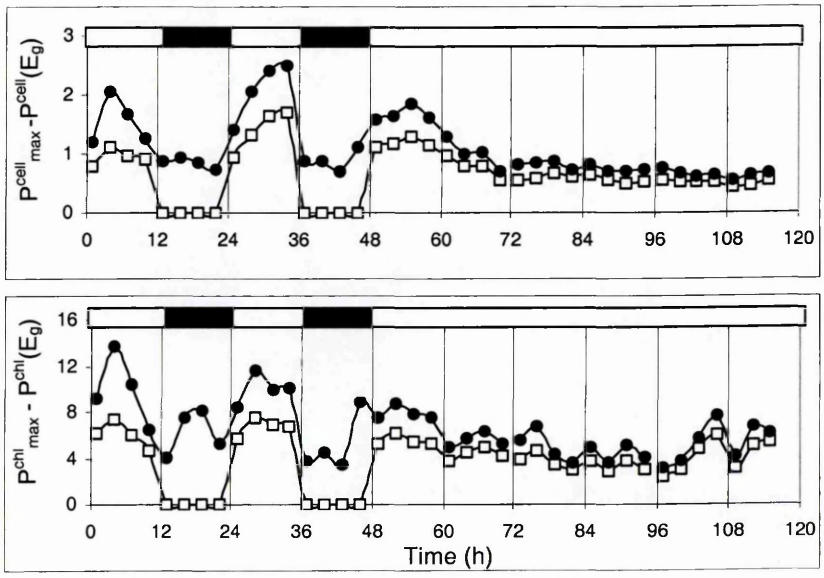

Fig. 6.14. Time distribution of P^B_{max} and $P^B(E_g)$ during INTRO exp. Upper panel: cell normalized coefficients. Lower panel: Chl a-normalized coefficients

Therefore, one component of the

photosynthetic machinery does not significantly change its performance and periodicity in continuous light. On the other hand, the time distribution of $rETR_{MAX}$ and $rETR(E_g)$ in the two light regimes (LD vs LL) shows strong similarities with what has been reported for P^B_{max} and $P^B(E_g)$, since the maximum electron transport rate in LL converges to the rate actually achieved under the growth irradiance (Fig. 6.16).

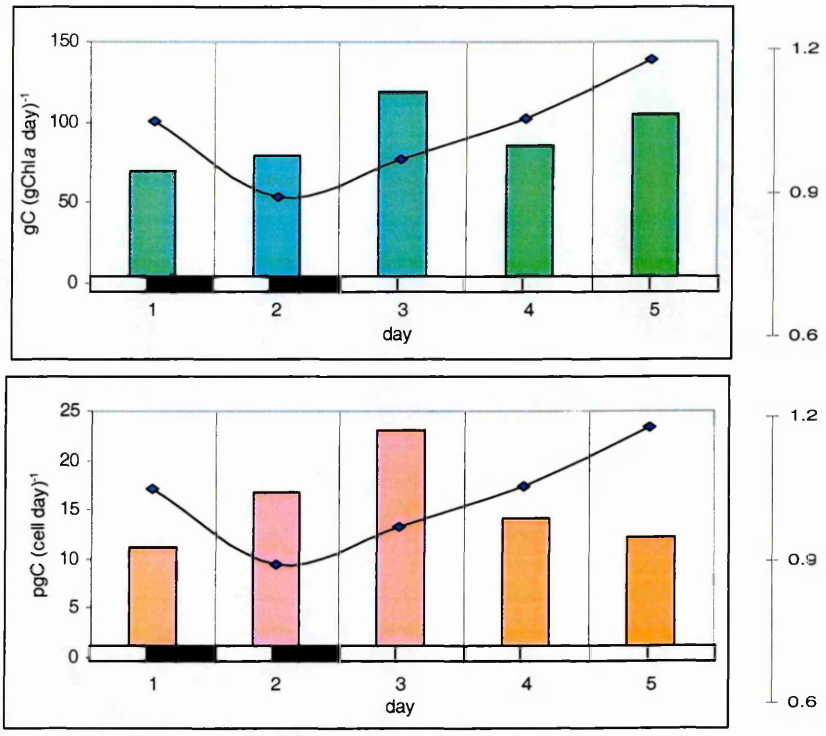

Fig. 6.15. Daily-integrated estimates of primary production during the experiment INTRO. Green bars: total C-fixed per Chl *a* per day. Orange bars: total C-fixed per cell per day. Superimposed (black line) the daily growth rate (μ)

This is true also for cells adapted to continuous light conditions (Exp. LL24) where the difference between $rETR_{MAX}$ and $rETR(E_g)$ spans from 9 to 16% (not shown). This indicates loss of plasticity, as it is also evident in NPQ data based on measurements performed at high light (Exp. PHYSIO, Fig. 4.12). In that case SV coefficients drastically drop in the first subjective night, keeping typically nocturnal values all over the LL period. This suggests that L-D and D-L transitions regulate the functionality of the photosynthetic machinery, reducing during dark the capability of the cell to respond to light fluctuations which occur in the natural environment during the light period.

When the L-D and D-L transitions are removed, cells simply adjust to the steady light intensity, becoming incapable to respond to light fluctuations.

The pattern of σ_{PSII} shows also periodicity in LL. Its variations are likely to be due, as discussed above, to the persistence of periodicity in the synthesis of PPC.

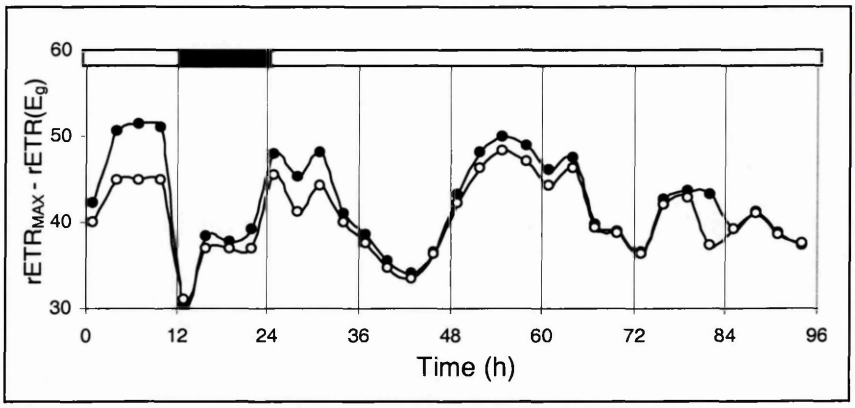

Fig. 6.16. Time distribution of $rETR_{MAX}$ (closed circles) and $rETR(E_g)$ (open circles) during PHYSIO exp.

Finally, the persistence of oscillations in the rETR vs. their disappearance in P^B_{max} during LL cycles indicates that a fraction of electrons generated by RC activity are not utilized for carbon fixation. This suggests that the energy is likely to be used in alternative pathways as, for example, repair mechanisms.

Finally experiments in continuous dark regime highlight the persistence of circadian patterns in $rETR_{MAX}$ (Fig. 4.20) even in absence of light, strengthening the above-discussed findings about this coefficient. On the other hand, all the other investigated parameters display quite constant values since the first DD cycle. As for pigments, this is in some way expected, since my results showed that their synthesis is related to the presence of light. This is also confirmed by recent studies on the genome of diatoms that pointed out the absence of genes for chlorophyll biosynthesis in the dark (A. Falciatore, personal communication) that are, conversely, present in other phytoplankton groups (e.g. cyanobacteria, green algae (Timko, 1998).

6.5 Cell cycle

Cell cycle appears strongly phased to the LD cycle, while the removal of dark periods rapidly induces the loss of rhythmicity, as shown in cell cycle data acquired over the LL periods of INTRO experiment. From cell cycle data (i.e. the relative percentage of cells in each stage) it was also possible to derive the duration of stages on a daily basis by means of the "cell cycle method" proposed by Carpenter and Chang (1988). They demonstrated that under periodic (i.e. L:D) conditions the total duration of the phases S and G_2+M is given by:

$$t_{S+G_2+M} = 2\left(t_{G2+M\,\max} - t_{S\,\max}\right) \qquad \textit{Eq. 6. 1}$$

where $t_{G2+Mmax}$ and t_{Smax} are the times at which the percentages of cells in G_2+M and S stages are at their maximum. Then, the durations of S and G_2+M are derived coupling equation 6.1 with the following:

$$\frac{t_S}{t_{G2+M}} = \frac{\sum_{i=1}^{n}\left(1+f_S+f_{G2+M}\right)}{\sum_{i=1}^{n}\left(1+f_{G2+M}\right)} - 1 \qquad \textit{Eq. 6. 2}$$

with n being the number of samples collected at fixed times of the diel cycle and f the percentage of the indicated (subscribed) stage of the cell cycle. In addition, from the duration of stages, an independent estimate of the daily growth rate may be derived (Eq. 7 in Valulot, 1995).

DAY	μ_{cc} (d^{-1})	Duration of G_2 (h)	Duration of S (h)
EXP. INTRO			
1	0.68	9.89	2.11
2	1.15	5.01	0.99
3	1.52	5.15	0.85
EXP. SPRING			
1	0.58	10.69	1.31
2	0.42	15.27	2.73
3	0.25	26.02	3.98

Table 6.1. Estimates of daily growth rates and duration of cell cycle stages from cell cycle method (Carpenter and Chang (1988)) applied on FCM-cell cycle data reported in Fig. 5.2 and 5.5.

The comparison between the daily growth rates as calculated from cell counts (Table 5.1) and from the above described method (shown in table 6.1 together with the estimated duration of stages) revealed some discrepancies. Accordingly, also the estimates of the duration of G_2 and S stages in some cases showed unexpected variability among different days (see for instance the first two days of INTRO experiment). The inconsistency of the data may be due either to the relatively low sampling resolution of cell cycle samples (a better sampling frequency would be 2 hours or less (Vaulot, 1995), or to the absence of replicate samples.

Thus, to better understand whether the estimated average durations of the stages could reproduce the circadian patterns observed in different light regimes, I used a simplified model of population dynamics, realized *ad hoc* by Dr. V. Botte (Centro Italiano Ricerche Aerospaziali, Capua (Italy)), which describes the growth of a *P. tricornutum* population in terms of the progression through the four phases of the cell cycle (G_1, S, G_2, M). Cells are forced to spend a certain time in each stage of the cell cycle, after which they pass into the following stage. The duration of this time is given for each cell by the following expression:

$$t_{stage(j)} = T_{stage(j)} \pm (stdev_{stage(j)} \cdot rand) \qquad Eq.\ 6.3$$

where $t_{stage(i)}$ is the time that the cell elapses in the stage j; $T_{stage(j)}$ is the average duration of the stage j; $stdev_{stage(j)}$ is the standard deviation on $T_{stage(j)}$; rand is a random number chosen from a normal distribution with mean zero, variance one and standard deviation one.

$T_{stage(j)}$ and $stdev_{stage(j)}$ are given as inputs of the model (consistently with the growth rate) and retained all through the simulation if not specified. The cells are randomly distributed among the four stages at the start point of each simulation. The only external control is

represented by the effect that dark conditions have on DNA synthesis due to the light restriction point, i.e., the progression from G_1 to S is blocked if cells are in the dark.

The output of the model is the time distribution of cells in the different stages of the cell cycle.

I performed several simulations, both in LD and LL regime, introducing different input values (reported in table 6.2), both for average durations of the stages and standard deviations. The results are shown in Fig. 6.17, 6.18 and 6.19. All the simulations clearly demonstrate that the LD alternation by itself is able to induce circadian oscillations since the second LD entraining cycle. The obtained time patterns are similar to those usually observed in my data with peaks of G_1 at the beginning of L periods and peaks of G_2 at the beginning of the dark, using a growth rate of 0.9 d^{-1} (Fig. 6.17 and 6.19). On the other hand, the use of a doubled daily growth rate and of halved stage durations generates nocturnal G_1 peaks, as occasionally observed (e.g. 1st day of INTRO experiment). Oscillations persisted in continuous light with period depending only on the total duration of the cell cycle, only when standard deviation is set to 20% of the average stage duration. On the contrary, if the standard deviation is increased to 40%, oscillations disappear rapidly, as observed in the experimental data (Fig. 5.2).

Cell cycle stage	Average duration (h)	Standard deviation	
Figure 6.17			
		Panel a)	Panel b)
G_1	9.78	20%	40%
S	1.31	20%	40%
G_2	6.72	20%	40%
M	0.67	20%	40%
Division rate (d^{-1})	1.3		
Growth rate (d^{-1})	0.9		
Figure 6.18			
		Panel a)	Panel b)
G1	4.89	20%	40%
S	0.65	20%	40%
G2	3.36	20%	40%
M	0.33	20%	40%
Division rate (d^{-1})	2.6		
Growth rate (d^{-1})	1.8		
Figure 6.19			
LD regime		Panel a)	Panel b)
G_1	9.78	20%	40%
S	1.31	20%	40%
G_2	6.72	20%	40%
M	0.67	20%	40%
Division rate (d^{-1})	1.3		
Growth rate (d^{-1})	0.9		
LL regime		Panel a)	Panel b)
G_1	7.50	20%	40%
S	1.00	20%	40%
G_2	5.17	20%	40%
M	0.50	20%	40%
Division rate (d^{-1})	1.7		
Growth rate (d^{-1})	1.18		

Table 6.2. Input parameters used for the simulation of the number of cells in the different stages of the cell cycle, reported in Fig. 6.17, 6.18, 6.19 (see text for details).

In Fig 6.19 I report a case where the duration of the cell cycle stages is changed, i.e. shortened, during the LL period, according to the daily growth rates measured over INTRO experiment. The results show that peaks occur more frequently in LL, but oscillations dampen out only at higher values of the standard deviation. It is worth noting that this last pattern is the closest one to my results, which clearly suggests that desynchronization occurs quickly after the removal of the dark period.

Another aspect is that from my data it is not clearly distinguishable whether different physiological performances would correspond to different stages of the cell cycle. Under LD alternation, high abundance of cells in the stage G_2 correspond to high values of cell pigment content and size, suggesting that size increase and in-cell pigment accumulation continues during the G_2 stage, whereas their decrease is due to cell division and the recruitment of G_1 cells.

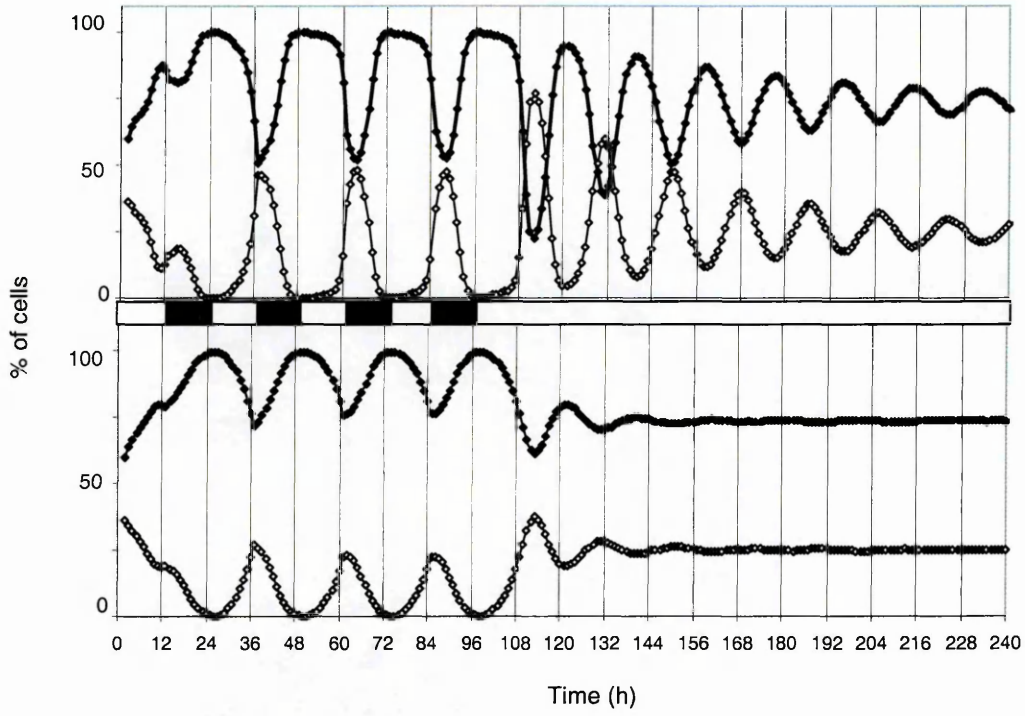

Fig. 6.17. Simulation of the time distribution of the percentage of cells in G_1 (closed diamonds) and G_2 (open diamonds) over six LD and four LL cycles using a population dynamic model (see text for details). The input parameters are reported in table 6.2.

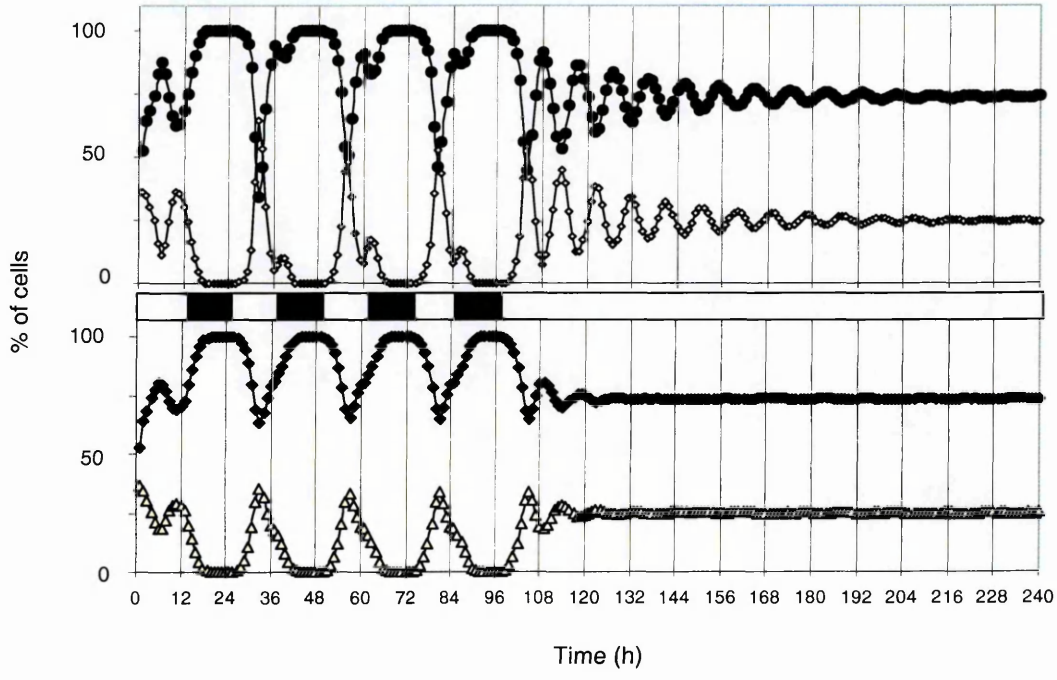

Fig. 6.18. Simulation of the time distribution of the percentage of cells in G_1 (closed diamonds) and G_2 (open diamonds) over six LD and four LL cycles using a population dynamic model (see text). The input parameters are reported in the table 6.2

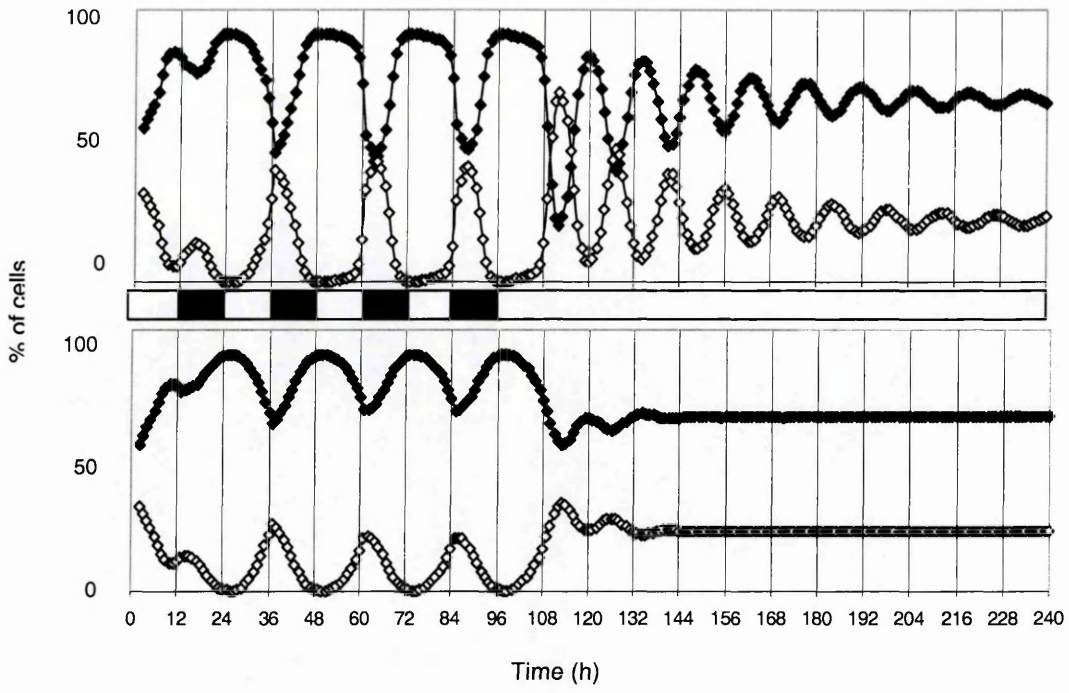

Fig. 6.19. Simulation of the time distribution of the percentage of cells in G_1 (closed diamonds) and G_2 (open diamonds) over six LD and four LL cycles using a population dynamic model (see text). The input parameters are reported in the table 6.2

This pattern is substantiated by the cross-correlation analysis performed on INTRO and SPRING experiment between RED and G_2 cells abundance (not shown). The results indicated that in AL the correlation is maximum at time lag 0 ($p<0.05$, i.e. the two parameters are in phase), while in SPRING RED and G_2 display the cross-correlation max at time lag =3 ($p<0.05$) but lag=0 is statistically relevant as well ($p<0.05$).

On the other hand, when the cell cycle is decoupled from the LD cycle, e.g., when multiple peaks of G_2 occur during a day, the G_2 time course is also decoupled from RED time course that continues to follow the LD cycle (exp C24 and C36, in Chapter 5). The results suggest that pigment synthesis may be, at least partially, decoupled from cell cycle.

This is confirmed also by the experiments in continuous light conditions. In this light regime, the cell cycle lost the phase since the first LL cycle, and the abundance of

cells in the different stages became rather flat over time. Also, chlorophyll synthesis became confused but completely decoupled from any pattern related to cell cycle.

In addition, I reported in the last section that the chlorophyll distribution continued to show some periodical trend, at least at the level of the whole suspension. This supports the idea that the removal of night is more critical for the cell cycle than for chlorophyll synthesis, probably because of the removal of the light restriction point.

The coupling of $rETR_{MAX}$ with cell cycle data (experiment SPRING) reveals a close relation with variations of the abundance of G_2 cells. $rETR_{MAX}$ systematically anticipates by 3 hrs the occurrence of peaks of $\Delta G_2/\Delta T$ (Fig. 6.20, upper panel). Conversely, cell division occurs in correspondence of low values of $rETR_{MAX}$. Likewise the maximal photosynthetic capacity (P^B_{max}, exp. INTRO) precedes by three hours the distribution of $\Delta G_2/\Delta T$ (Fig. 6.17, lower panel). The pattern is consistent with a close dependence of cell growth from C fixation rates.

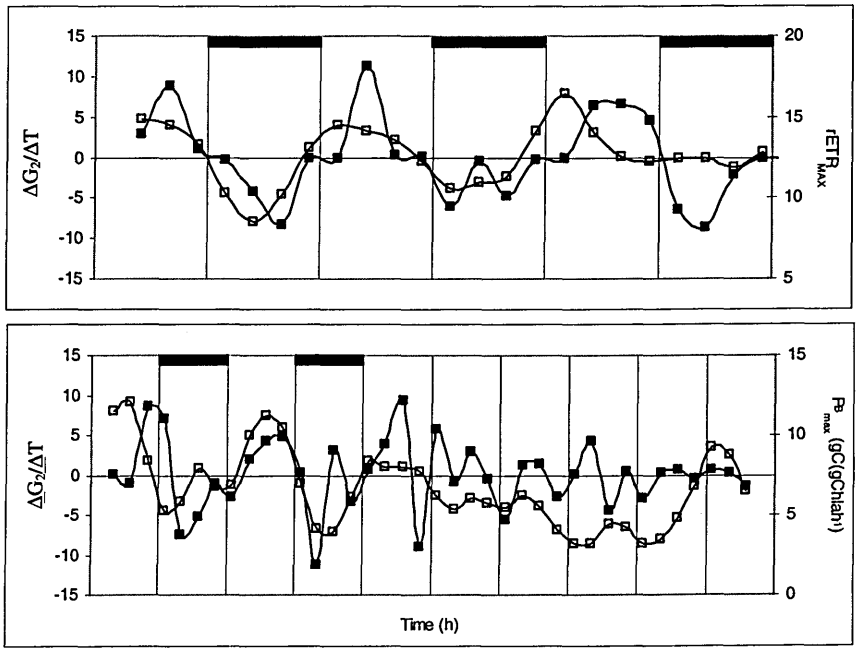

Fig. 6.20. Upper panel: time course of $rETR_{MAX}$ (open squares) and $\Delta G_2/\Delta T$ (closed squares) over the exp. SPRING. Lower panel: time course of P^B_{max} (open squares) and $\Delta G_2/\Delta T$ (closed squares) over the exp. INTRO

In conclusion, high levels of photosynthetic performance, both in terms of electron transport and C fixation, are achieved "far" from cell division and close to the transition to stage G_2.

In LD regime the maximum percentage of G_2 cells is observed at the end of the day, i.e., when photosynthesis was still possible. When photosynthesis is turned down by the lack of light and the rearrangement of the machinery, cells proceed in the G_2 stage until the division, without any increase in pigment content and with an increase in total biovolume relying on the internal storage. The only difference in the SPRING experiment is in the absence of total biovolume increase during the D period. This may be attributed to the reduced amount of chemical energy stored during the L period because of the sinusoidal light pattern (lower daily integrated PAR values).

6.6 Conclusions

I synthetically outline the main conclusions of my study, principally focused on the diatom *P. tricornutum.*

- L-D shifts are crucial for regulating the timing of the physiological activity (photosynthetic performance and machinery, pigment synthesis, cell cycle).

  The impact is independent from light intensity (similar time patterns are observed under different growth irradiance), unless it is very low (e.g., diurnal Ddx relative accumulation is prevented).
- Different physiological processes run at different paces in the different stages of the cell life, which makes the cells better suited to alternating light. This suggests a synchronization of cell processes probably due to internal entrainer/s.
- The entrainer, as most of zeitgebers, needs to be externally phased.

- When this phasing (reset) does not occur, the cells lose the global coordination, i.e., at the level of the whole suspension, mainly due to the desynchronization of the cell cycle, which does not imply the concurrent desynchronization of the timing of physiological processes on a cell basis. The latter span from the coupling and decoupling of pigment synthesis, the partitioning of electrons among different physiological needs (e.g., nitrate reduction, ATP synthesis, etc.), the activation/inactivation of the photosynthetic machinery and the assembling/dismantling of the photosynthetic machinery.

Actually it remains to be seen whether cells grown in continuous light are, on the long run, as healthy as the ones grown in LD alternation. It is clear that they are able to divide more rapidly, but they do not double the daily growth rate or the daily carbon fixation (consequently the efficiency of the use of light is lower), and are less flexible in facing light variations (e.g. rETR and P^B close to $rETR_{MAX}$ and P^B_{max}, respectively).

- The use of resources and the capability to adjust to environmental changes are more efficient if they are organized over the day. Thus, a proper rhythm would increase the efficiency in the use of the energy and the capability to respond to perturbations.
- The phasing of different processes is much more easily explainable if one assumes the presence of time giver(s) within the cell that is (are) reset by L-D and D-L transitions.

Since such 'tools' are linked to specific genes, and since biochemical-biomolecular investigations were outside the scope of my research, I cannot propose robust hypotheses on their nature. However, preliminary investigations on the genome of the diatoms *T. pseudonana* and *P. tricornutum* seem to exclude the presence of the genes commonly involved in the systems for circadian rhythms, i.e. *per*, *tim*, *clk*, (C. Bowler, personal

communication), but highlighted the presence of phytochrome and cryptochrome photoreceptors which are known to have a role in the control of clock-regulated processes in other organisms. The latter findings are also consistent with the model-derived results presented in Chapter 2.

All the above makes sense also in an evolutionary perspective. LD alternation is a permanent pattern in the Earth system. Obligatory autotrophs, i.e., organisms requiring light to survive and grow, would be strongly hampered during dark period, unless the D period is utilized to perform processes that would somehow relieve and prepare the activity taking place during the L periods (mainly photosynthesis and its regulation), and my data demonstrate that this is in fact occurring.

Acknowledgments

I wish to sincerely thank my external supervisor, Prof. Marlon Lewis for the kind and helpful attitude demonstrated during his pleasant visits to Naples through the four years of supervision of my PhD program. In particular I am very grateful for his precious help in yearly addressing my work and in critically reviewing my manuscripts.

I would like to thank all the people from SZN who made my life in the lab friendly and the work experience stimulating. In particular I warmly thank Fabrizio, my invaluable officemate, colleague and friend; Italia and Fabio, always ready to listen to me and say the right words at the right time; Serena and Enzo, precious during "impossible" experiments and close to me in any hard or pleasant moment (Serena, I owe you a summer cruise!); Rosario, Aurea, Imma, Francesca, Iole, Patrizio for sharing nice coffee breaks (Rosario also for making coffee!), lunches, and cruises; Ferdinando, Christophe, Céline for tolerating my "chaotic" presence in the office over the last years, Grazia, for her kind, warm and always motivating attitude since I was an undergraduate student.

Further, all the others "living" at the third floor: Augusto, Ciro, Alex, Daniele, Olga, Angela, Raffaella, François, Sabina, Giovanna, Margherita, Manuela, Diana for sharing daily not only the space, but also a smile.

I want to warmly thank Silvia and Gabriella for their kind and precious help in the contacts with the Open University and the supervisors.

I thank Dr. Raffaella Casotti for the support on the use of the flow cytometer and the interpretation of FCM data, Dr. Christophe Brunet and Augusto Passarelli for the helpful suggestions about the HPLC technique, Dr. Vincenzo Vellucci for the help with spectrophotometry and spectroradiometry, Dr. Immacolata Santarpia and Dr. Francesca Margiotta for performing PvsE measurements during the *in situ* experiment, Dr. Vincenzo Botte (C.I.R.A.) for developing the model of population dynamics using cell cycle data, Dr. Chris Bowler and Dr. Angela Falciatore for the stimulating scientific discussions about photoperception at sea, and for the revision of my manuscripts.

Sincere thanks to Dr. Vincenzo Saggiomo who approached me to the study of primary production at sea, but mainly because he was able to understand and support me in a particularly bad moment.

The greatest "grazie" is for Dr. Ribera d'Alcalà. Maurizio has represented my "reference point" since I was an undergraduate student, when he involved me with his enthusiasm and curiosity in the study of the Biological Oceanography. From the first, unforgettable, cruise to the completion of this thesis, through eight years of experiments, cruises, scientific discussions, rushed preparations of seminars, conferences, papers, I have appreciated his contagious passion for work, his honesty and humanity, his capability to be close to young people and to people in general, which make him far from being a boss and at the same time being a great boss!

Finally, I wish to thank the people who have always believed in me: mamma, papà, and Edo, who make my life serene....and Luigi who makes it important.

References

Armbrust, E.V., Berges, J.A., Bowler, C., Green, B.R., Martinez, D., Putnam, N.H., Zhou, S., Allen, A.E., Apt, K.E., Bechner, M., Brzezinski, M.A., Chaal, B.K., Chiovitti, A., Davis, A.K., Demarest, M.S., Detter, J.C., Glavina, T., Goodstein, D., Hadi, M.Z., Hellsten, U., Hildebrand, M., Jenkins, B.D., Jurka, J., Kapitonov, V.V., Kroger, N., Lau, W.W., Lane, T.W., Larimer, F.W., Lippmeier, J.C., Lucas, S., Medina, M., Montsant, A., Obornik, M., Parker, M.S., Palenik, B., Pazour, G.J., Richardson, P.M., Rynearson, T.A., Saito, M.A., Schwartz, D.C., Thamatrakoln, K., Valentin, K., Vardi, A., Wilkerson, F.P., Rokhsar, D.S. (2004) The genome of the diatom *Thalassiosira pseudonana*: ecology, evolution, and metabolism. *Science*, **306**, 79-86.

Allali, Bricaud, A. and Claustre, H. (1997) Spatial variations in the chlorophyll specific absorption coefficients of phytoplankton and photosynthetically active pigments in the equatorial Pacific. *J. Geophys. Res.*, **102**, 12413-12423.

Arsalane, W., Rousseau, B. and Duval, J.-C. (1994) Influence of the pool size of the xantophyll cycle on the effects of light stress in a diatom: competition between photoprotection and photoinhibition. *Photochem. Photobiol.*, **60**, 237-243.

Babin, M., Morel, A. and Gagnon, R. (1994) An incubator designed for extensive and sensitive measurements of phytoplankton photosynthetic parameters. *Limnol. Oceanogr.*, **39**, 694-702.

Barinaga, M. (1998) Clock photoreceptor shared by plants and animals. *Science*, **282,** 1628-1630.

Beaver, L.M., Gvakharia, B.O., Vollintine, T.S., Hege, D.M., Stanewsky, R. and Giebultowicz, J.M. (2002) Loss of circadian clock function decreases reproductive fitness in males of *Drosophila melanogaster*. *Proc. Nat. Acad. Sci. USA*, **99**, 2134-2139.

Behrenfeld, M.J., Prasil, O., Babin, M. and Bruyant, F. (2004) In search of a physiological basis for covariations in light-limited and light-saturated photosynthesis. *J. Phycol.*, **40**, 4-25.

Bidigare, R.R., Ondrusek, M.E., Morrow, J.H. and Kiefer, D.A. (1990). *In vivo* absorption properties of algal pigments. Proceedings of SPIE #1302 (Ocean Optics X), Orlando.

Bird, R.E. and Riordan, C. (1986) Simple solar spectral model for direct and diffuse irradiance on horizontal and tilted planes at the earth's surface for cloudless athmospheres. *J. Climatol. Appl. Meteorol.*, **25**, 87-97.

Borowitzka, M.A. and Volcani, B.E. (1978) The polymorphic diatom *Phaeodactylum tricornutum*: ultrastructure of its morphotypes. *J. Phycol.*, **14**, 10-21.

Bouvier, T., Troussellier, M., Anzil, A., Courties, C. and Servais, P. (2001) Using light scatter signal to estimate bacterial biovolume by flow cytometry. *Cytometry*, **44**, 188-194.

Boczar, B.A. and Prezelin, B.B. (1989) Organisation and comparison of chlorophyll-protein complexes from two fucoxanthin-containtening algae: *Nitzschia closterium* (Bacillariophyceae) and *Isochrysis galbana* (Prymnesiophyceae). *Plant Cell Physiol,* 30, 1047-1056.

Bricaud, A., Morel, A. and Prieur, L. (1981) Absorption by dissolved organic matter of the sea (yellow substance) in the UV and visible domains. *Limnol. Oceanogr.*, **26**, 43-53.

Brzezinski, M.A., Olson, R.J. and Chisholm, S.W. (1990) Silicon availability and cell-cycle progression in marine diatoms. *Mar. Ecol. Prog. Ser.*, **67**, 83-96.

Bunning, E. and Stern, K. (1930) Uber die tagesperiodischen Bewegungen der Primarblatter von *Phaseolus multiflorus*. II. Die Bewegungen bei Thermokonstanz. *Ber. Dtsch.Bot. Ges.*, **48**, 227-252.

Byrne, T.E., Wells, M.R. and Johnson, C.H. (1992) Circadian rhythms of chemotaxis to ammonium uptake in *Chlamydomonas*. *Plant Physiol.*, **98**, 879-886.

Casal, J.J., Sánchez, R.A. and Gibson, D. (1990) The significance of changes in the red/far-red ratio associated either to neighbour plants or to twilight for tillering in *Lolium multiflorum* Lam. *The New Phytol.*, **116**, 565-572.

Casper-Lindley, C. and Bjorkman, O. (1998) Fluorescence quenching in four unicellular algae with different light-harvesting and xanthophyll-cycle pigments. *Photosynth. Res.*, **56**, 277-289.

Chambers, P.A. and Spence, D.H.N. (1984) Diurnal changes in the ratio of underwater red to far red light in relation to aquatic plants photoperiodism. *J. Ecol.*, **72**, 495-503.

Chisholm, S.W. (1981). Temporal patterns of cell division in unicellular algae. In: Physiological Bases of Phytoplankton Ecology. Platt, T. Ottawa, *Can. Bull. Fish. Aquat. Sci.* **210**.

Chisholm, S.W., Morel, F.M.M. and Slocum, W.S. (1980). The phasing and distribution of cell division cycles in marine diatoms. In: Primary Productivity and Biogeochemical Cycles in the Sea. Falkowski, P. G., Plenum Press, NY: 281-300.

Crews, C.M. and Shotwell, J.B. (2003) Small-molecule inhibitors of the cell cycle: an overview. *Progr. in Cell Cycle Res.*, **5**, 125-133.

Delvin, P.F. and Kay, S.A. (2000) Chryptochromes are required for phytochrome signaling to the circadian clock not for rhythmicity. *The Plant Cell*, **12**, 2499-2509.

Demmig, B., Winter, K., Krüger, A., Czygan, F.-C. (1987) Photoinhibition and zeaxanthin formation in intact leaves. A possible role of the xanthophyll cycle in the dissipation of excess light energy. *Plant Physiol.*, **84**, 218–224.

Doty, M.S. and Oguri, M. (1957) Evidence for a photosynthetic daily periodicity. *Limnol. Oceanogr.*, **2**, 37-40.

Dring, M.J. (1988) Photocontrol of development in algae. *Annu. Rev. Plant. Physiol. Plant Mol. Biol.*, **39**, 157-174.

Dunlap, J.C. (1999) Molecular Bases for Circadian Clocks. *Cell*, **96**, 271-290.

Eilers, P.H.C. and Peeters, J.C.H. (1993) Dynamic behaviour of a model for photosynthesis and photoinhibition. *Ecol. Modell.*, **69**, 113-133.

Eppley, R.W., Holmes, R.W. and Paasche, E. (1967) Periodicity in cell division and physiological behavior of *Dytilum brightwelii*, a marine plankton diatom, during growth in light-dark cycles. *Arch. Microbiol.*, **56**, 305-323.

Eriksson, M.E. and Millar, A.J. (2003) The Circadian Clock. A Plant's Best Friend in a Spinning World. *Plant Physiol.*, **132**, 732-738.

Falciatore, A. and Bowler, C. (2002) Revealing the molecular secrets of marine diatoms. *Annu. Rev. Plant Biol.*, **53**, 109-130.

Falciatore, A., Ribera d'Alcalà, M., Croot, P. and Bowler, C. (2000) Perception of environmental signals by a marine diatom. *Science*, **288**, 2363-2366.

Falkowski, P.G. and Raven, J.A. (1997). Aquatic photosynthesis. Blackwell, Oxford

Ferrari, G.M. (2000) The relationship between chromophoric dissolved organic matter and dissolved organic carbon in the European Atlantic coastal area and in the West Mediterranean Sea Gulf of Lions. *Mar. Chem.*, **70**, 339-357.

Ferrari, G.M. and Tassan, S. (1999) A method using chemical oxidation to remove light absorption by phytoplankton pigments. *J. Phycol.*, **35**, 1090–1098.

Furukawa, T., Watanaba, M. and Shihira-Ishikawa, I. (1998) Green- and blue-light-mediated chloroplast migration in the centric diatom *Pleurosira laevis*. *Protoplasma*, **203**, 214-220.

Gathman, S.G. (1983) Optical properties of the marine aerosols as predicted by the Navy aerosol model. *Opt. Engin.*, **22**, 57-62.

Geider, R.J., Osborne, B.A. and Raven, J.A. (1985) Light dependence of growth and photosynthesis in *Phaeodactylum tricornutum* (Bacillariophyceae). *J.Phycol.*, **21**, 609-619.

Granbon, M. and Pedersen, M. (2001) Circadian rhythm of photosynthetic oxygen evolution in *Kappaphycus alvarezii* (Rhodophyta): dependence on light quantity and quality. *J.Phycol.*, **37**, 1020-1025.

Green, R.M., Tingay, S., Wang, Z.-Y. and Tobin, E.M. (2002) Circadian rhythms confer a higher level of fitness to *Arabidopsis* plants. *Plant Physiology*, **129**, 576-584.

Gregg, W.W. and Carder, K.L. (1990) A simple spectral solar irradiance model for cloudless maritime atmospheres. *Limnol. Oceanog.*, **35**(8), 1657-1675.

Hader, D.-P. and Lebert, M. (1998) The photoreceptor for phototaxis in the photosynthetic flagellate *Euglena gracilis*. *Photochem. Photobiol.*, **68**(3), 260-265.

Haltrin, V.I. and Kattawar, G.W. (1991) Light fields with Raman scattering and fluorescence in sea water. Technical Report. College Station, Dept of Physics, Texas A&M Univ., 74 pp.

Haltrin, V.I. and Kattawar, G.W. (1993) Self-consistent solutions to the equation of transfer with elastic and inelastic scattering in ocean optics: I. model. *Appl. Opt.*, **32**(27), 5356-5367.

Hastings, S.W. and Sweeney, B.M. (1958) A persistent diurnal rhythm of luminescence in *Gonyaulax polyedra*. *Biol. Bull.*, **115**, 440-458.

Højerslev, N.K. and Aas, E. (2001) Spectral light absorption by yellow substance in the Kattegat–Skagerrak area. *Oceanologia*, **43**, 39–60.

Hughes, J.E., Morgan, D.C., Lambton, C.R., Black, C.R. and Smith, H. (1984) Photoperiodic time signals during twilight. *Plant, Cell Env.*, **7**, 269-277.

Ianora, A., Miralto, A., Poulet, S., Carotenuto, Y., Buttino, I., Romano, G., Casotti, R., Pohnert, G., Wichard, T., Colucci-D'Amato, L., Terrazzano, G. and Smetacek, V. (2004) Aldehyde suppression of copepod recruitment in blooms of a ubiquitous planktonic diatom. *Nature*, **429**, 403-407.

Iwasa, K. and Shimizu, A. (1972) Motility of the diatom *Phaeodactylum tricornyutum. Exp. Cell Res.*, **74**, 552-558.

Jacquet, S., Partenski, F., Lennon, J.-F. and Vaulot, D. (2001) Diel patterns of growth and division in marine picoplankton culture. *J. Phycol.*, **37**, 357-369.

Johnson, C.H. (2001) Endogenous timekeepers in photosynthetic organisms. *Annu. Rev. Physiol.*, **63**, 695-728.

Kaftan, D., Meszaros, T., Whitmarsh, J. and Nebdal, L. (1999) Characterization of Photosystem II activity and heterogeneity during the cell cycle of the green alga *Scenedesmus quadricauda. Plant Physiol.*, **120**, 433-441.

Kohata, K. and Watanabe, M. (1988) Diel changes in the composition of photosynthetivc pigments and cellular carbon and nitrogen in *Chattonella antiqua* (Raphidophyceae). *J. Phycol.*, **24**, 58-66.

Kohata, K. and Watanabe, M. (1989) Diel changes in the composition of photosynthetic pigments and cellular carbon and nitrogen in *Pyramimonas parkeae* (Prasinophyceae). *J. Phycol.*, **24**, 58-66.

Kolber, Z.S. and Falkowski, P.G. (1993) Use of active fluorescence to estimate phytoplankton photosynthesis *in situ. Limnol. Oceanog.*, **38**, 1646-1665.

Kolber, Z.S., Prasil, O. and Falkowski, P.G. (1998) Measurements of variable chlorophyll fluorescence using fast repetition rate techniques: defining methodology and experimental protocols. *Biochim. Biophys. Acta*, **1367**, 88-106.

Kraml, M. and Herrmann, H. (1991) Red-blue interaction in *Mesotaenium* chloroplast movement - blue seems to stabilize the transient memory of the phytochrome signal. *Photochem. Photobiol*, **53**, 255-259.

Lamparter, T., Mittmann, F., Gartner, W., Borner, T., Hartmann, E. and Hughes, J.E. (1997) Characterization of recombinant phytochrome from the cyanobacterium *Synechocystis. Proc. Natl. Acad. Sci. USA*, **94**, 11792–11797.

Latasa, M., Berdalet, E. and Estrada, M. (1992) Variation in biochemical parameters of *Heterocaspa* sp. and *Olisthodiscus luteus* grown in 12:12 light:dark cycles. II. Changes in pigment composition. *Hydrobiologia*, **238**, 149-157.

Lavaud, J., Rousseau, B., van Gorkom, H.J. and Etienne, A.-L. (2002a) Influence of the diadinoxanthin pool size on photoprotection in the marine planktonic diatom *Phaedactylum tricornutum. Plant Physiol.*, **129**, 1398-1406.

Lavaud, J., van Gorkom, H.J. and Etienne, A.-L. (2002b) Photosystem II electron transfer cycle and chlororespiration in planktonic diatoms. *Photosynth. Res.*, **74**, 51-59.

Leedale, G.F. (1959) Periodicity of mitosis and cell division in the Euglenineae. *Biological Bulletin of the Marine Biologiacal Laboratory, Woods Hole*, **116**, 162-174.

Lewin, J. and Hellebust, J.A. (1975) Heterotrophic nutrition of the marine pennate diatom *Navicula pavillardi* Hustedt. *Can. J. Microbiol.*, **21**, 1335-1342.

Lohr, M. and Wilhelm, C. (1999) Algae displaying the diadinoxanthin cycle also possess the violaxanthin cycle. *Proc. Nat. Acad. Sci. USA*, **96**, 8784-8789.

Lohr, M. and Wilhelm, C. (2001) Xanthophyll synthesis in diatoms: quantification of putative intermediates and comparison of pigment conversion kinetics with rates constant derived from a model. *Planta*, **212**, 382-391.

Lopez-Figueroa, F. (1992) Diurnal variation in pigment content in *Porphyra laciniata* and *Chondrus crispus* and its relation to the diurnal changes of underwater light quality and quantity. *P.S.Z.N.I: Mar. Ecol.*, **13 (4)**, 285-305.

Lopez-Figueroa, F. (1998) Diel migration of phytoplankton and spectral light field in the Ria de Vigo (NW Spain). *Mar. Biol.*, **130**, 491-499.

Luning, K. (2001) Circadian growth in *Porphyra umbricalis* (Rhodophyta): spectral sensitivity of the circadian system. *J. Phycol.*, **37**, 52-58

Mancinelli, A.L. (1994). The physiology of phytochrome action. In: Photomorphogenesis in plants. Kendrick, R. E. and Kronenberg, G. H. M. Dordrecht, Kluwer Academic Publishers: 211-269.

Maritorena, S., Morel, A. and Gentili, B. (2000) Determination of the fluorescence quantum yield by oceanic phytoplankton in their natural habitat. *Appl. Opt.*, **39**, 6725-6737.

Marra, J. (1978) Effect of short-term variations in light intensity on photosynthesis of a marine phytoplankter: a laboratory simulation study. *Mar. Biol.*, **46**, 191-202.

Marra, J. and Heinemann, K. (1982) Photosynthesis response by phytoplankton to sunlight variability. *Limnol. Oceanogr.*, **27**, 1141-1157.

Marshall, B.R. and Smith, R.C. (1990) Raman scattering and in-water ocean optical properties. *Appl. Opt.*, **29**, 71-84.

Marsot, P., Cembella, A.D. and Colombo, J.C. (1991) Intracellular and extracellular amino acid pools of the marine diatom *Phaeodactylum tricornutum* (Bacillariophyceae) grown on unenriched seawater in high-light-cell-density dialysis culture. *J. Phycol.*, **27**, 478-491.

Mitchison, J.M. (1971) The biology of the cell cycle. Cambridge, Cambridge University Press.

Moore, J.K. and Villareal, T.A. (1996) Buoyancy and growth characteristics of three positively buoyant marine diatoms. *Mar. Ecol. Prog. Ser.*, **132**, 203-213.

Morel (1988) Optical modeling of the upper ocean in relation to its biogenous matter content (Case 1 water). *J. Geophys. Res.*, **93**, 10749-10768.

Morel, A. (1991) Light and marine photosynthesis: a spectral model with geochemical and climatological implications. *Prog. Oceanog.*, **26**, 263-306.

Morel, F.M.M., Hudson, R.J.M. and Price, M.M. (1991) Limitation of productivity by trace metals in the sea. *Limnol. Oceanog.*, **36**, 1742-1755.

Mueller, J.L. and Austin, R.W. (1995). Ocean optics protocols for SeaWiFS validation, Technical Report Series. In: NASA Technical Memorandum 104566, Rev. 1. Hooker, S. B., Firestone, E. R. and Acker, J. Greenbelt, Maryland.

Neckel, H. and Labs, D. (1984) The solar spectrum between 3300 and 12500 Å. *Solar Physics*, **90**, 205-258.

Nikaido, S.S. and Johnson, C.H. (2000) Daily and circadian variation in survival from ultraviolet radiation in *Chlamydomonas reinhardtii*. *Photochem. Photobiol.*, **71**, 758-765.

Olaizola, M., La Roche, J., Kolber, Z. and Falkowski, P.G. (1994) Non-photochemical fluorescence quenching and the diadinoxanthin cycle in a marine diatom. *Photosynth. Res.*, **41**, 357-370.

Ouyang, Y., Andersson, C.R., Kondo, T., Golden, S.S. and Johnson, C.H. (1998) Resonating circadian clocks enhance fitness in cyanobacteria. *Proc. Nat. Acad. Sci. USA*, **95**, 8660-8664.

Owens, T.G., P. G. Falkowski and Withledge, T.E. (1980) Diel periodicity in cellular chlorophyll content in marine diatoms. *Mar. Biol.*, **59**, 71-77.

Palmer, J.D., Livingston, L. and Zusy, F.D. (1964) A persistent diurnal rhythm in photosynthetic capacity. *Nature*, **203**, 1087-1088.

Platt, T., Ed. (1981). Physiological bases of phytoplankton ecology. Ottawa, *Can. Bull. Fish. Aquat. Sci.* (210).

Platt, T., Gallegos, C.L. and Harrison, W.G. (1980) Photoinhibition of photosynthesis in natural assemblages of marine phytoplankton. *J. Mar. Res.*, 38, 687-701.

Pope, R.M. and Fry, E.S. (1997) Absorption spectrum (380-700 nm) of pure water. II. Integrating cavity measurements. *Appl. Opt.*, **36**, 8710-8723.

Post, A.F., Dubinsky, Z., Wyman, K. and Falkowski, P.G. (1984) Kinetics of light-intensity adaptation in a marine planktonic diatom. *Mar. Biol.*, **83**, 231-238.

Prasil, O., Kolber, Z., Berry, J.A. and Falkowski, P.G. (1996) Cyclic electron flow around Photosystem II in vivo. *Photosynth. Res.*, **48**, 395-410.

Prezelin, B.B., Meesson, B.W. and Sweeney, B.M. (1977) Characterization of photosynthetic rhythms in marine Dinoflagellates: I. Pigmentation, photosynthetic capacity and respiration. *Plant Physiol.*, **60**, 384-387.

Prezelin, B.B. and Sweeney, B.M. (1977) Characterization of photosynthetic rhythms in marine dinoflagellates: II. Photosynthesis-irradiance curves and in vivo chlorophyll *a* fluorescence. *Plant Physiol.*, **60**, 388-392.

Putt, M., Rivkin, R.B. and Prezelin, B.B. (1988) Effect of altered photic regimes on diel pattern of species-specific photosynthesis I. Comparison of polar and temperate phytoplankton. *Mar. Biol.*, **97**, 435-433

Quigg, A. and Berdall, J. (2003) Protein turnover in relation to maintenance metabolism at low photon flux in two marine microalgae. *Plant Cell Env.*, **26**, 693-703.

Ragni, M. and Ribera d'Alcalà, M. (2004) Light as an information carrier underwater. *J. Plankton Res.*, **26**, 433-443.

Reed, R.K. (1977) On estimating insolation over the ocean. *J. Phys. Oceanogr.*, **7**, 482-485.

Reinfelder, J.R., Kraepiel, A.M.L. and Morel, F.M.M. (2000) Unicellular C4 photosynthesis in a marine diatom. *Nature*, **407**, 996-999.

Riebesell, U., Wolf-Gladrow, D.A. and Smetaceck, V. (1993) Carbon dioxide limitation of marine phytoplankton growth rates. *Nature*, **361**, 249-251.

Roenneberg, T. (1996) The complex circadian system of *Gonyaulax polyedra. Physiol. Plantarum*, **96**, 733-737.

Roenneberg, T. and Foster, R.G. (1997) Twilight times: light and the circadian system. *Photochem. Photobiol.*, **66**, 549-561.

Roenneberg, T. and Merrow, M. (2002) "What watch?...such much" Complexity and evolution of circadian clocks. *Cell Tissue Res.*, **309**, 3-9

Roenneberg, T. and Morse, D. (1993) Two circadian oscillators in one cell. *Nature*, **362**, 362-364.

Sakshaug, E., Bricaud, A., Dandonneau, Y., Falkowski, P.G., Kiefer, D.A., Legendre, L., Morel, A., Parslow, J. and Takahashi, M. (1997) Parameters of photosynthesis: definitions, theory and interpretation of results. *J. Plankton Res.*, **19**, 1637-1670.

Sathyendranath, S. and Platt, T. (1988) The spectral irradiance field at the surface and in the interior of the ocean: a model for applications in oceanography and remote sensing. *J. Geophys. Res.*, **93**, 9270-9280.

Scala, S., Carels, N., Falciatore, A., Chiusano, M.L. and Bowler, C. (2002) Genome Properties of the Diatom *Phaeodactylum tricornutum*. *Plant Physiol.*, **129**, 993-1002.

Sineshchekov, O. and Govorunova, E.G. (2001) Rhodopsin receptors of phototaxis in green flagellate algae. *Biochemistry*, **66**, 1300-1310.

Smith, H. (2000) Phytochromes and light signal perception by plants - an emerging synthesis. *Nature*, **407**, 585-591.

Smith, R.C. and Baker, K. (1981) Optical properties of the clearest natural waters. *Appl. Opt.*, **20**(2), 177-184.

Somers, D.E. (1999) The Physiology and Molecular Bases of the Plant Circadian Clock. *Plant Physiol.*, **121**, 9-19.

Sournia, A. (1974) Circadian periodicities in natural populations of marine phytoplankton. *Adv. Mar. Biol.*, **12**, 325-389.

Stal, L.J. and Krumbein, W.E. (1985) Nitrogenase acrivity in the non-heterocystous cyanobacterium *Oscillatoria sp.* grown under alternatng light-dark cycles. *Arch. Microbiol.*, **143**, 67-71.

Suzuki, L. and Johnson, C.H. (2001) Algae know the time of the day: circadian and photoperiodic programs. *J.Phycol.*, **37**, 933-942.

Sweeney, B.M. (1960) The photosynthetic rhythm in single cells of *Gonyaulax polyedra*. *Cold Spring Harb. Symp. Quant. Biol.*, **25**, 145-148.

Sweeney, B.M. (1963) Resetting the biological clock in *Gonyaulax* with ultraviolet light. *Plant Physiol.*, 704-708.

Timko, M.P. (1998). Pigment biosynthesis: Chlorophylls, heme, and carotenoids. Dordrecht, Kluwer Academic Publishers.

Ting, C.S. and Owens, T.G. (1993) Photochemical and nonphotochemical fluorescence quenching processes in the diatom *Phaeodactylum tricornutum*. *Plant Physiol,* **101**, 1323-1330.

Trees, Clark, Bidigare, Ondrusek and Mueller (2000) Accessory pigments versus chlorophyll *a* concentrations within euphotic zone: a ubiquitous relationship. *Limnol. Oceanog.*, **45**(5), 1130.

Vaulot, D. (1995) The cell cycle of phytoplankton: coupling cell growth to population growth. *Molecular ecology of Aquatic Microbes (Nato ASI series)*, **38**, 303-322.

Vaulot, D. and Chisholm, S.W. (1987) A simple model of the growth of phytoplankton population in light/dark cycles. *J. Plankton Res.*, **9**, 345-366.

Vermeulen, K., Van Bockstaele, D.R. and Berneman, Z.N. (2003) The cell cycle: a review of regulation, deregulation and therapeutic targets in cancer. *Cell Prolif.*, **36**, 131-149.

Vidussi, F., Claustre, H., Bustillos-Guzman, J., Cailliau, C. and Marty, J.C. (1996) Determination of chlorophylls and carotenoids of marine phytoplankton: separation of chlorophyll *a* from divinil chlorophyll *a* and zeaxanthin from lutein. *J. Plankton Res.*, **12**, 2377-2382.

Villareal, T.A. (1991) Nitrogen-fixation by the cyanobacterial symbiont of the diatom genus *Hemiaulus*. *Mar. Ecol. Prog. Ser.*, **76**, 201-204.

Villareal, T.A. and Carpenter, E.J. (1990) Diel buoyancy regulation in the marine diazotrophic cyanobacterium *Trichodesmium thiebautii Ehr. Limnol. Oceanogr.*, **35**, 1832-1837.

Zinn, J.G. (1759) Von dem Schlafe der Pflanzen. *Hambugisches Magazine*, **22**, 49-50.